BULLETIN OF THE DEPARTMENT OF GEOLOGY

TRIBHUVAN UNIVERSITY

Volume 24
December 2023

Puhbished by
Central Department of Geology
Tribhuvan University
Kirtipur, Kathmandu
NEPAL

Bulletin of the Department of Geology
Tribhuvan University, Kathmandu, Nepal
ISSN: 1996-3491

Cover Photo: Excavation of a pit at Dumrighari, Sarlahi for soil investigation and water table measurement.
(Photo by: Dr. Kabi Raj Paudyal)

INSTRUCTIONS TO AUTHORS FOR SUBMISSION

Submission of manuscripts

Manuscripts should be submitted to the email address of Chief Editor of the Bulletin of the Department of Geology. Submission of manuscript implies that it has not been published previously, that is not under consideration elsewhere, and that if accepted it will not be published elsewhere in the same form in English or any other language.

Preparation of manuscripts

Authors are suggested to follow a recent edition for the styling. The manuscripts would be presented in word documents files, with 30 mm margins at all sides and with a double spaced Times New Roman font of size 12 points. The corresponding author should be identified including a complete mail and email addresses and a phone number. The electronic files should be labelled with the manuscript title, and the authors' and files' name. The manuscript should not exceed 12 pages including tables and figures although in special cases longer manuscripts will be considered. Manuscripts should be typed according to following orders. Title, author's full name(s), affiliation(s), address(es), email address of the corresponding author and abstract (<300 words), which will be followed by the main text. The corresponding author should be identified with a number and footnote, no other footnote should be used. International system of unit (SI) should be used. Only internationally agreed abbreviations should be used. Symbols should be accompanied with explanations.

References

For the publications to be cited in the text, refer to the author's surname, followed by the year of publication. All the publications cited in the text should be presented in the list of references. It should be arranged alphabetically by author's surname. Refer the recent publication for the pattern of citation and list of references. Some examples are:

Hesse, M., Halbritter, H., Zetter, R., Weber, M., Buchner, R., Frosch-Radivo, A., and Ulrich, S., 2009. Pollen Terminology: An Illustrated Handbook. Springer-Verlag/Wien, 223 p.

Martin, A.J., DeCelles, P.G., Gehrels, G.E., Patchett, P.J., and Isachsen, C. 2005. Isotopic and structural constraints on the location of the Main Central Thrust in the Annapurna Range, central Nepal Himalaya. Geol. Soc. America Bull., v. 117, pp. 926–944.

Yagi, H., Maemoku, H., Ohtsuki, Y., Saijo, K., and Nakata, T., 2000. Recent activities faults distributed in and around Kathmandu valley, Lower Himalayan Zone. In: Okumura, K. (Ed.) Active faults research for the new millennium. Proceedings of the Hokudan International Symposium and School of Active Faulting. pp. 557-560.

Illustrations

The illustrations (photographs, diagrams and maps) are all to be referred as 'Fig.' followed by the corresponding number. All illustrations should be submitted in a print ready format, the size of which should be kept within a printable size of the bulletin and should be of high quality. The electronic version of the line drawings should be presented in TIFF or JPG format having resolution not less than 300 dpi. Figures and maps should not be drawn in colours. In geological maps legends should be used instead of colours. Text used in the figures should be Arial 9 to 10 points. The figure captions should be listed separately.

Tables

The tables are to be referred to as 'Table', followed by the corresponding number, e.g. Table 1:. All the tables should be of printable size and the caption should contain in the upper part. Footnotes should be given below the table and referred to by superscript lowercase letters. Tables should be prepared in Excel files and all the text should be of Times New Roman (TNR) plain and 10 points.

Publishing policy

The editorial board will review manuscripts in order to verify that they follow the format of BDG. Only those manuscripts, which follow the format, will be considered for further review process. The manuscript will be forwarded to at least two reviewers for peer review and the results of the evaluation will be communicated to the corresponding author for making corrections or modifications. The manuscript will be accepted for publication only when author(s) have fully reviewed and corrected the manuscript following comments of the referees. If one of the referees rejects the manuscript, the editorial board will take the final decision. After the acceptance of the manuscript for publication, when necessary the manuscript will be revised by the editorial board. All the ideas and interpretations expressed in the publication are responsible to their authors.

Bulletin of Department of Geology, Tribhuvan University, Kathmandu, Nepal, vol. 24, 2023, pp. 1-14
DOI:https://doi.org/10.3126/bdg.v24i.68372

Water Management in Hariwan Municipality of Nepal: Groundwater Harvesting from Riverbeds and Aquifers

Kabi Raj Paudyal*[1], Ram Bahadur Sah[2], Prem Nath Paudel[3], Prakash Chandra Acharya[4], Mamata Sayami[5], Goma Khadka[6], Aneeta Thapa[7], and Khum Narayan Paudayal[8]
1, 2, 6, 7, 8. Central Department of Geology, Tribhuvan University, Kirtipur, Kathmandu, Nepal
3. President Chure Terai Madhesh Conservation Development Board, Khumaltar, Nepal
4. Chandragiri Municipality-14, Kathmandu, Nepal
5. Department of Geology, Tri-Chandra Campus, Ghantaghar, Kathmandu, Nepal

ABSTRACT

Most of the regions of the Siwalik and Northern Terai (Bhabar) have a scarcity of water due to the water level beyond the suction limit of ordinary centrifugal pumping. In the present study, the Lakhandehi River section in the Sarlahi district is selected for shallow aquifer prospecting. The objective of this study was to assess potential zones of shallow aquifers including riverbeds. It was also aimed to assess the status of the existing subsurface water conditions, and distribution system, and find out suitable locations for groundwater harvesting and uses. The methodological part of the present study covers the field data collection and finding the appropriate shallow aquifer for groundwater extraction. In the field study, both the geological as well as hydrogeological maps were prepared on a 1:25,000 scale to assess the aquifer condition. A social survey was also carried out to find the most water scarcity areas and water availability conditions in the region. The main water scarcity area is found in the Hariwan Municipality, around the northern part of Bhabar and the southernmost region of the Chure region. The water insufficiency area for the present study was found in the places like Hariyon Khola section (Dumrighari), Sano Dume and Dume Khola sections (Samari Bhanjyang), Kothi Khola section (Kothikholagaun), and Attrauli Khola section (Atrauli village) of Hariwan Municipality due to the presence of impermeable layers in shallow depth. The concept of the development of swamp wells by retaining the groundwater flow from the shallow depth of the river channel is proposed in areas like the Samari Bhanjyang and Atrauli villages. Similarly, the development of shallow wells is proposed for the other two regions. To ensure a cost-effective water supply to the communities, it is advisable to implement a water lifting system to elevate the reservoir, followed by gravity-flow distribution.

Keywords: Shallow aquifer, Dug wells, Sump wells, Lakhandehi River

Received: 17 August 2022 **Accepted:** 5 February 2023

INTRODUCTION

Many places in the Siwalik region have water scarcity due to the rapid drainage of rainwater which reduces the availability of groundwater. Similarly, the Babhar zone of the region has water unavailability due to highly porous gravelly mass with greater thickness. As a result, the rivers that flow through this zone lose a significant amount of their discharge, which gradually infiltrates the subsurface, recharging the southern part of the region. Typically, the water that percolates through the Bhabar zone emerges at the junction of the Bhabar and Middle Terai or further south of the region. In the present study, the watershed of the Lakhandehi River is chosen for groundwater resource prospecting and utilization. This river is the largest in the district, spanning approximately 25 kilometers. This river is a perennial river and a tributary of the Bagmati River. Its major tributaries include Mathe Khola, Madar Khola, Dayani Khola, Narayan Khola, Hattibanda Kholsi, Baune Khola, and Chapani Khola, which merge with the Lakhandehi Khola to form a single river system. The Lakhandehi River originates from the northern hills of the Chure region. The streams of the river originate from the fractures in the sandstones or at the geological contact between the permeable sandstone and impermeable mudstone. The dendritic pattern of this river is controlled by the regional joints. In the well inventory survey, the SWL of the dug well found varies from 12 m in some places to 20-24 m in others. As per the hydrogeological classification, the southern part of the present study belongs to the Babar zone which is the northernmost flank of the Indo-Ganga Plain. It extends from the piedmont of the Siwalik southward to a maximum width of 8-10 km. This region in the study area is extremely poor in surface water availability. The rainwater in this region either seeps underground immediately or runs as overland flow resulting the flash floods. The Bhabar Zone is the major recharge zone for the Terai region of the country. Rivers crossing these areas lose their water content.

**Corresponding author*:
Email : kabiraj.paudyal@cdgl.tu.edu.np (Kabi Raj Paudyal)

Geologically, the study area encompasses the Siwalik range to the north, the Bhabar zone in the middle, and the southern Terai region to the south. Within the Lakhandehi watershed, the water scarcity areas of the Hariwan and the Lalbandi municipalities were targeted areas facing water scarcity. However, the northern part of the Hariwan was found to have the most severe water scarcity, making it the focal point of this study. The main objective was to prospect the shallow aquifer either from the terraces or from the riverbed materials and recommend an appropriate water distribution system for the communities. The dendritic pattern of this river seems to be influenced by regional joints (Neupane and Paudyal, 2021). The study area is located administratively in the Sarlahi district of the Madhesh Province of Nepal (Fig. 1). The climate of the region falls within the mild tropical region.

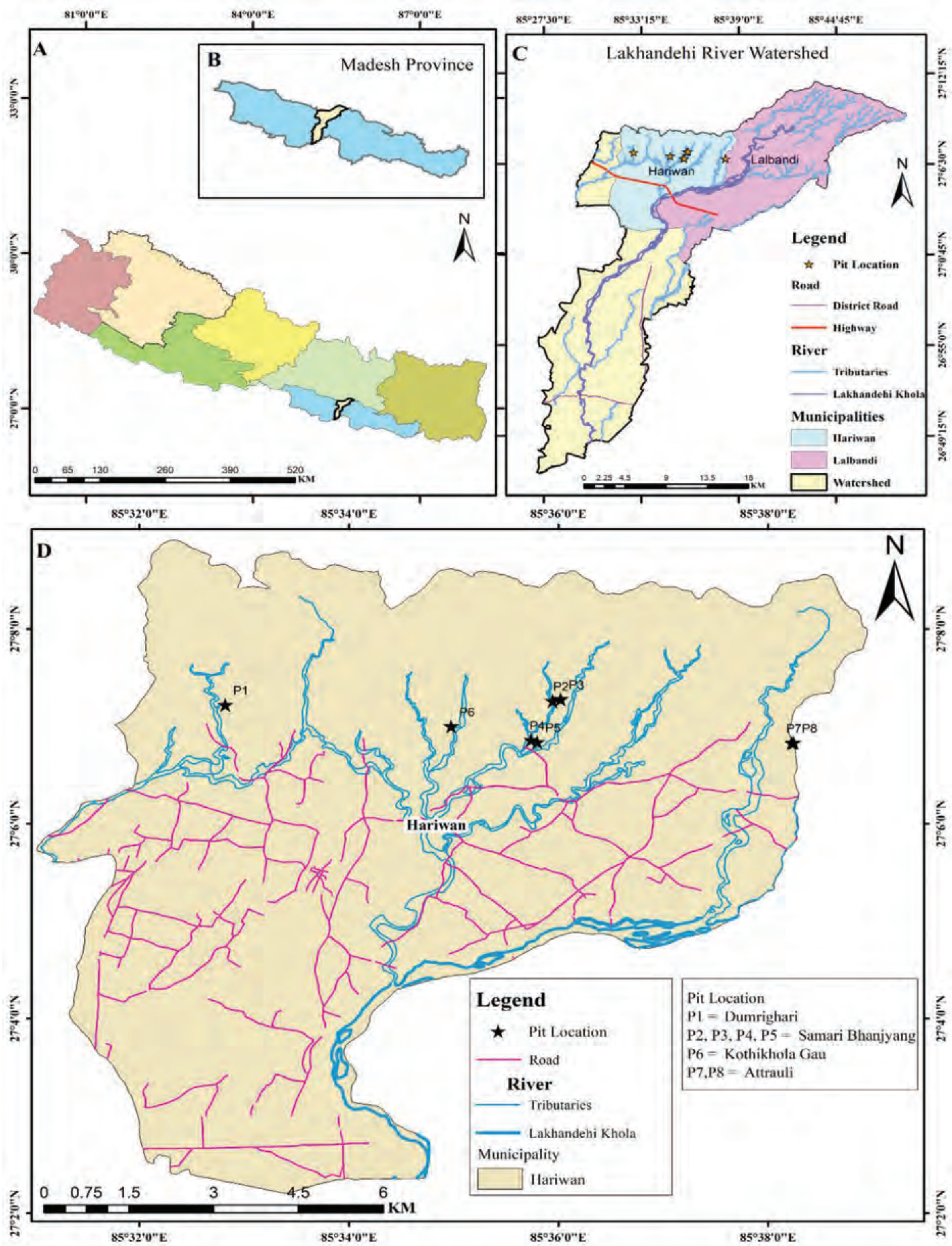

Fig. 1: Location map of the Lakhandehi watershed showing the Hariwan municipality and some adjacent regions (study area). A. Map of Nepal. B. Madesh Province. C. Lakhandehi River Watershed. D. Present study area.

The primary aim of this study is to investigate the shallow aquifer including riverbeds to provide drinking water in water scarcity areas of the Hariwan Municipality of Sarlahi district. The specific objectives are as follows:

i. To evaluate the status of the groundwater and find the water insufficiency regions,

ii. To propose the necessary infrastructures for groundwater harvesting and recommend an appropriate system for distributing the harvested water.

PREVIOUS STUDIES AND RESEARCH GAPS

The history of hydrogeological studies in the Terai Plain of Nepal dates to the early 1960s. The initial exploration of groundwater resources in Nepal was executed by the Department of Mines and Geology (DMG) during the 1959/1960 A.D. period, with the support of the Indian government. Duba (1982) was the first to investigate the groundwater resources in the Terai region of Nepal. Sharma (1995) compiled and presented a plethora of data concerning the hydrogeological characteristics, description of shallow and deep aquifers in Terai, tube well yield, and distribution in different parts of the Terai at that time of the Sarlahi district. Pradhan et al. (2002) conducted a comprehensive study on the Siwalik region of the Lakhandehi area, wherein they categorized the Middle Siwalik into two distinct geological sub-units based on the presence of pebbly sandstone beds. Sah (1998) proposed a unified lithological unit from different sections of the Siwalik of Nepal. The units in ascending order are the Bhorlegaon, Bankas, Jungali Khola, Chor Khola, Surai Khola, Dobata, Dudhaura Khola, Dhan Khola, and Deurali Formations. In a separate investigation, Sah et al. (2002) constructed a geological cross-section of the Terai zone specifically in the Sarlahi district. They have shown the distribution of aquifer zones in this region. Neupane and Paudyal (2021) prepared a detailed geological map of the Lakhandehi watershed area in 1:25,000 scales. More recently, Neupane and Paudyal (2021) have carried out some hydrogeological works in Lalbandi Municipality which lies in the Lakhandehi watershed area. They have focused on the hydrogeological condition of the Bhabar zone in this investigation. Their investigation revealed significant insights, including the variation in dug well depth ranging from 12 meters to 24 meters within this region. In this watershed, the region experiencing water scarcity is relatively smaller, and no prior local geological investigations have been undertaken by researchers or institutions. Additionally, tapping water from the riverbed materials is new for the Terai region of Nepal. Both the collection and distribution systems of groundwater are also discussed in this work. Under the UNDP/GWRDP/Shallow Aquifer Investigation program, altogether 20 STWs were installed for groundwater monitoring (average depth 31.4 m) in Sarlahi and established the subdivision of the shallow aquifer (DoI 1994). The actual situation of the availability of water in some of the Terai region is that there is flooding during the monsoon and drought in the rest of the year (Pokhrel, 2019). The same case exists in the present study. The proposed study area consists of the Himalayan Frontal Thrust in its northern part. Pathak (2016) has described the role of the HFT in hydrogeological significance in Terai. He suggests making use of a hard rock aquifer in Siwalik, installing a deep tube well within the Bhabar zone tapping groundwater in the Marshy zone, and supplying to the Bhabar zone to solve the water scarcity problems.

Extraction of groundwater is usually done through shallow tube wells, deep tube wells, and dug wells in the Terai region. In the study area, there is an adequate number of tube wells and dug wells in the Bhabar and Middle Terai (Marshy land) region. There are several artificial as well as natural ponds. The water scarcity problem that the Bhabar zone has been facing since a long time ago has been reduced after the construction of deep tube wells in different places. Recently, Lalbandi municipality has started distributing drinking water through the pipeline for 11 wards among 17 wards in the whole municipality. The water is supplied from a deep tube well developed at five different places. A similar case can be seen in Harion municipality too where water supplied from a deep tube well has fulfilled the water demand. There is not much problem of drinking water and irrigation water around this area now. They depend fully upon the deep tube well water for drinking and household work so negligence of the sources such as dug wells has led to dryness of the well. However, the people residing in Siwalik and the foothills of Siwalik have a major problem with drinking water and irrigation water, especially in the pre-monsoon. During these months most of the sources of water level either decrease or completely dry out. This has significantly affected domestic and wild animals around the region.

METHODOLOGY

A methodological flow chart to carry out the present work is shown in Fig. 2.

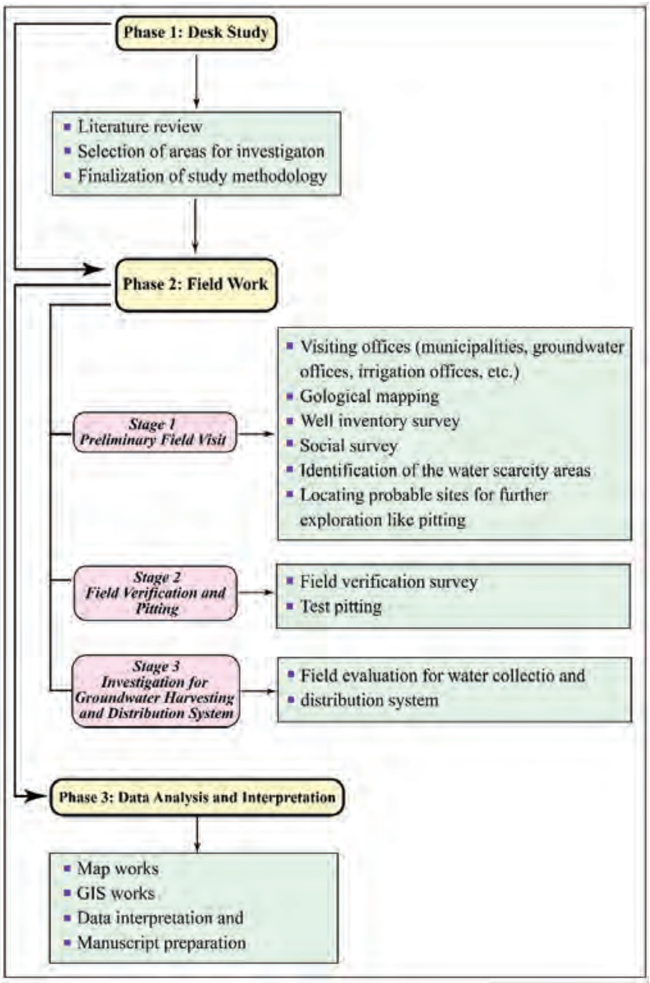

Fig. 2: Flow chart of the methodological framework.

RESULTS

Geology of the Hariwan area

The whole area of the present investigation lies within two geological zones: the Siwalik and Terai (Fig. 3). Within the rock successions of the Lower Siwalik, two geological units have been identified (Fig. 7): the Jangali Khola Formation and the Chor Khola Formation (Sah 1998). The typical lithology of the Jangali Khola Formation is variegated mudstone with thin sub-ordinate beds of loosely cemented, medium-grained grey sandstone. Similarly, the Chor Khola Formation compromises medium-to thick-beds of grey, medium-grained, laminated salt-and-pepper type sandstone. The channel of the Hariwan Khola flows from the axis of an antiformal structure. Many areas of the Siwalik region especially at and around the Main Himalayan Thrust (MFT), have been covered by the alluvial and colluvial admixtures in the form of different levels of terraces. The description of such terraces is made based on their stratigraphic position, geomorphic position, and elevation. Two levels of terraces, designated as T1 and T2 for older and younger respectively, and one active floodplain are distinguished in this area. Based on the grain size of the sediments and topographic breakage, the Terai zone in the present study can be divided into the Bhabar land, Middle Terai (Marshy land), and Southern Terai.

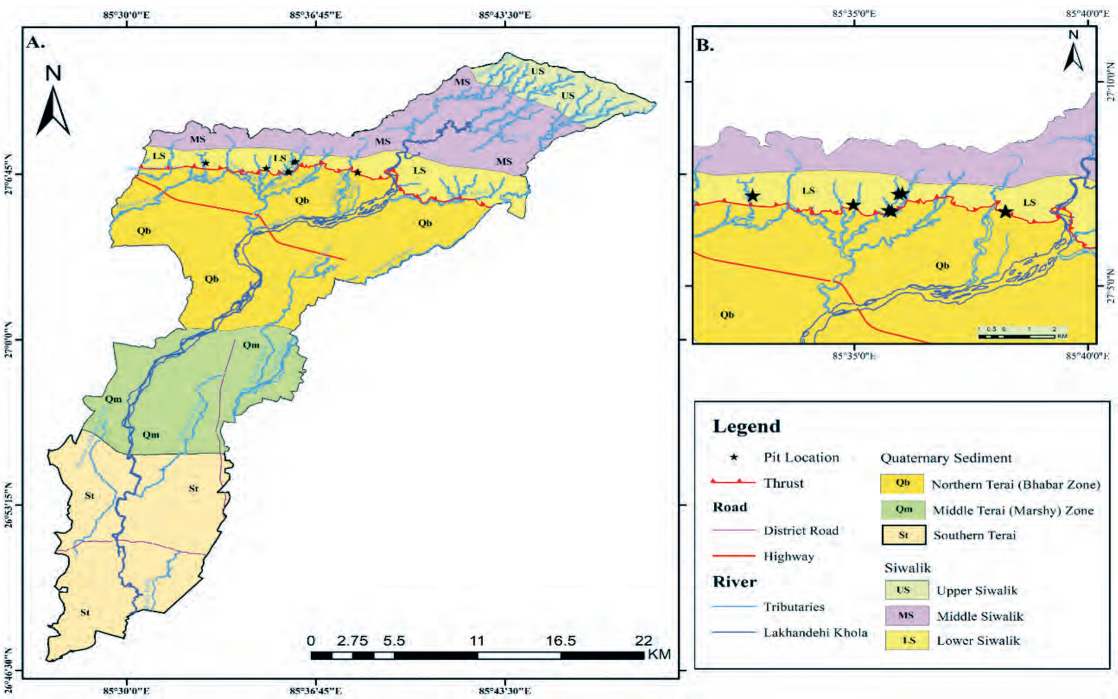

Fig. 3: Regional geological map of the Lakhandehi River watershed (modified after Neupane and Paudyal, 2021, and authors' observation (A) and geological map of the present study (B).

The corridor lying at the base of the south of the Churia hills is the Bhabar zone which is the northernmost flank of the Indo-Gangatic plain. It extends from the piedmont of the Siwalik southward to a maximum width of 8-10 km. This region in the study area is extremely poor in surface water availability.

The rainwater in this region either seeps underground immediately or runs as overland flow resulting the flash floods. Rivers crossing the Bhabar areas lose their water content. It is mainly composed of boulders, pebbles, cobbles, and coarse sand derived from the immediate northern vicinity of the Chure and the Mahabharat Range. In the study area, the Bhabar zone was observed around the Hirapur, Nawalpur, Patharkot, Atrauli, Sasapur, Daubari, Setibhir, Jiyajor, etc. The middle Terai consists of flat land of marshy nature and there exists artesian conditions. This zone is characterized by the dominance of clay, mud, sand silt, pebbles, and cobble at the surface. This is an extremely flood-affected area (Fig 4).

Water Insufficiency Areas

Water scarcity is described as a condition where water demand exceeds over available water supply. In the present study, the scarcity was evaluated based on the water availability vs demand by users. Local governmental bodies and water management authorities in the region were contacted to gather information about the watershed and any water scarcity issues during the data collection. Discussions were held with local body authorities of the Lalbandi municipality, Hariwan municipality, and their ward offices to obtain information about the water sources and distribution system within the study area and assess the major sites of water scarcity. The local people of the respective places were consulted to determine the locations of wells, natural ponds, and springs. The condition of water supply facilities to the local people was also assessed during the field survey. Public interaction played a crucial role in identifying the problems in the area, as connecting with people familiar with the region provided more specific insights.

The hydrogeological well inventory survey (Fig. 5) and social survey covered the Siwalik, Bhabar, and Middle Terai regions of the study area. The results showed that a few settlements in the Siwalik region and villages near the boundary of the Bhabar and Siwalik zone at Hariwan municipality lacked water supply and were still facing water scarcity. In these rural areas, accessing clean water is a challenge, particularly during dry seasons.

Many households rely on springs in the Siwalik region, shallow wells (dug wells) in Bhabar, and rivers in the Terai region for their water supply, but these sources do not provide sufficient water throughout the year, resulting in water-deficient conditions. From the field survey, it was found that the northern part of the study area, including Dumrighari, Kothikholagau, Samari Bhanjyang, and Attrauli villages in Hariwan municipality, experienced a high scarcity of water (Fig. 6). Detail geological and hydrogeological survey was carried

Fig. 4: The geomorphic view showing the Bhabar (recharge zone) and Middle Terai (discharge zone).

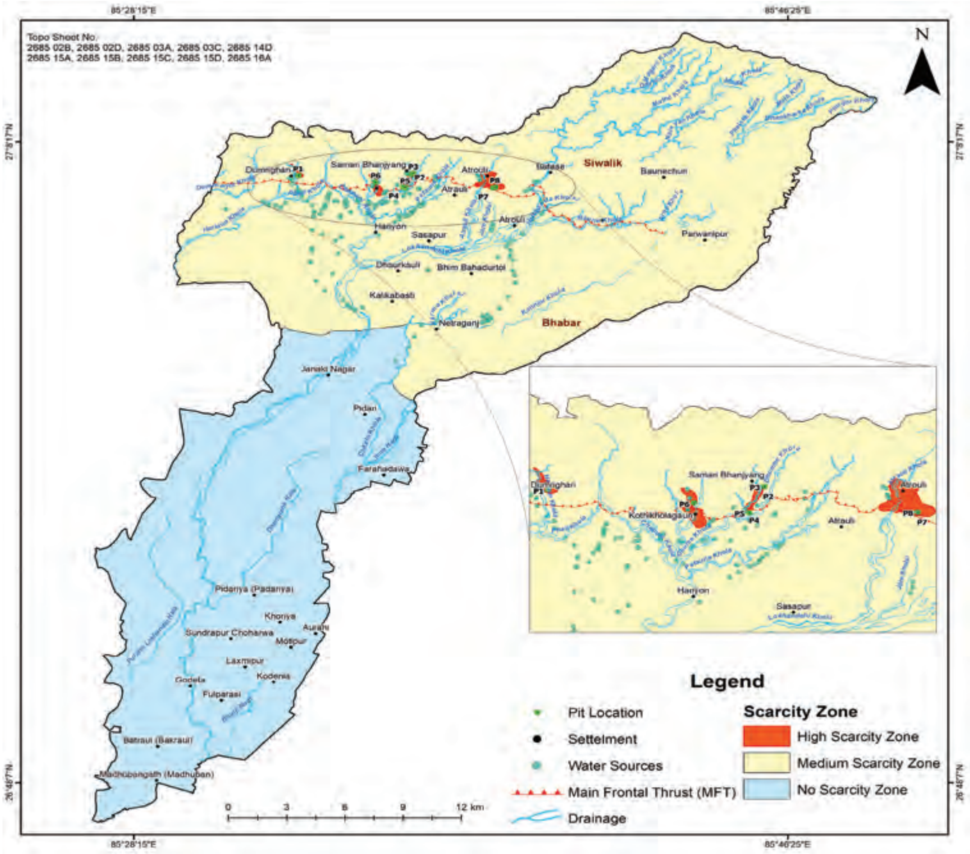

Fig. 5: Water scarcity mapping in the Bhabar-Siwalik section of the Lakhandehi Khola.

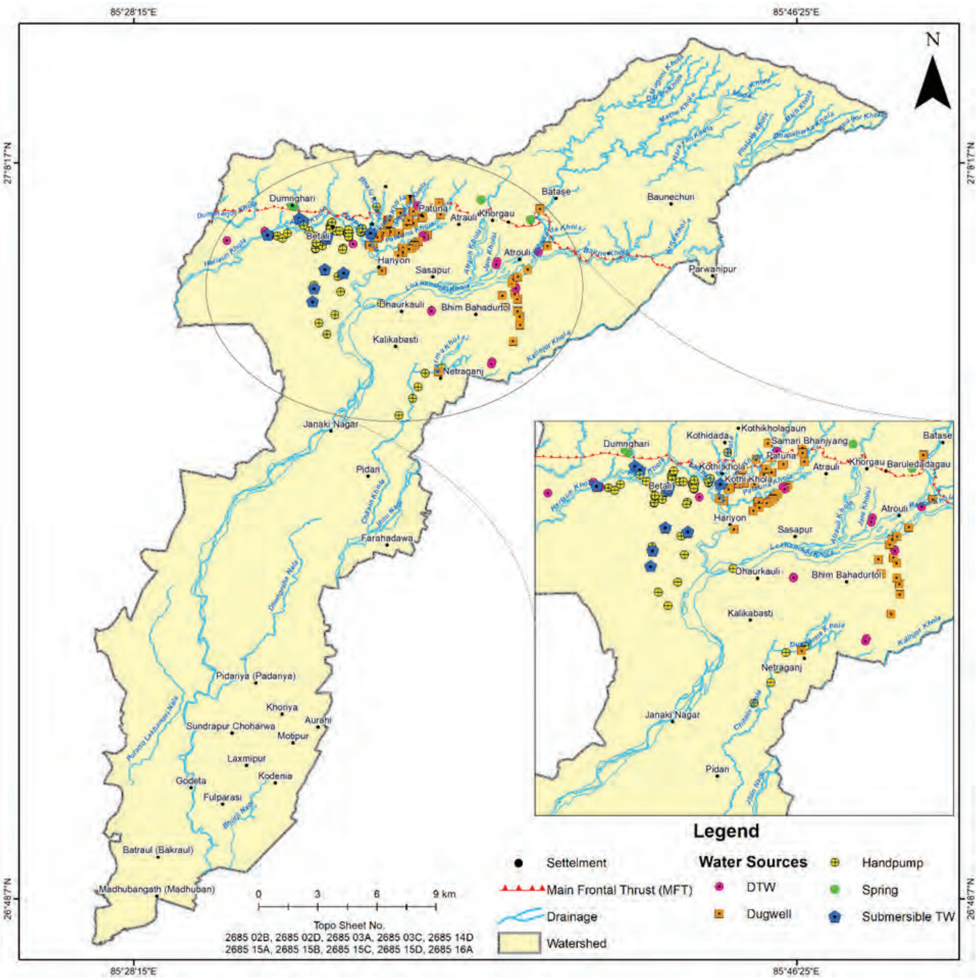

Fig. 6: Inventory mapping of water resources in water scarcity areas (shallow tube wells with single phase pump operated submersible pump).

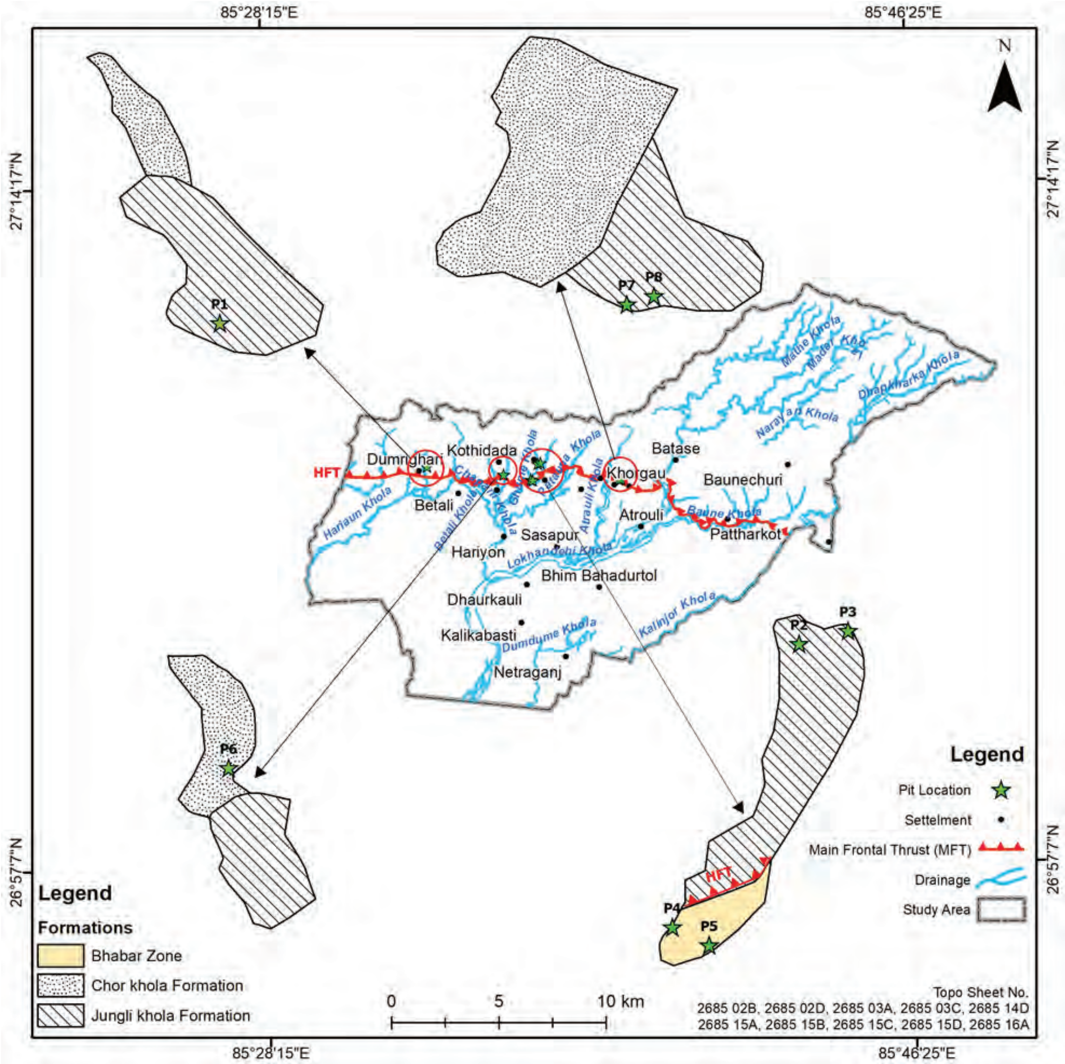

Fig. 7: Map depicting the site geology and location of investigation pits within the water-deficient region.

out in water scarcity areas (Fig. 7). Possible shallow aquifer sites including riverbeds were investigated for pitting in those areas to determine water availability at shallow depths.

The depth of pervious and impervious layers was determined directly through newly prepared pits of dimensions ~ 3 m x 2 m (length and breadth) with the depth varying from 2 m to 4 m. The depth of size was determined based on site conditions for water tapping, storing, and distribution. The local geological, and hydrogeological conditions and the subsurface litho-log details from each of the pits of each scarcity region are described in the following sections.

Geological and Hydrogeological Condition of Dumrighari Area

The Hariwan Khola section, located in the water scarcity region of Dumrighari areas, is characterized by rocks belonging to the Siwalik Group. In this vicinity, the rocks can be classified into two geological units: the Jangali Khola Formation and the Chor Khola Formation. The former unit primarily consists of variegated mudstone, with a smaller proportion of loosely cemented, medium-grained grey sandstone. On the other hand, the latter unit comprises medium-to-thick beds of medium-grained grey laminated salt-and-pepper type sandstone. Within the vicinity, there are two levels of river terraces along the Hariwan Khola, as well as a recent floodplain representing Quaternary deposits. The groundwater water indications in the area include seepages and springs that originate from the contact between the older terraces and Siwalik rocks (Fig. 8).

The existence of water-bearing layers at shallow depths in this region is indicated by both the contact springs and seepages. The alluvial cover is mainly composed of loosely held sand and gravels, with a finer matrix. The Dumrighari area consists of a few types of aquifers along the Hariwan Khola section and its adjacent regions.

Fig. 8: a) Field photographs of the contact spring with discharge 4 liters/minute (left) (GPS: 355890E, 3000949N) and b) seepage with discharge 2 liters/minute (right) (GPS: 355772E, 3001065N) on the older terrace and younger terrace respectively at Dumrighari.

Test Pitting (P1)

The site is located at latitude 27.118732 and longitude 85.543326. It is situated on the younger terrace (Fig. 9). The shallow aquifer discovered after digging is made up of gravelly sand, with a thickness of 2 meters. The discharge is about 6 liters per minute on average as a continuous flow. This aquifer level corresponds to the riverbed channel. The water extracted from this aquifer is suitable for the establishment of drinking water resources as a point source.

Geological and Hydrogeological Condition of Samari Bhanjyang Area

The geological condition of this site closely resembles that of the Hariwan Khola. The rock sequence consists mainly of variegated mudstone with a smaller proportion of loosely cemented, medium-grained grey sandstone. Many surface areas are covered by the terraces of the Sano Dume and Dume Khola. The MFT is located immediately south of this region. An indication of groundwater on the surface is evident from a dug well present there. The presence of a shallow aquifer can be inferred from the water available at a depth of about 4.0 meters in the existing dug well, situated in a flood plain. The aquifer is developed within the younger alluvial deposits. Geological observation reveals that water is flowing from the contact between the alluvial deposits and the mudstone and claystone of the Jangali Khola Formation. Four pits, one at the older terrace, another at the younger terrace of the Sano Dume Khola, and two in the Bhabar zone near Dume Khola, were excavated to determine the water table in this region.

Test Pitting

Test pits designated as P2, P3, P4, and P5 were excavated in this area. The pit site P2 is situated on the left bank of the Sano Dume Khola, on the older terrace (Terrace 1), at latitude 27.122785 and longitude 85.597321. The site of the pit construction lies slightly in depressed topography (Fig. 10).

Although the surface appears moist, no shallow

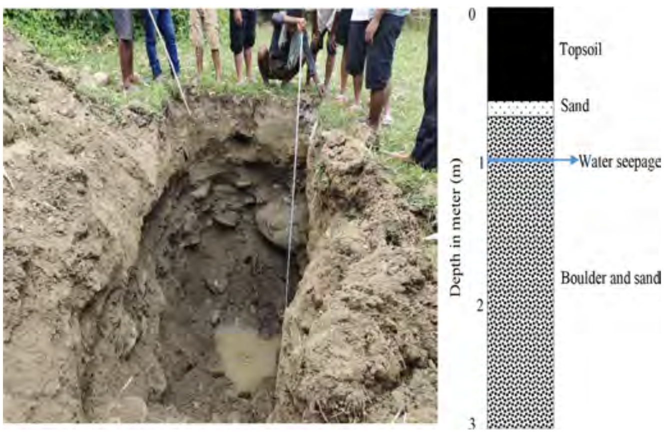

Fig. 9: Excavation of Pit (P1) at Dumrighari (left) and detail lithology of the pit (right) (GPS: 27.118732N, 85.543326E)

Fig. 10: Excavation of pit P2 (left) and lithology (right) at Samari Bhanjyang (GPS: 27.122785N, 85.597321E).

aquifer was found within the pit up to a depth of 3.5 meters. The topsoil and silty soil (B horizon of soil) were moist. However, the moisture gradually diminished in the underlying layers and became dry upon reaching the claystone and mudstone layers of the Siwalik rock. No shallow aquifer was identified at P2, and it is abandoned for water collection purposes.

The P3 site is situated on cultivable depressed land adjacent to the ridge on the right bank of Sano Dume Khola at Latitude 27.121266 and Longitude 85.597892, on the younger terrace (Terrace II). The selection of this site was based on recommendations from residents, as it remains consistently moist throughout the year. The lithology of the pit reveals a 1.9-meter-thick layer of moist topsoil overlaying mudstone (Fig. 11).

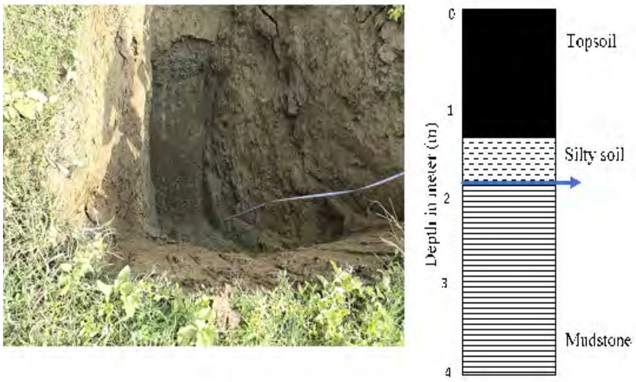

Fig. 11: Excavation of Pit (P3) (left) and litho-log (right) at Samari Bhanjyang (GPS: 27.121266N, 85.597892E).

Indications of groundwater couldn't find in this pit as mudstone is found at the bottom. Site P4 is located on cultivable land near the Dume Khola at latitude 27.115343 and longitude 85.595407. The area falls under the Bhabar zone. No shallow aquifer was found since the area acts as a recharge zone (Fig. 12). Pit P5 is located on the right bank of the Dume Khola on the river channel at latitude 27.114024 and longitude 85.59488 (Photograph 30). It lies in the Bhabar zone. The shallow aquifer was not found as the digging was made up to 4.1 m depth in the riverbed (Fig. 13).

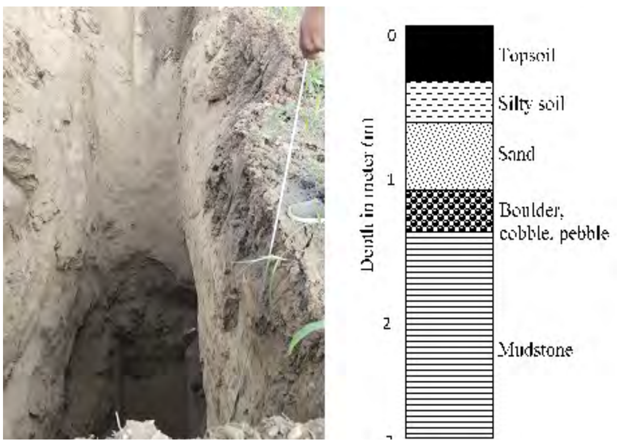

Fig. 12: Excavation of Pit (P4) (left) and lithology (right) at Samari Bhanjyang (GPS: 27.115343N, 85.595407E).

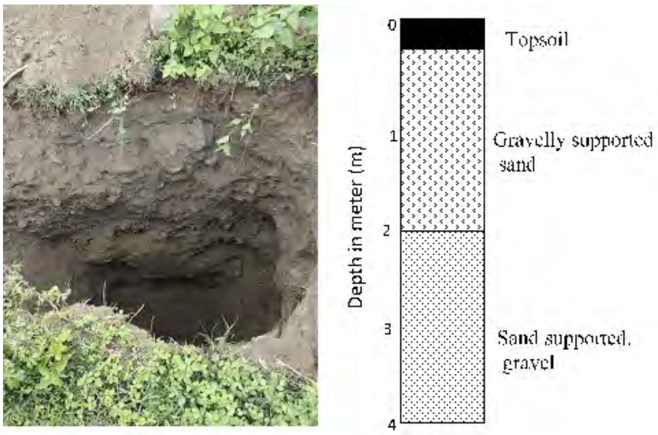

Fig. 13: Excavation of Pit (P5) (left) and corresponding lithology (right) at Samari Bhanjyang (GPS: 27.114024N, 85.59488E).

Geological and hydrogeological condition of the Kothi Khola Section

The area comprises Siwalik rock succession with alluvial deposits over it. The major geological units of the section area are the Jangali Khola Formation and the Chor Khola Formation. Water availability in the form of spring and seepage is found in three places in the area in older terrace (Terrace II), the younger terrace (Terrace I), and the riverbed channel. There are contact springs developed from the contact of the alluvial cover and the Siwalik rock.

The pit designated as P6 is located on the right bank of Kothi Khola on the wide ground of the old school at the younger terrace. The pit is at latitude 27.118175 and longitude 85.581944. The location is in Terrace II at around 2 m in height from the riverbed channel. The shallow aquifer was observed at a depth of 1.8 m in a gravelly sand layer (Fig. 14).

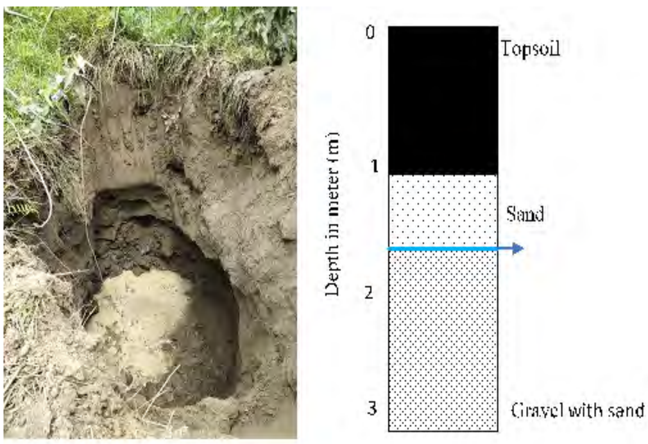

Fig. 14: Excavation of Pit (P6) (left) and lithology (right) at Kothikhholagau (GPS: 27.118175N, 85.581944E).

The discharge from observation at P6 is around 10 liters per minute as measured by the bucket method.

Geological and hydrogeological condition of the Atrauli Khola Section (Atrauli)

The rock successions of this area can be mapped under the Jungli Khola Formation, and the Chor Khola Formation of the Siwalik Group in the northern section while there is the Bhabar zone in the south. The attitude of beds is different from other sections. In this section, beds are dipping locally towards the south. Many places in this region are covered by alluvial and colluvial deposits. Some seepage and wetlands are also observed on the floodplain of the Atrauli Khola and its tributaries. Along the Atrauli Khola section towards the western side of Chisapani Village, there is a wetland. The seepage is likely to be the contact springs as signs of water flowing from the contact between soil and calcareous sandstone. Within the colluvium, a well is developed, and local people are using the groundwater available in the well (Fig. 15). Test Pit P7 was developed on the right bank of the Atrauli Khola on the river terrace at longitude 85.630264 and latitude 27.116205.

Fig. 15: a) Field photograph showing the seepage at the left bank of the Atrauli Khola (GPS: 364490E, 3000967N) and b) wetland in the western hill of Chisapani village (right) (GPS: 363910E, 3001039N).

Within the range of 2 m depth, a mudstone layer (bedrock) is found which was completely dry in field condition (Fig. 16). Pit (P8) was located on the existing channel of the Atrauli Khola. Seepages were found at about 0.9 m depth at the contact of upper river deposits (topsoil) and lower mudstone layers (Fig. 17).

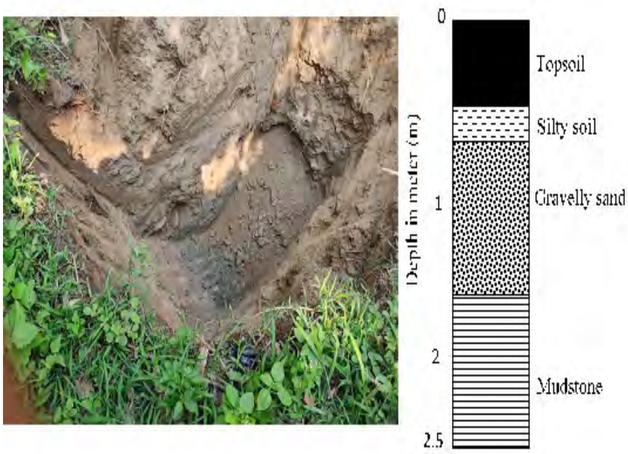

Fig. 16: Excavation of Pit (P7) (left) and litho-log (right) at Atrauli (GPS: 85.630264E, 27.116205N).

Groundwater Harvesting and Distribution System

The present study area has identified the development of shallow wells as a suitable method for initial water collection at the source (Fig. 18).

Both dug wells and sump wells are recommended for this area. Shallow wells especially dug wells, are considered the most appropriate water source in groundwater supply systems due to their cost-effectiveness and shorter construction periods. The relatively low yield of shallow wells makes them ideal for rural areas with minimal water consumption,

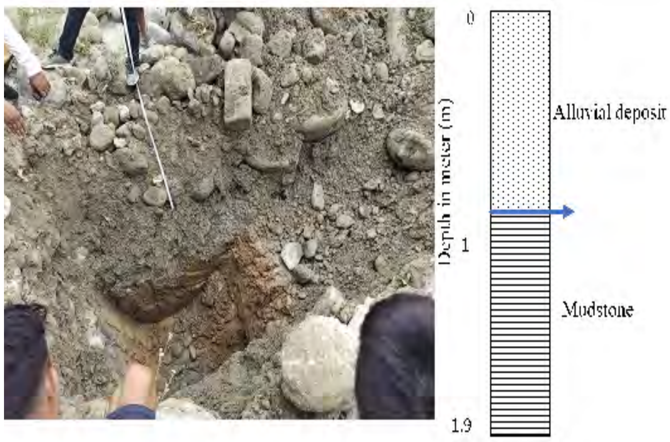

Fig. 17: Excavation of pit (P8) (left) and litho-log (right) at Atrauli (GPS: 85.630474 and latitude 27.115989).

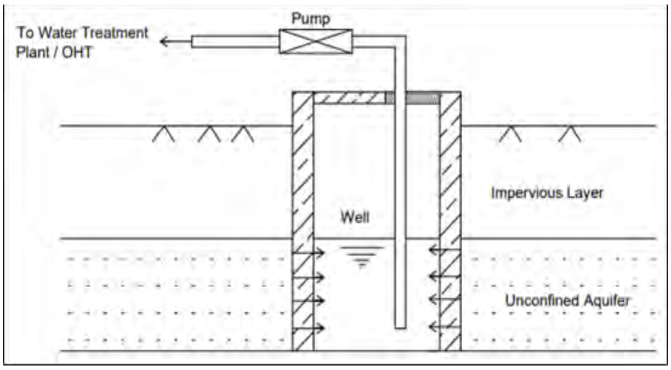

Fig. 18: Idealized schematic diagram of the shallow well as recommendation (Not to scale).

primarily for domestic purposes (Sharma, 1981). In the Atrauli area, it is recommended to utilize sump wells to tap the groundwater as an improved version of a shallow aquifer.

These sump wells are shallow wells constructed along the riverbed or directly at the river channel to collect water seeping through their bottoms (Fig. 19). The water collected in the shallow wells like dug wells and sump wells can initially be pumped to a water treatment plant for physical and chemical treatment before being distributed to the community across all groundwater sources under study. The treated water will then be pumped to a water storage tank before being supplied to the community.

A water reservoir tank (RVT) is another essential component of the water supply system, required to store water to meet the hourly fluctuation of consumers' water demand and ensure peak flow in the distribution network. RVTs are constructed at ground level on hilltops higher than the service area. In areas with flat topography, the tanks may be elevated above the ground on towers to provide adequate water pressure, known as overhead tanks (OHT). For all sources in the study area, an overhead tank (OHT) is recommended to store the water. Water can be pumped from the source (dug well or sump well for this case) and stored in the OHT, from where it can be distributed to consumers through the distribution system. Distribution lines are another crucial component of the water supply system, responsible for carrying water from the storage tank to its end-use points, such as household taps, yard connection taps, or public stand posts. The distribution pipelines should consist of a main pipeline connected to the RVT, sub-main pipes connected to the main pipeline, and service/branch pipes connected to the sub-main pipes for distribution to households. Based on the available discharge and water demand, yard connections and public stand posts are recommended for the present investigated area. Efficient distribution requires water to reach its end-use points with the required flow rate and adequate pressure in the piping system. There are three main types of distribution systems commonly adopted these days.

(a) Gravity-Fed Distribution: Water flows in the distribution pipeline due to gravity, eliminating the need for pumping. This system is highly reliable and cost-effective.

(b) Pumping System: Water is supplied through continuous pumping in this type of system.

(c) Dual or Combined System: This system utilizes both gravity and pumping systems for water distribution.

In the case of all our study areas, a Dual system, i.e., pumping (from shallow well to water treatment plant and then to OHT) and gravity-fed distribution (OHT to stand post through distribution pipelines) is necessary as per the topography of the source location and service area. The recommended groundwater supply system is shown in Fig. 20.

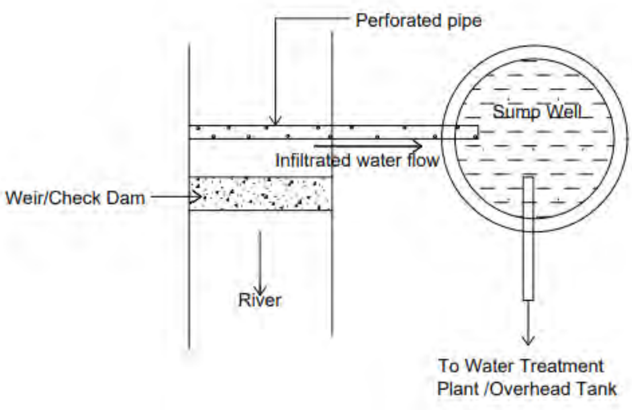

Fig. 19: A typical schematic diagram showing the plan for a sump well development (Not to scale).

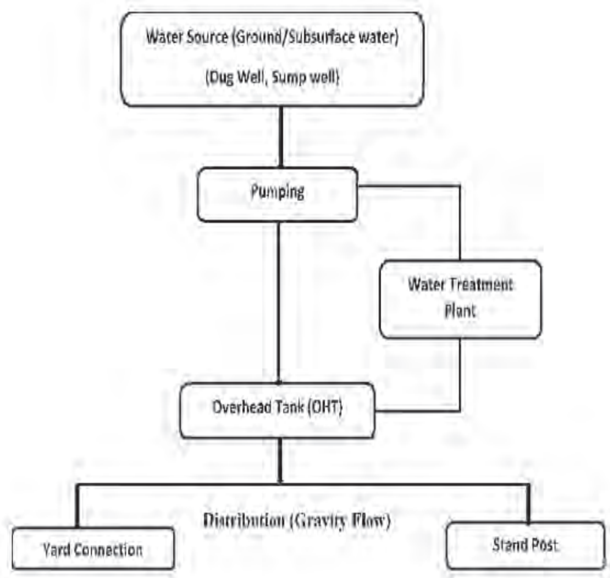

Fig.20: Recommended groundwater supply system components in the study area.

DISCUSSIONS AND CONCLUSIONS

The present study is targeted to assess the source of water from the shallow depth in the Hariwan municipality. Both geological as well as hydrogeological investigation was carried out on the paleo-river channels, active river channels as well areas near the riverbanks. The areas of water scarcity were identified based on well-inventory mapping followed by the questionnaire surveys on the communities. The possible sources of groundwater were investigated based on the geological as well as hydrogeological knowledge of the experts. It is a preliminary type of study to assess the location of groundwater, especially the shallow aquifer.

Detail aerial mapping, geophysical investigation for sub-surface information, and deep drillings are not applied in this study. In the present work, four water scarcity areas were selected for the detailed study to prospect shallow-level groundwater. For direct observation of groundwater location and its discharge, several pits were constructed using an excavator that could dig to make a pit of desirable size up to a depth of five meters. After determining the depth to water level, type of aquifer, and discharge of water to the pits, an appropriate water distribution system was suggested based on site conditions and the location of settlements. The use of Single-phase submersible pumps (cost-effective for STWs) is considered the best for extracting water from the wells.

Altogether, four places were found as the main water scarcity region within the Hariwan Municipality. Geologically, all the studied areas lie in the immediate north of the Bhabar region, however, some parts of the study location lie in the boundary between the Bhabar and the Chure region. There is a distinct geological boundary to separate the Bhabar and the Chure region which is called the Main Frontal Thrust (MFT). The presence of such boundary was demarcated based on the topographical breakage, the appearance of inclined bed rocks, and fault breccias and slickensides. In a regional geological map, the concept of Lower, Middle, and Upper Siwalik is used in this study (Fig. 3). However, in the water scarcity region, further classification is made locally to understand the aquifer condition of the region. Two units like the Jungali Khola and Chor Khola Formations are distinguished by comparing the lithological similarity from different sections (Fig. 7).

As the first location of the study, the Dumrighari area of Hariwan-9 lies about 2 km north of the Bhabar zone. It is located immediately north of the MFT region. Geological units like the Jungli Khola Formation and the Chor Khola Formation are found in this region as hard rocks while the two levels of terraces are found as the Quaternary deposits in addition to recent deposits of rivers. The Jungli Khola Formation is composed of dominantly mudstone and shale with a minor proportion of sandstone and siltstone while the Chor Khola Formation consists of a dominantly salt-and-pepper type of sandstone with a lesser proportion of mudstone and shale. The source of water is found in two locations: one at the paleo-flood plain of the Hariwan Khola while the other at the up-hill section of the same river. The water in the first case is found about 3 m depth from the surface as an unconfined aquifer composed of gavel-rich porous material while in the second case, it is found at the interface between the colluvium soil and bed rocks of the Siwalik Group lying below it. There are other possibilities for finding such types of water sources based on the geological criteria and judgment of experts.

The second water scarcity zone was assessed in the Samari Bhanjyang area of Hariwan Municipality- It also lies at the foot of the Chure hills, immediately north of the Bhabar region crossing the MFT region. Locally, the region consists of the Jangli Khola unit from a geological perspective. In general, there is no groundwater till 4 m depth from the surface. Two pits developed in this area revealed that there are mudstone beds of the Chure region below the 4 m without any water seeps. This shows that there is no water horizon above the bed rocks and to get the water level, the depth of hard rock aquifer should be reached. However, there is one well near the Sano Dume Khola, where there is a water level about 3.5 m depth from the surface. This well lies at the paleo river channel of the Sano Dume Khola. Therefore, the region around this well (especially at the right bank of this river as the settlement is on this side) is proposed as a suitable site for groundwater tapping and harvesting. Similarly, an investigation was made around the Dume Khola section of the Samari Bhanjyang village. The groundwater level couldn't find till 4 m depth from the existing dry channel of this Dume Khola. It shows that deep borings are necessary for such regions. The third water scarcity zone was found in the Kothi Khola village of Hariwan Municipality-1. It geologically lies in the foothills of the Siwalik region and the rocks found in this area can be mapped under the Jangli Khola Formation and the Chor Khola Formation. In the paleo-flood plain of Kothi Khola, at the right bank side, groundwater is found at a depth of 2.5 m from the surface. The discharge of water is satisfactory in this region. Water bearing horizon is composed of poorly graded gravel with admixtures of silt and sand in various proportions and the aquifer is unconfined in nature. Therefore, this area is proposed as the groundwater harvesting site after detailed studies and investigation. The fourth site reported for water scarcity lies in Atrauli village of Hariwan Municipality-2. Geologically, this area also lies at the foothill of the Siwalik. The rock in this region dominantly consists of sandstone with a minor proportion of mudstone and shale. Two pits were developed at the banks of the Atrauli Khola where mudstone beds are found at a depth of 2 m from the surface. Further, another pit was constructed at the present channel of the Atrauli River, and the layer of mudstone (an impervious layer) is found at a depth of 2 m from the surface. Then the concept of water collection by blocking the running groundwater through the riverbed and the development of a sump well at the riverbank is proposed to fulfill the water demand in this area. It is considered one of the best conjunctive uses of groundwater (Sharma 1997).

Lifting of groundwater from the wells in a reservoir located at a certain height and distribution of water through gravity flow is proposed as the distribution system of the water to the communities. However, the tapping and harvesting of groundwater varies from site to site depending upon the site condition.

Previous studies show that there is a decreasing trend in the overall groundwater table in the Bhabar zone of Nepal. In the Siwalik region, most of the natural sources of water such as streams, sloughs, arroyos, rivers, etc. are either completely dried up or the water level decreases significantly during the winter season. This may be due to several reasons as many landslides lying immediately north of the Bhabar region due to activity of the Main Frontal Thrust which has diverted the water sources, high rate of deforestation, newly constructed roads through the region, and unscientific mining of construction materials without considering even the basic principles of mining and its severity on the environment. Therefore, the status of soil erosion and mass movement should be studied thoroughly to assess the stability condition of the hills and ultimately to conserve the water sources of the region. In this region under consideration, the water demand encompasses domestic usage along with various other applications like gardening and small-scale irrigation purposes. Abundance prevails during the monsoon season and persists for approximately two to three months thereafter. However, water scarcity becomes apparent during the remaining months, primarily attributed to natural factors, specifically the subsurface geology and the presence of unconsolidated materials i.e., the Bhabar region at the foothills of the Siwalik range. It is noteworthy that the present study was carried out during the pre-monsoon peak dry season and immediately after the monsoon season. The pit development and observation were carried out during the peak dry season. The following conclusions are made from the present study:

1. There is no water scarcity problem in the southern part of the Lakhandehi River watershed. The demand for water is easily fulfilled by tube wells, dug wells, and deep tube wells.
2. The major water-scarce areas are found in the northern part of the Lakhandehi Khola watershed. These areas are Dumrighari, Kothi Khola Gau, Samari Bhanjyang, and Atrauli of Hariwan Municipality. The main cause of water scarcity is the unavailability of groundwater at shallow depths. Deep tube wells might be the alternative source for water supply system in the area, however detail hydro-geological study should be carried out to ensure the sustainable and adequate discharge.
3. In Dumrighari, Samaribhanjyang, and Kothi Kholagau, new possible sites for shallow groundwater harvesting are found. Similarly, for the Atrauli areas, a source of groundwater from the adjacent riverbeds is recommended.
4. In the Atrauli area, the concept of developing sump wells by retaining the groundwater flow from the relatively shallow sections of the river channel is proposed.
5. Water lifting system to the elevated reservoir and distribution of water to the communities through gravity flow is proposed as the use of water in the region.

ACKNOWLEDGMENT

The present research is a part of a G-to-G project between the President Chure Terai Madhesh Conservation Development Board (PCTMCD) and the Central Department of Geology (CDG), Tribhuvan University on the title: Study of the uses of subsurface water Resources in Province 2 (Madesh province). Financial support was provided by the PCTMCD and technical and managerial part was supported by the CDG. We are grateful to these governmental organizations of Nepal. We highly acknowledge Prof. Dr. Dinesh Pathak, Dr. Ranjan Kumar Dahal, Dr. Kiran Paudyal, Dr. Susmita

Dhakal, Narayan Gopal Ghimire, Shrijana Shrestha, Susma Giri, and Pawan Kumar Acharya for their technical, administrative, and moral support.

REFERENCES

DoI., 1994. Re-assessment of the groundwater development strategy for irrigation in the Terai. Department of Irrigation Groundwater Resources Development Project, v. 3, 202 p.

Duba, D., 1982. Groundwater Resources in the Terai of Nepal. WECS, Singh Durbar, Kathmandu, Nepal, 125 p.

Neupane, A., and Paudyal, K., 2021. Lithological control on landslides in the Siwalik section of the Lakhandehi Khola watershed of Sarlahi district, south-eastern Nepal. Jour. Dev. Innov., (Karma Quest International, Canada), v. 5(2), 2021, pp. 44 – 65.

Pokhrel, G.S., 2019. Short critical note water wealth of Nepal. Jour. Nepal Geo. Soc., v. 58 (Sp. Issue), pp. 13-19.

Pradhan, U.M.S., Shrestha, R.B., KC, S., & Sharma, S.R., 2002. Geological map of petroleum exploration block 7, Malangawa, Central Nepal (Scale: 1: 250,000). Petroleum Exploration Promotion Project, Department of Mines and Geology, Kathmandu.

Pathak, D., 2016. Water availability and hydrogeological condition in the Siwalik foothill of east Nepal. Nepal Jour. Sci. Tech., v. 17(1), pp. 31-38.

Radojicic S., 1975. Nepal water resource availability: water supply and sanitation sector study, Kathmandu, Nepal. UNICEF, available at https://www.ircwash.org/sites/default/files/822-NP75.pdf.

Sah R.B., 1998. Lithostratigraphy of Nepalese Siwaliks: An appraisal for standardization. Journal of Nepal Geological Society, Vol. 18, pp. 217-226.

Sah R.B., Paudyal K.R., and Gurmaita H.N., 2002. Natural sources of arsenic poisoning in groundwater of Terai plain. Nepal. Journal of SAN, v. 4, pp.1-12.

Sharma, C.K., 1981. Ground Water Resources of Nepal. Publisher: Sangeeta Sharma, 23/281 Bishalnagar Kathmandu, Nepal, Second Edition, 162 p.

Sharma, C.K., 1995. Shallow (Phreatic) Aquifers of Nepal. Publisher: Sangeeta Sharma. 175 p.

Sharma, C.K., 1997. A Treatise on Water Resources of Nepal. Publisher: Sangeeta Sharma. 493 p.

Bulletin of Department of Geology, Tribhuvan University, Kathmandu, Nepal, vol. 24, 2023, pp. 15-28
DOI:https://doi.org/10.3126/bdg.v24i.68374

Study on Rock Characteristics for Assessing the Hydraulic Erodibility of Sandstones in the Manahari River Section, Sub-Himalaya, Central Nepal

Jit Bahadur Gurung, Naresh Kazi Tamrakar*
Central Department of Geology, Tribhuvan University, Kirtipur, Kathmandu

ABSTRACT

The long-term erosion of the bed rock is steered by the power of the stream of variable magnitude and frequency which would give us the idea about bed rock incision and its channel morphology. Large numbers of infrastructural development work such as roads, bridges are undergoing in the Manahari Area. Hence, hydraulic erosion of the rocks is always a topic of interest while carrying out these construction works. Therefore, the main aim of this study is to determine the hydraulic erodibility of the Siwalik rocks under the action of stream power. Erodibility of the rocks and the stream powers of the Manahari River were determined by extensive field survey and laboratory analysis of rock material properties. Rock mass strength, block particle size, discontinuity/inter-particle bond shear strength, the shape of materials units, and their orientation relative to the flow were assessed to determine erodibility of the rocks. The longitudinal and cross-sectional surveys were carried out to find out the hydraulic parameters to calculate the erosive power of the stream i.e., slope of the channel surface, hydraulic radius, and velocity. The erodibility index ranges from 22 to 198 on the basis of their rock mass properties whereas the stream power value ranges from 1 to 6 kW/m^2. The value of the stream power obtained at the bankfull condition at different flow time intervals i.e., 10, 25, 50, and 100 years ranges from 5 to 25 kW/m^2. With this range of stream power at different time interval flow, the Manahara River has the capacity to erode maximum of the sandstones present in the riverbed as all the values of the erodibility plot above the threshold line of erosion. However, the relation between the erodibility index and stream power at normal flow condition shows that the Siwalik sandstones of the study area are not erodible under the influence of the available stream power.

Keywords: Erodibility, Stream Power, sandstones, Hydraulic Erodibility Index, Siwalik

Received : 12 March 2023 **Accepted:** 5 September 2023

INTRODUCTION

“Erodibility” term here sketches the remarkable erosion of the rock that transpires when the rock is submitted to hydraulic erosive power or in other word when water moves over the surface of the rocks, it exerts forces that dislodge and transport rock particles, leading to erosion. The various rock mass properties such as intact rock strength, block size, discontinuous conditions, bedding orientation, and groundwater condition have a major influence on the erosion of bedrock (Whipple et al. 2000). Kristen (1982) and Annandale (1995) have proposed a semi-empirical model known as Erodibility index method (EIM) that is based on field observations of scour threshold in various earth materials and is used for measuring the erosion resistance of earth materials and to relate the critical stream power (Kirsten 1982; Annandale and Smith 2001; Annandale 2005).

The erosional process is triggered by physical and chemical weathering, which coherently decreases rock strength and enhances susceptibility to abrasion, expanding fractures along which blocks are removed by plucking and pulverizing rock into small fragments (Hancock et al. 2011; Bizzi and Lerner 2015). The erodibility of rock is influenced by many interrelated geologic factors including material properties of the rock itself, as well as characteristics of the rock mass, particularly structural and stratigraphic discontinuities which determine the overall integrity of the rock mass. The erodibility of earth materials is determined by plotting the erodibility Index for a given earth material and the magnitude of the stream power. To elucidate stream power, it uses various geo-morphic parameters such as hydraulic radius, slope of channel, Bank full width, area, and velocity of stream. The fluctuation of stream power causes the jointed rock to be jacked out followed by dislodgement and finally displacement from its parent rock. A log-log plot of the erodibility index (K_h) and the rate of energy dissipation (P) of various

*Corresponding author
Email: naresh.tamrakar@cdgl.tu.edu.np
(Naresh Kazi Tamrakar)

materials are related to the critical threshold that can trigger the erosion of material. In cases, where the stream power exceeds the threshold line or point then the material will scour. The erodibility of the bedrock is also influenced by the shape of the river longitudinal profiles (Duvall et al. 2004). Shobe et al. (2017) have found that there is a great influence of weathering in the erodibility of the channel morphology. Sparacino (2012) has observed weathering is the dominant cause for the bedrock erodibility variation but the range and dominant form is highly variable, depending on climate conditions and rock type. The erosion was more rapid in the sandstone channel than in the limestone channel. Abundant coarse sediment can inhibit fluvial incision by armoring channel beds (Cook et al. 2012). High sediment transport rates can be more important than thresholds of coarse sediment motion for setting channel slope and limiting bedrock incision (Small et al. 2015). Pells (2016) have concluded that the main factor that triggers the erosion is the geological factors such as orientation, persistence, spacing, and nature of rock defects including bedding partings, joints, foliation, and shears.

A large number of developmental works are being carried out in the Siwalik area and also will be carried out in the forthcoming time. Large numbers of road alignments and bridges are under construction and will be constructed in the future in the Manahari-Chainpur area (Fig. 1). Bedrock erosion can be a severe threat to the river infrastructures in the Manahari River section that is mainly composed of weak sedimentary rocks. Hence, there has occurred a concern about hydraulic erosion of bedrock on the channel and near bridge pier foundation. The main aim to account this study was to see if this river could be able to scour river bed bringing instability in the structures such as bridge and embankment.

GEOLOGICAL SETTING

The Siwalik Groups sediments were deposited in a basin in the Himalayas by a major river system in the between the Middle Miocene and the Early Pleistocene period. Four stratigraphic units were mapped in the study area namely, the Midland Group, the Lower Siwalik Subgroup, the Middle Siwalik Subgroup and, the Recent Alluvial Deposits. The Lower Siwalik and the Middle Siwalik are too

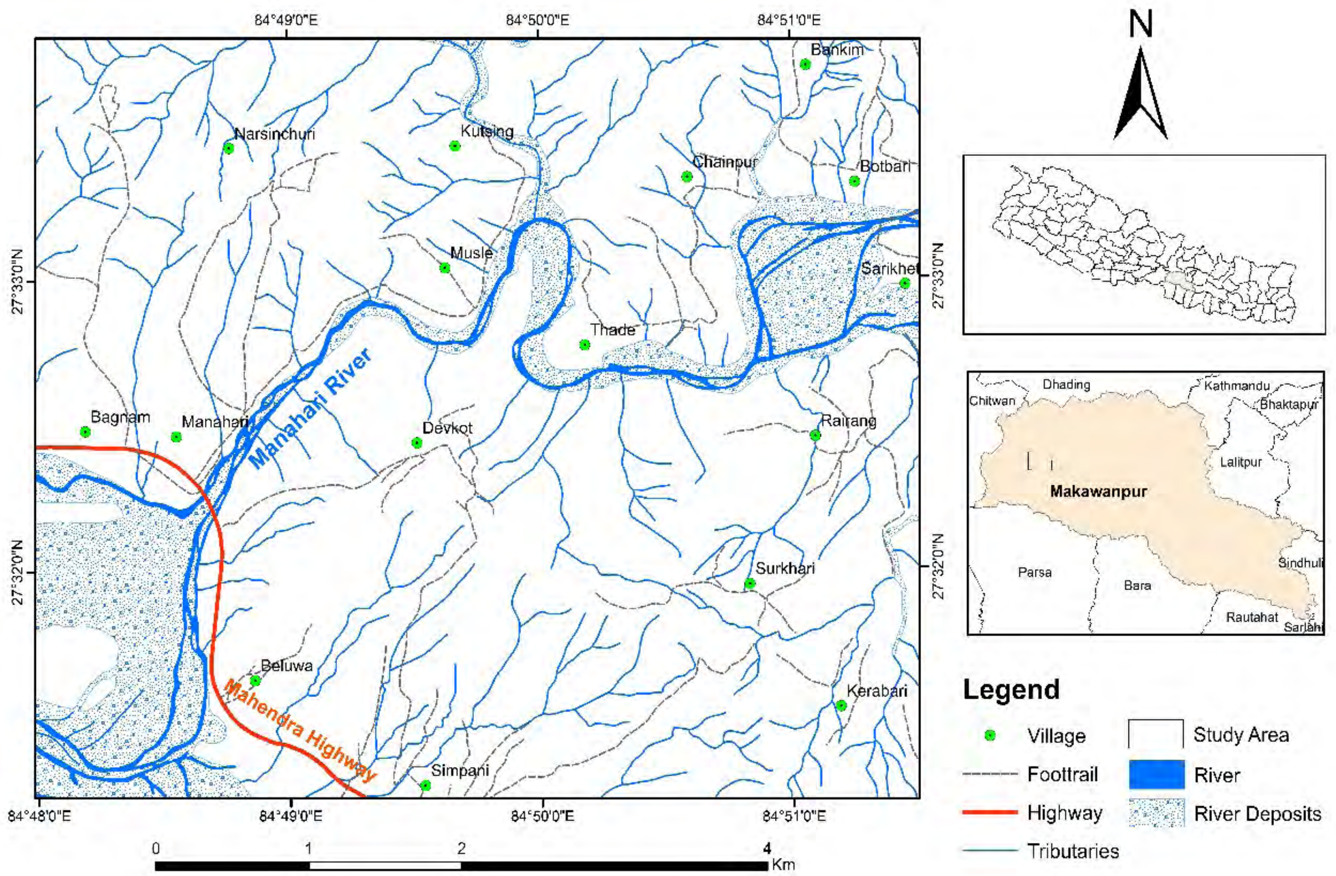

Fig. 1: Location Map of Study area

thick to assign them formation. Therefore, they have been considered Subgroup of the Siwalik Group, and the Subgroups nomenclature has been known for the Siwalik Group of India (Kumar et al. 2004; Kumar et al. 2007). The lithological changes between Siwaliks and Lesser Himalaya are due to the ongoing tectonic processes associated with the Himalayan orogeny, which is due to the collision between the Indian and Eurasian tectonic plates. The relief towards the southern part of Main Boundary Thrust (MBT) i.e., the Siwalik Hills is comparatively low with gentle slopes due to continuous erosion by rivers and other geological processes while that of the Lesser Himalaya which is towards the northern side of MBT has higher relief with steeper slopes and more rugged terrain because of more resistant to erosion.

The Midland Group mainly consists of light grey to greenish grey slate of the Benighat Slate which is observed on the Northern part of the study area (Fig. 2). The general lithological composition of the Lower Siwalik Subgroup is fine to medium-grained, greenish-grey to brown sandstones (Fig. 3), grey siltstones, and variegated mudstone and shale in some parts. The sandstone of the Lower Siwalik Subgroup becomes highly calcareous as the sequence goes up along with calcareous leaching. The grain size is coarse together with salt and pepper appearance brown sandstone having a very massive bed indicates the lithology of the Middle Siwalik Subgroup (Fig. 4). The coarse-grained micaceous sandstone is interbedded with purple to greyish siltstone which possesses a nodular weathering pattern and also with a thin bed of black mudstone in some sections. Pebbly sandstones were observed in the upper part of the Middle Siwalik Subgroup. Cross laminated sandstones of the Middle Siwalik Subgroup are also observed on the right bank of the Manahari River (Fig. 5). The Southern section represents the recent alluvium deposit, which is mainly comprised of loose alluvial materials along with gravel whose size ranges from, pebbles to boulders. The materials are mainly composed of quartzite, sandstone, granite, mudstones, etc. having sand, clay, and silt as supporting matrices. Stratigraphic section (Fig. 6) exposed along the Manahari River mainly comprises of the Lower and the Middle Siwalik Subgroups, and the Benighat Slate of the Lesser Himalaya (Shrestha 2019).

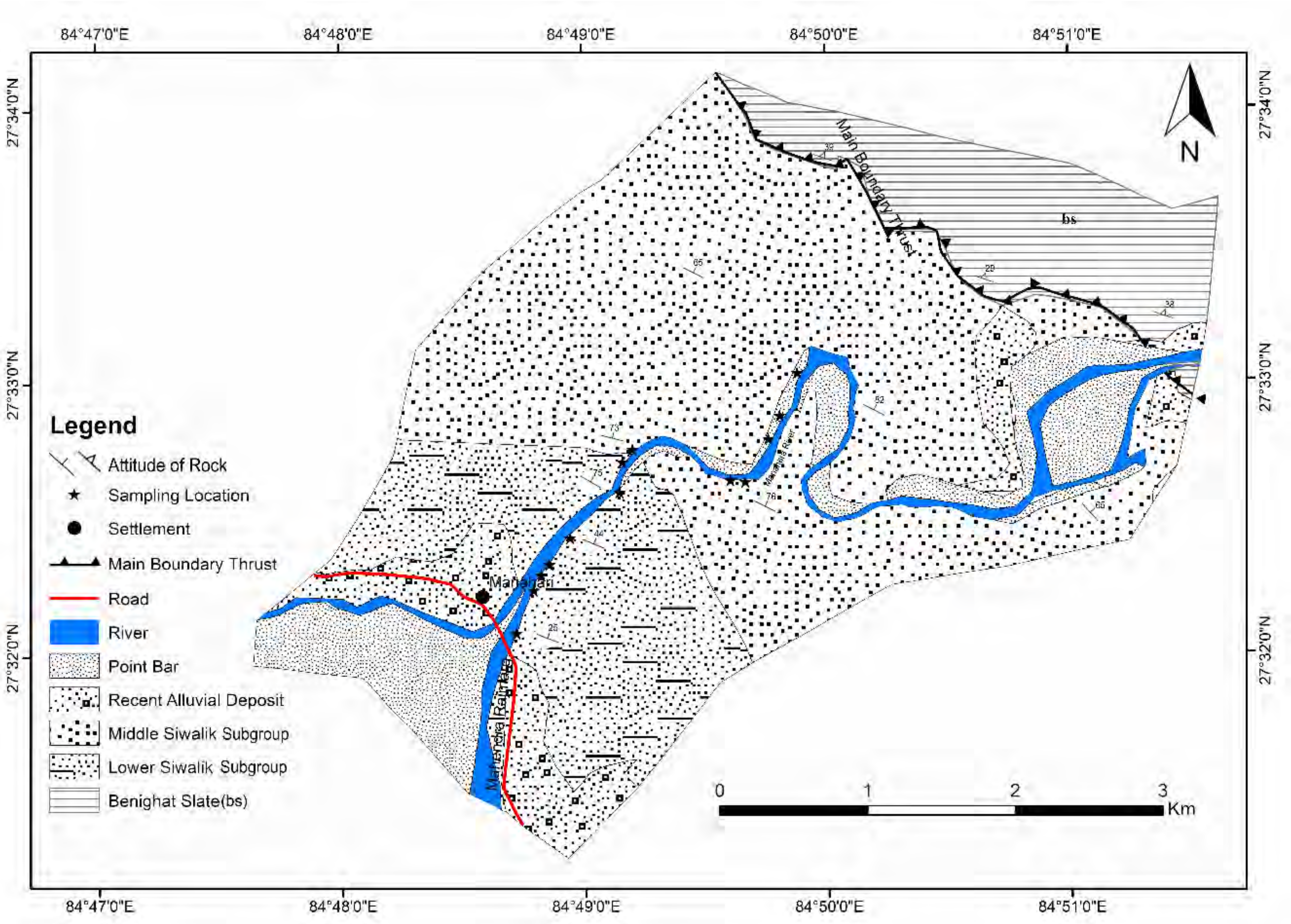

Fig. 2: Geological Map of the Study area

Fig. 3: Medium to thick bed of sandstone of the Lower Siwalik Subgroup on the left bank of the Manahari River

Fig. 4: Thick to massive bed of vertical sandstone interbedded with mudstone on the left bank of the Manahari River of the Middle Siwalik Subgroup

Fig. 5: Cross-laminated thick bed of sandstone of the Middle Siwalik Subgroup on the right bank of the Manahari River

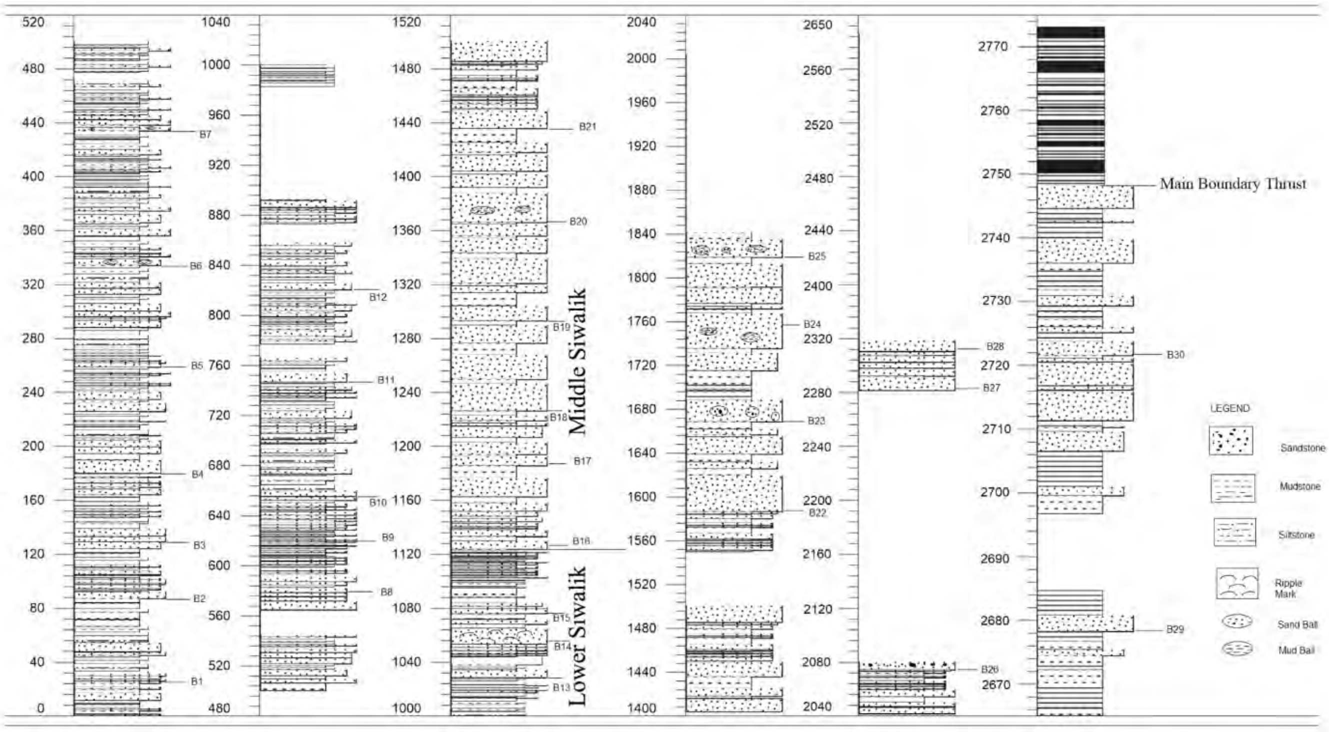

Fig. 6: Stratigraphic Section of the Lower and the Middle Siwalik Subgroups exposed along Manahari River (Shrestha 2019)

METHODOLOGY

Six locations were selected, of which three were from the Middle Siwalik area and three from the Lower Siwalik area to study erodibility and erosivity. Along with that, detailed information about rock type, lithology, orientations, weathering patterns, texture, and structures was also carried out in the fieldwork. Erodibility index parameters such as mass strength, joint roughness, and alternation, no. of Joints, joint orientation, river flow direction of every 13 locations were noted during the fieldwork. The total scores of the given parameter's values were calculated to find out the Erodibility index. The values for different parameters of erodibility index were assigned according to the criteria based on Kristen (1982). Therefore, the plot of the Erodibility Index and stream power as suggested by Annandale (1995) was followed to find out the erosivity of the sandstones.

Calculation of Erodibility Index (K_h)

The primary geological parameters like rock strength, block or particle size, discontinuity/inter-particle bond shear strength and shape of material units and their orientation relative to the flow were determined to figure out the Erodibility Index after Annandale (1995) as;

$$K_h = M_s. K_b. K_d. J_s \text{ .... } (1)$$

Where, K_h -Erodibility index, M_s -Mass strength, K_b-Particle or fragment size of the rock blocks, K_d -Inter-block strength, and J_s-Relative shape and orientation of blocks.

The mass strength number (M_s), represents the relative ability of the rock mass to resist fracture and failure, is a function of the rock density and the rock unconfined compressive strength (UCS).

The block size number (K_b), represents the relative size of rock blocks, was estimated from the ratio of rock quality designation (RQD) and the joint set number (J_n).

$$K_b = RQD/J_n \text{ .... } (2)$$

where, RQD= rock quality designation and J_n= Joint set number.

The shear strength number (K_d), represents the relative resistance offered by the rock discontinuities, was determined by the ratio of the joint roughness number (J_r) to the joint alteration number (J_a).

$$K_d = J_r/J_a \text{ .... } (3)$$

Where, J_r= joint roughness and J_a= joint surface alternation

The relative ground structure number (J_s), represents the ability of rock materials to resist erosion caused by the structure of the ground, was a function of the rock block shape and the least favorable joint orientation relative to the flow direction.

These four parameters of the erodibility index were taken to jointly represent the resistance of rock mass to the scour process of plucking.

Calculation of Stream Power (P)

Detail study on stream power parameters such as velocity, channel slope, the hydraulic radius was done in the Manahari River during the field study taking cross-section profile (Fig. 7) and longitudinal profile. Stream power (P) or erosive power is a parameter to ascertain the Hydraulic erodibility index. The erosive capacity of the Manahari River was determined from the equation derived by Bagnold (1966):

$$P = (\rho . g . Q . S_f)/w \quad \ldots\ldots\ldots (4)$$

Where, ρ = density of water (1000 kg/m^3), Q = discharge (m^3/s), g = acceleration due to gravity (9.8 m/s^2), S_f = slope, w = width of flow. The above obtained power is in W/m^2 and can be transferred to kW/m^2 after dividing by 10^3.

During high discharge exceeding the bank full discharge, the cross-sectional area, width of channel and velocity of flow increases, hence increasing the stream power. Density of water and slope are more or less constant whereas discharge may vary depending on velocity and cross-sectional area of stream.

Relation between Erodibility Index (K_h) and Stream Power (P)

Whether the rock will erode or not is represented by the correlation between stream power and the erodibility index of the materials by the below mentioned function after Annandale (1995).

$$P = K^{0.75} \ldots\ldots\ldots (5)$$

At the erodibility threshold, if, $P>K^{0.75}$ the erodibility threshold is exceeded, scouring is expected (Annandale 1995; Annandale and Smith 2001). While, if $P<K^{0.75}$ the erodibility threshold is not exceeded, and scouring is not favorable. Combining both, the Erodibility index and stream power one can estimate scour potential as proposed by Annandale (1995) and Annandale and Smith (2001). Altogether, 150 field observation were reviewed in order to develop a curve illustrating the threshold of erosion. Concurrently, a best fit line for the line separating the erosion and non-erosion cases was also drawn from same sets of data. The correlation defined by Stream power (P) and the Erodibility index (K_h), forms a continuous curve for the whole range of earth materials which encompasses from silt to hard intact rock.

RESULTS

Erodibility Index Parameters

Based on field investigation and some of them in laboratory, the different parameters were calculated for measuring Erodibility index. With a sole aim of studying bedrock erosion, 13 locations were selected for the hand specimen collection, including the rocks of the Lower Siwalik Subgroups and the Middle Siwalik Subgroups so as to calculate the erodibility indices. The parameters include the mass strength number (M_s), rock block size (K_b), joint shear strength (K_b), a block's shape and orientation relative to the flow direction of river or stream (J_s), and the joint spacings.

Fig. 7: Cross-sectional survey of the Manahari River to calculate the Hydraulic parameters

Mass strength number (M_s)

The rating for M_s was specified according to the UCS value of the sandstones which was obtained from the lab work. The highest rating of the M_s value has been assigned to locations 2,5,8,9 and 13 i.e., 17.7 as it has the greater UCS value, and the lowest rating i.e., 8.39 to location1,3,4,6,7,10,11 and 12 because of the lower UCS value (Table 1). The value of UCS shows that the rock sample collected from the study area falls under the hard rock category. Kristen (1982) has suggested a table regarding the UCS value of the rock in which the UCS value is assigned with a rock strength number. The strength of sandstones can also be calculated in the field by calculating the different parameters as suggested by Bieniawski (1989). The variability in the rock mass strength in bedrock channels is due to the interactions between weathering erosion, and hence erodibility of rock, across bedrock channels. Weathering is one of the most convincing mechanisms for reducing rock tensile strength and thereby reducing the critical stress necessary to alter rock which makes rock more prone to erosion by abrasion.

Particle/Block size number (K_b)

For the calculation of block size number, two basic parameters are required i.e., Rock Quality Designation (RQD) value and no. of joint sets of the desired location. The value of RQD ranges from 5-100 whereas the values of J_n ranges from 1-5. Consequently, the value of K_b ranges from 1-100. Knowing the joint sets, the corresponding J_n rating is determined by following the Kristen's (1982) table. The joint sets normally observed in the field were of 3 sets whereas in some locations 4 types of joint sets were also observed along with the maximum and minimum joint spacing of each joint set from every location. The RQD value was calculated in the laboratory from the hand sample and the value ranges from 55-62. The highest value of K_b was detained by location 7 i.e., 18.44 and the lowest value by location 12 i.e., 14.4 Table 1).

Inter-particle shear strength number (K_d)

The shear strength number (K_d) also uses the two parameters i.e., joint roughness no. (J_r) and joint alternation no. (J_a) The joint roughness number refers to the roughness condition of the facing walls of a discontinuity whereas the joint alternation number reflects the weathering condition of the joint face materials. The roughness of the joint surface along with its weathering pattern was noted down in the field and with their characteristics, and a number was assigned to each parameter for each location, and then inter particle shear strength number was deliberated adapting the table as suggested by Kristen (1982). For this parameter, the joint spacing also plays some role. The sampling location 10, K_d value was found to be 0.231 while for location 5,8 and 9, K_d value was 0.752 (Table 1).

Table 1: Table showing values of Rock mass strength number (M_S), Block size number (K_b) and Inter-particle shear strength number (K_d)

	Mass strength number (M_s)			Block size number (K_b)				Inter-particle shear strength number (K_d)		
Location	I_{s50} (MPa)	UCS (Mpa) = n $(I_{s50})^{0.6818}$	M_s	RQD	No. of Joint sets	J_n	K_b	J_r	J_a	K_d
DSL1	2.57	11.1	8.39	55	3	3.34	16.47	3	7.33	0.41
DSL2	4.07	13.76	17.7	61.1	4	4.09	14.94	2	7.33	0.27
DSL3	1.86	9.014	8.39	59.8	4	4.09	14.62	2	7.33	0.27
DSL4	3.44	11.44	8.39	57.3	3	3.34	17.16	2	7.33	0.27
DSL5	4.72	15.68	17.7	57	3	3.34	17.07	2	2.66	0.75
DSL6	4.20	12.8	8.39	56.2	3	3.34	16.83	2	7.33	0.27
DSL7	3.53	11.8	8.39	61.6	3	3.34	18.44	3	8.66	0.35
DSL8	4.26	14	17.7	58.5	3	3.34	17.51	2	2.66	0.75
DSL9	7.96	19.5	17.7	61.4	4	4.09	15.01	2	2.66	0.75
DSL10	1.64	7.94	8.39	61.3	3	3.34	18.35	2	8.66	0.23
DSL11	2.62	10.6	8.39	59.1	3	3.34	17.69	2	7.33	0.27
DSL12	3.50	12.2	8.39	58.9	4	4.09	14.40	2	7.33	0.27
DSL13	6.21	17.4	17.7	58	3	3.34	17.37	2	7.33	0.27

UCS = Uniaxial compressive strength, RQD = Rock quality designation, J_n = Joint set number, J_r = Joint roughness number, J_a = Joint alternation number

Table 2: Joint structure number (J_s)

Sample	Joints Sets	Joint Spacing Max. (m)	Joint Spacing Min. (m)	Average Joint Spacing (m)	y/x	r = (1: y/x)	Dip amount	Dip Direction	River Flow Direction	|DD-FD|	GS		Strike	Strike-FD	AD	ED
DSL_1	J_0	0.70	0.015	0.36	2.04	0.49	29	28	210	182	1.89	against	298	88	29.0	27.1
	J_1	0.66	0.014	0.34			51	154	210	56		along	64	146	34.6	32.7
	J_2	0.34	0.010	0.18			53	224	210	14		along	134	76	52.2	50.3
DSL2	J_0	2.10	0.020	1.06	3.31	0.30	47	33	210	177	1.89	against	303	93	47.0	45.1
	J_1	1.30	0.200	0.75			66	290	210	80		along	200	10	21.3	19.4
	J_2	1.25	0.030	0.64			45	210	210	0		along	120	90	45.0	43.1
	J_3	0.60	0.040	0.32			73	130	210	80		along	40	170	29.6	27.7
DSL3	J_0	1.10	0.030	0.57	3.71	0.27	61	15	210	195	1.15	against	285	75	60.2	59.0
	J_1	1.20	0.080	0.64			77	265	210	55		along	175	35	68.1	66.9
	J_2	0.73	0.090	0.41			44	156	210	54		along	66	144	29.6	28.4
	J_3	0.33	0.015	0.17			65	307	210	97		against	217	7	14.6	13.5
DSL4	J_0	0.80	0.020	0.41	2.18	0.46	61	25	210	185	1.15	against	295	85	60.9	59.8
	J_1	1.06	0.030	0.55			58	210	210	0		along	120	90	58.0	56.9
	J_2	0.49	0.010	0.25			74	310	210	100		against	220	10	31.2	30.0
DSL5	J_0	1.10	0.020	0.56	3.81	0.26	75	25	230	205	1.322	against	295	65	73.5	72.2
	J_1	0.35	0.010	0.18			86	285	230	55		along	195	35	83.0	81.7
	J_2	1.25	0.122	0.69			26	306	230	76		along	216	14	6.7	5.4
DSL6	J_0	0.68	0.020	0.35	1.20	0.84	72	22	236	214	1.322	against	292	56	68.6	67.3
	J_1	0.57	0.015	0.29			65	307	236	71		along	217	19	34.9	33.6
	J_2	0.56	0.015	0.29			14	224	236	12		along	134	102	13.7	12.4
DSL7	J_0	1.04	0.040	0.54	2.94	0.34	79	19	230	211	1.29	against	289	59	77.2	75.9
	J_1	2.06	0.050	1.06			20	117	230	113		against	27	203	8.1	6.8
	J_2	3.00	0.180	1.59			49	281	230	51		along	191	39	35.9	34.6
DSL8	J_0	0.95	0.020	0.49	2.02	0.50	81	39	245	206	1.29	against	309	64	80.0	78.7
	J_1	1.21	0.100	0.66			52	138	245	107		against	48	197	20.5	19.2
	J_2	0.61	0.040	0.33			17	305	245	60		along	215	30	8.7	7.4
DSL9	J_0	1.80	0.040	0.92	1.60	0.63	23	66	240	174	1.109	against	336	96	22.9	21.8
	J_1	1.40	0.050	0.73			78	207	240	33		along	117	123	75.8	74.7
	J_2	2.00	0.030	1.02			75	292	240	52		along	202	38	66.5	65.4
	J_3	1.20	0.070	0.64			77	101	240	139		against	11	229	73.0	71.9
DSL10	J_0	2.30	0.050	1.18	1.90	0.53	83	29	200	171	1.109	against	299	99	82.9	81.8
	J_1	1.70	0.020	0.86			28	217	200	17		along	127	73	27.0	25.8
	J_2	1.20	0.040	0.62			60	283	200	83		along	193	7	11.9	10.8
DSL11	J_0	2.80	0.050	1.43	1.49	0.67	78	33	200	167	2.049	against	303	103	77.7	75.6
	J_1	2.30	0.050	1.18			80	120	200	80		along	30	170	44.6	42.5
	J_2	3.40	0.090	1.75			9	306	200	106		against	216	16	2.5	0.5
DSL12	J_0	1.50	0.080	0.79	2.50	0.40	82	37	230	193	2.049	against	307	77	81.8	79.7
	J_1	0.80	0.020	0.41			84	110	230	120		against	20	210	78.1	76.1
	J_2	0.90	0.030	0.47			12	307	230	77		along	217	13	2.7	0.7
	J_3	2.00	0.050	1.03			75	216	230	14		along	126	104	74.6	72.5
DSL13	J_0	1.50	0.040	0.77	4.49	0.22	67	71	230	159	2.049	against	341	111	65.5	63.5
	J_1	3.00	0.050	1.53			62	119	230	111		against	29	201	34.0	31.9
	J_2	0.65	0.030	0.34			58	292	230	62		along	202	28	36.9	34.9

GS – Ground Slope, FD – Flow Direction, AD – Apparent Dip, ED – Effective Dip, DD – Dip Direction, r – ratio

Relative joint structure number (J_s)

The relative ground structure number (J_s) parameter describes the relationship between the block's shape and orientation relative to the direction of flow direction of the river or stream and it simplifies that whether the river flow can penetrate the discontinuities and dislocate the rock blocks. To find out the J_s value all we need is the effective dip of each joint sets of every location and joint spacing ratio (r). The value of J_s is expressed in terms of the relative spacing of the two joint sets, the dip angle, and the dip direction of the closer spaced set relative to the direction of flow of the river. The rating for the J_s is determined as a function of the dip and dip direction of the rock block as well as the joint spacing ratio. It's rating, as proposed by Kristen (1982), ranges from 0.37 to 1.5. The data obtained from the field showed us that the highest rating value was from location 10 i.e., 1.09 while the lowest value from location 1 i.e., 0.55 (Table 2).

Erodibility index (K_h)

The Erodibility index is the scalar product of the indices of its constituent parameters. The rock masses when subjected to the action of flowing water, causes the pressure fluctuation that progressively results in the jacks out the rock masses from its position of rest. When the rock mass is pulled out by the turbulence of water, then finally it will be displaced. Weathering is one of the most convincing mechanism for receding rock tensile strength and thereby lowering the critical stress necessary to alter rock, which makes rock more vulnerable to erosion (Sklar and Dietrich 2001).The Erodibility index (K_h) of the site 5 which falls in the Lower Siwalik Subgroup has the highest value of 197.59 whereas the site 4 which also falls in the Lower Siwalik Subgroup has the lowest value of Erodibility index (K_h) i.e., 22.1 (Table 3). Location 5 has the highest erodibility value because of very hard rock, along with unaltered rock with joint separation of less than 5 mm and the orientation of the bed is along the flow direction of the river. Higher joint sets, hard rock with less UCS value, the weathered rock having joint separation more than 25 mm and the orientation of bed is against the flow direction of the river, these are the characters possesses by location no. 4 that's why it has the lowest value of erodibility.

In addition to that, when we look at the Erodibility index value of the Lower Siwalik sandstone there is a remarkable fluctuation, ranging from the highest to the lowest value, whereas the value of Erodibility index of Middle Siwalik sandstone shows not that much fluctuation or can say have lower Erodibility index value compared to the Lower Siwalik sandstone value except at Location 9 which lies in between the boundary of the Middle Siwalik Subgroup and Lower Siwalik Subgroup. Being said that we are well aware that the Lower Siwalik Subgroup is lithologically composed of interbedding of siltstones and mudstones which will ultimately cause the mineral composition to mix up. It is a

Table 3: Hydraulic Erodibility index (K_h)

Location	Mass strength (M_s)	Block Size Number (K_b)	Shear Strength Number (K_d)	Relative Ground Structure (J_s)	Erodibility Index (K_h)
DSL_1	8.39	16.47	0.41	0.53	29.97
DSL_2	17.7	14.94	0.27	0.68	48.70
DSL_3	8.39	14.62	0.27	0.69	22.93
DSL_4	8.39	17.16	0.27	0.56	22.10
DSL_5	17.7	17.07	0.75	0.87	197.59
DSL_6	8.39	16.83	0.27	0.83	31.97
DSL_7	8.39	18.44	0.35	0.78	41.81
DSL_8	17.7	17.51	0.75	1.08	181.81
DSL_9	17.7	15.01	0.75	0.62	124.27
DSL_{10}	8.39	18.35	0.23	1.09	27.74
DSL_{11}	8.39	17.69	0.27	0.75	30.38
DSL_{12}	8.39	14.40	0.27	1.03	25.71
DSL_{13}	17.7	17.37	0.27	0.61	51.41

factual truth that, whenever there is an alternation in mineral composition there is a lowering of the strength of the rock which applies to the sandstone of the Lower Siwalik Subgroup. Handin et al. (1963) studied fine and coarse limestone and found that the fine-grain limestone is generally harder than the coarse-grain limestone. From the above statement it is clear that grain size is also one of the important factors for determining the mechanical properties of the rock. Hence, with the grain size greater than the sandstones of the Lower Siwalik Subgroup, the sandstones of the Middle Siwalik Subgroup have weak mechanical properties compared to that of the sandstones of the Lower Siwalik Subgroup which will alternatively impact the erodibility value and the variation in value of erodibility.

Stream Power Parameters

The morpho-hydraulic characteristics of the river such as channel slope, bank-full area (A_{bkf}), bank full depth (D_{bkf}), bank full width (W_{bkf}) also riverbank sediments were evaluated in order to get the knowledge about the stream power and the present condition of the river section in 6 different transects. The field studies have shown that the bank full discharge commonly approximates a flow event with a 1.4-1.6-year recurrence interval in the annual maximum series (Rosgen 1994; Annandale 1995). Rock erodibility may also vary within and across channel cross-sections (Small et al. 2015), and may play a significant role in setting channel geometry and gradient (Hancock et al. 2011). Table 4 shows the value of all these geomorphologic parameters.

- **Velocity of stream (V)**

  Velocity of the stream is also a common simplification for the examination of streamflow which is generally downstream. Here, the calculations were made on the basis of the average velocity at a given cross section because the actual velocities may vary markedly from top to bottom, side to side, and in direction varying with time and space. The velocity of the stream was taken from six transects including both the Lower Siwalik Subgroup section and the Middle Siwalik Subgroup section. The velocities of the Manahari River were determined in the upstream reach and in the downstream reach. Transect no. 6 has highest velocity of 7.79 m/s whereas transect no. 2 has lowest velocity of 3.95 m/s. Bringing together, the slope gradient and the hydraulic radius, the velocity of the stream was assessed.

- **Hydraulic radius (R)**

  For the Hydraulic radius (R_h), the cross-sectional survey was carried out for the geometrical and geomorphological parameters of the stream comprehending bank full width and height, width of flood prone width and bank materials. Transect no.5 has highest hydraulic radius i.e., 2.46 m and transect no. 2 has the lowest value of hydraulic radius i.e., 1.19 m. The area of bank full has increased in the upstream part of the Middle Siwalik Subgroup but as we move towards the transection zone between the Middle and the Lower Siwalik Subgroups there is decreasing trend in the bank full area. As we move down from the transection zone towards the Manahari Bazar area then again, the bank full area has shown the increasing trend which will subsequently increase or decrease the hydraulic radius. Hydraulic radius is directly proportional to its stream cross-sectional area of stream. Therefore, the more the hydraulic radius more the stream will feel free to flow which will initially cause more flow of water in the stream that means an increase in the stream power.

Table 4: Values of Morpho-Hydraulic Parameters

Site	Max. Bankfull Depth D_{bkf} (m)	Max. Bankfull width W_{bkf} (m)	Max. Bankfull area A (m^2)	Wetted Perimeter W_p (m)	Hydraulic radius R_h	Manning (n)	Stream slope S (m/m)	Velocity V (m/s)
1	1.98	50	99	53	1.83	0.04	0.033	6.74
2	1.24	61	76	49	1.19	0.04	0.020	4.00
3	1.41	58	82	37	1.35	0.04	0.023	4.57
4	1.51	49	74	32	1.42	0.04	0.023	4.77
5	2.46	81	200	55	2.32	0.04	0.019	5.68
6	2.23	88	197	60	2.13	0.04	0.036	7.80

- **Slope (S)**

  To determine the stream slope, longitudinal survey of 6 sections were done in terms of the width and nature of the channel of the river, with 3 sections in the Middle Siwalik Subgroup section and 3 in the Lower Siwalik Subgroup section. The ratio of the measured water level in upstream and downstream transects determines the sloping channel or the vertical drop of the stream bed from upstream to downstream in comparison with the adjacent floodplain features. Transect no. 6 has the highest slope gradient (tan θ) with the value of 0.036 and the lowest value of 0.019 for transect no. 5. In the end, there is not much a drastic change in the river slope of the Manahari River.

Stream Power (P)

The amount of energy that a stream has available for carrying materials such as rock, woody vegetation, and sediment is referred to as stream power. Water flowing in an open channel typically gains kinetic energy as it flows from a higher elevation to a lower elevation. The stream power here comes to be in a unit of W/m. Then, this stream power is converted into a unit stream power by dividing it by the bankfull width and we get values in W/m^2 which can be converted to kW/m^2 by dividing by 1000. The transect no. 6 has the highest stream power of 6.1 kW/m^2 while the lowest stream power is 0.974 kW/m^2 of the transect no. 2 (Table 5). The transect which has the greater bank full area (A_{bkf}) and bank full depth (D_{bkf}) and sometimes bank full width (W_{bkf}) also, usually have high stream power than the other transects with a smaller bank full area and bank full depth. For this reason, the stream power values fluctuate from different transect sections. The role of the slope is found to be not that significant for the stream power as we can conclude from the data of slope gradient that there is barely a fluctuation in the slope gradient of the channel slope. But, whenever the value of the channel slope has increased, we can see an increase in the velocity of the stream, which has been proved true from the relation between slope and velocity in transects no. 1 and 6.

Table 5: Stream Power of the six transects

Location	Siwalik Sub Group	Bankfull Area A_{bkf} (m^2)	Velocity V (m/s)	Slope S (m/m)	Density of water ƒ (Kg/m^3)	Acceleration due to gravity g (m/s^2)	Discharge Q (m^3/s)	Stream Power P (kW/m^2)
DSL1	Lower Siwalik	98.5	6.74	0.033	1000	9.8	663.89	4.34
DSL2	Lower Siwalik	76	4.1	0.02	1000	9.8	300.2	0.97
DSL3	Lower Siwalik	82	4.57	0.023	1000	9.8	374.74	1.46
DSL4	Middle Siwalik	74	4.77	0.023	1000	9.8	352.98	1.59
DSL5	Middle Siwalik	200	5.68	0.019	1000	9.8	1136.21	2.67
DSL6	Middle Siwalik	197	7.81	0.036	1000	9.8	1534.63	6.10

Table 6: Stream Power at different consecutive time intervals (Log Pearson III Method)

Location	Siwalik Sub Group	Stream Power at 10 years interval (kW/m^2)	Stream Power at 25 years interval (kW/m^2)	Stream Power at 50 years interval (kW/m^2)	Stream Power at 100 years interval (kW/m^2)	Threshold Stream Power (kW/m^2)
DSL1	Lower Siwalik	9.54	14.05	18.22	23.14	15.67
DSL2	Lower Siwalik	4.75	6.99	9.07	11.52	10.35
DSL3	Lower Siwalik	5.73	8.43	10.93	13.89	33.07
DSL4	Middle Siwalik	6.61	9.74	12.63	16.04	32.97
DSL5	Middle Siwalik	3.44	5.07	6.57	8.35	24.61
DSL6	Middle Siwalik	5.84	8.60	11.15	14.16	14.49

The power of the Manahari River at a different consecutive time is listed in Table 6. The consecutive time includes several time intervals i.e., 10, 25, 50, and 100 years. The discharge of the Manahari River at these intervals of time was calculated by using the Log Pearson III method with the data collected from the Department of Hydrology and Meteorology (DHM) and from that value of the discharge, the stream power was also calculated at the same time intervals.

And obviously, the discharge of the stream will increase in that interval of time which will ultimately trigger the power of the stream to be high as can be seen in Table 6. The normal stream power value ranges from 1 to 6 kW/m^2 but when we inspect the stream power value at different time interval periods in Table 6, the value ranges from 5 to 24 kW/m^2 which is more than 4 times greater than that of the value poses by normal stream power.

DISCUSSIONS

Hydraulic Erosion potential of the Siwalik bedrocks

The correlation between Stream power (P) and Erodibility index (K_h) represents an earth material's relative ability to resist erosion can, at the erosion threshold. The erosion Threshold parameter was obtained following Annandale's criteria of erodibility. The value above the dashed line indicates that the material is erodible whereas below that dashed line indicates the material is non-erodible.

The calculated value to the threshold line of scouring of the Lower Siwalik sandstone is about 10-55 kW/m^2 while for the Middle Siwalik sandstone is 10-40 kW/m^2. The calculated value of the present research gives the idea about the Middle Siwalik sandstone and the Lower Siwalik sandstone need greater stream power for the higher erodibility value and need low stream power for the low erodibility value of the sandstones. A similar result was also obtained from the analysis of the Hydraulic erodibility vs. Stream power in Fig. 8. The threshold line of scouring in the graphical representation is above from the samples of the Lower and the Middle Siwalik Subgroups. This also suggests that both the Siwalik Subgroup sandstones are rigid and need more stream power for the scouring. The Middle Siwalik sandstones are more likely to be softer than that of the Lower Siwalik sandstones in the present study. Both the Siwalik Subgroups seem to be equally resistible to the scouring from the stream power, achieved during the bankfull discharge of stream.

The result of the relation between Erodibility index and Stream power shows that some (mostly the Lower Siwalik sandstone) bed rocks of the Manahari River at the bankfull stage are not that favorable for erosion but few of the sandstones of the Lower and the Middle Siwalik Subgroup are near about the threshold to erosion under the action of stream power of the bankfull flow.

This result of the Hydraulic erodibility index (K_h) shown in Fig.8 is only valid for the normal flow of a stream having normal stream power but as river flow at different time intervals increases the value of the discharge will also increase which ultimately increases the stream power. As already mentioned, the stream power becomes four times more in different consecutive time intervals than in the normal stream power. In such conditions, the sandstones exposed in the Manahari River section will be in erodible condition which will definitely jeopardize the settlement area, infrastructures, and the ongoing developmental work being carried out.

Lithology versus erodibility

Erosion of bedrock by the action of water is itself a very complex method that was combined with various erosion processes. Why is the rock not favorable to erosion in the study area, various factors acting in this case. The first reason is the strength of the rock mass. As already discussed, the rocks are of hard type also the conditions of the discontinuities are also of very good conditions i.e., the weathering pattern of the rock is faintly or slightly while observing from the field condition. The spacing of the joints is also not that much (1-25 mm) and the continuity of the joint is also wide. Along with that, the dipping of most of the joint sets is along the flow direction of the river which is not a favorable condition for the erosion of bedrock. The depth of the bank full comparatively high, and it already mentioned in the above paragraph that, with greater depth, the flow will be contained within the channel bank causing the larger floodplain to decrease and as a result, the interaction between the channel bedrock and floodplain is reduced which automatically will decrease the incision of the bedrock. Besides that, the stream power is not that much enough to erode the rock type (sandstones) of the study area. Although, we can clearly see that there was the small scale to medium scale erosion of the mudstone and siltstone in many parts along the Manahari River section. Other than these factors, the probable reasons may be due to the mudrock that is interbedding with sandstones and

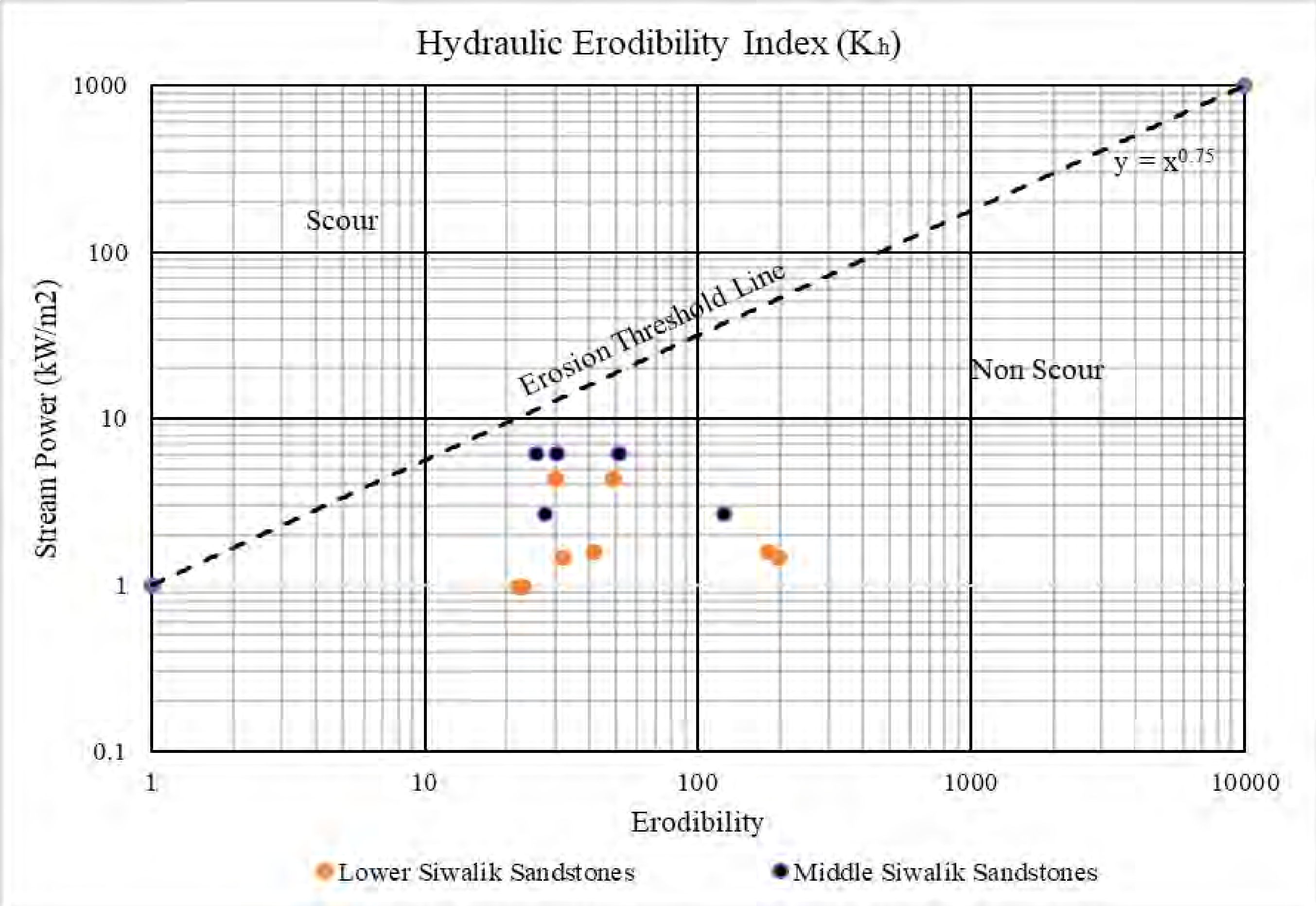

Fig. 8 Graphical representation showing relation between Hydraulic Erodibility Index (K_h) and Stream power (P) Annandale (1995)

whose erodibility is less than that of the interbedded sandstones are eroded by the stream power after which the sandstones bed are left with joints and may easily dislodged and eventually eroded. The same goes for the sandstones in hillslope, even if the sandstones are strong enough, once the mudrock interbed gets eroded away, the sandstones become unstable due to the void spaces and removal of underlying supports which later on fall and in due course erode away. In the case of hydraulic erosion of riverbeds, a similar situation arises and therefore erodibility of sandstones that we have calculated diminishes. When the erodibility diminishes, the plots on K_h vs. P lie above the curve and riverbed will be the potential for scour. The true intension of this research was to elucidating river channel stability, rather than linking with the study of tectonics along the Manahari River section.

CONCLUSIONS

- The erosive power of the Manahari River is not adequate for the erodibility of sandstones of both the Lower Siwalik Subgroup and the Middle Siwalik Subgroup. Sandstones can be eroded either due to increased level of stream power or due to diminish of erodibility by weathering and mass wasting of sandstones and associated lithology.
- The construction works for the road alignments and bridge can be carried out in the Manahari-Chainpur area in the present condition and in the near future without any obstruction. But this is only valid for the area with a large bed of sandstones.
- While, for the area with the lithology of shale, mudstones, and siltstones, necessary precautions should be taken while carrying out the developmental work in the Manahari-Chainpur road section along Manahari River.

ACKNOWLEDGEMENTS

This research is an outcome of the first author's MSc dissertation and the authors are thankful to the University Grants Commission (UGC) for funding this dissertation.

REFERENCES

Annandale. G.W., 1995. "Erodibility." Journal of Hydraulic Research, v. 33(4), pp. 471–494.

Annandale, G.W., 2005. Scour technology: Mechanics and engineering practice, 1st Ed., McGraw-Hill Professional, New York. 420p.

Annandale, G.W., and Smith, S., 2001. Calculation of Bridge Scour Using the Erodibility Index Method. Colorado Department of Transportation, Report no. CDOT-DTD-R-2000-9. 48p.

Bagnold, R.A., 1966. An approach to the sediment transport problem from general physics. US government printing office.

Bieniawski, Z.T., 1973. Engineering classification of jointed rock masses. Trans South Africa Institute Civil Engineering v. 15, pp. 335–344.

Bizzi, S. and Lerner, D.N., 2015. The use of stream power as an indicator of channel sensitivity to erosion and deposition processes. River Res. Appl., v. 31, pp. 16–27.

Cook, K.L., Turowski, J.M., and Hovius, N., 2012. A demonstration of the importance of bedload transport for fluvial bedrock erosion and knickpoint propagation: Earth Surf. Process. Landf., v. 38 (7), pp. 683–695.

Hancock, G.S., Small, E.E., and Wobus, C., 2011. Modeling the effects of weathering on bedrock-floored channel geometry: Jour. Geophy. Res., v. 116.

Handin, J., Hager Jr, R.V., Friedman, M., and Feather, J.N., 1963. Experimental deformation of sedimentary rocks under confining pressure: pore pressure tests. AAPG Bull., v. 47(5), pp. 717–755.

Kirsten, H.A.D., 1982. A classification system for excavation in natural materials, The Civil Engineer in South Africa. pp. 292-308.

Kumar, R., Sangode, S.J., and Ghosh, S.K., 2004. A multistory sandstone complex in the Himalayan Foreland Basin, NW Himalaya, India. Jour. Asian Earth Sci., v. 223(3), pp. 407–426.

Kumar, R., Suresh, N., Sangode, S.J., and Kumaravel, V., 2007. Evolution of the Quaternary alluvial fan system in the Himalayan foreland basin: Implications for tectonic and climatic decoupling. Quat. Int. v. 159, pp. 6–20.

Pells, S.E., 2016. Erosion of rock in spillways. Ph D Thesis, Kensington University of New South Wales. Physics, United States Geological Survey, Professional Paper 422-I, 37 p.

Rosgen, D.L., 1994. A classification of natural rivers. Catena, v. 22(3), pp. 169–199.

Shobe, C.M., Hancock, G.S., Eppes, M. C., and Small, E.E., 2017. Field evidence for the influence of weathering on rock erodibility and channel form in bedrock Rivers. Earth Surf. Process. Landf., v. 42, pp. 1997-2012. Doi: 10.1002/esp.4163

Shrestha, S., and Tamrakar, N.K., 2019. Mineralogical maturity and provenance of sandstones from Manahari River area, Sub-Himalaya, central Nepal. Unpublished M. Sc. Thesis submitted to Central Department of Geology, Tribhuvan University. 56p.

Sklar, L.S., and Dietrich, W.E., 2001. Sediment and rock strength controls on River incision into bedrock: Geology, v. 29 (12), pp. 1087–1090.

Small, E., Blom, T., Hancock, G.S., Hynek, B.M., and Wobus, C.W., 2015. Variability of rock erodibility in bedrock-floored stream channels based on abrasion mill experiments. Jour. Geophy. Res. Earth surf., v. 120 (8), pp. 1455–1469. https://doi.org/10.1002/2015JF003506

Sparacino, M.S., 2012. Variability of erodibility in bedrock-floored channels produced by differential weathering. Undergraduate Honors Thesis. 865p.

Whipple, K.., Hancock, G. ., and Anderson, R., 2000. River incision into bedrock: Mechanics and relative efficiency of plucking, abrasion and cavitation: Geol. Soc. America Bull., v. 112, pp. 490–503.

Bulletin of Department of Geology, Tribhuvan University, Kathmandu, Nepal, vol. 24, 2023, pp. 29-36
DOI:https://doi.org/10.3126/bdg.v24i.68375

Tectonic Stress Analysis of Shivnath-Salena Area, Using Stress Response Structure

Kabiraj Phuyal[1]* , Madhusudan Sapkota[1] , Kamala Kant Acharya[1] , Megh Raj Dhital[2]
1. Central Department of Geology, Tribhuvan University, Kirtipur, Kathmandu, Nepal
2. Department of Geology, Tri-Chandra Multiple Campus, Tribhuvan University, Kathmandu, Nepal

ABSTRACT

The geological mapping of the Shivnath-Salena area and structure analysis of the same area were conducted in the Lesser Himalayan sequence, Far West Nepal, unveiling the characteristics of kinematics and the associated stress field in the region. The area comprises of the Salena Formation and Chachura Formation. The Salena Formation is sandwiched between the Pachkora Thrust and Dudulakhan Thrust, and the Chachura Formation occurs between the North Dadeldhura Thrust and Pachkora Thrust. The Salena Formation is composed of light grey and white quartzite and black slates that are intensely deformed, with folds. The Malena Anticline and the Lamalek Syncline are the intraformational folds observed in the study area. Superimposed folding was also observed. The Chachura Formation comprises Paleocene to Late Eocene green sandstone, grey and purple shale, and approximately 1 m thick grey fossiliferous limestone. This study interprets stress-response structures to show the tectonic stress field in the Salena Formation. Twenty-seven fault slip data (slickenside) were collected in the field and used to determine the stress regime by applying the stress inversion technique. The direction of the maximum principal stress axes is interpreted as NE-SW. The average value of the stress index R' is about 0.30, indicating an extensional tectonic stress regime in the study area. As σ1 is vertical, R = R' in the study area suggests normal faulting in an extensional regime.

Keywords: Structure, Slickenside, Stress, Extensional, Tectonic.

Received : 12 April 2023 **Accepted:** 18 October 2023

INTRODUCTION

The Earth's processes are dynamic, and lithospheric movement continues to form divergent, convergent, and transverse tectonic plates. The collision between these tectonic plates results in fracture formations and reactivation, combining the driving pressure ratio (R'), stress ratio (R) and regional field stress (far-field stress). The superposition of many small strain increments is the product of continuous deformation. Under a specific stress level, the stress response structure demonstrates how strain increases in diverse directions and to varying degrees Slickensides are smoothly polished lineations that typically form within rocks along shear cracks and fault surfaces. They are assumed to record slide motion and mechanical abrasion that occurs during faulting (Ortega-Arroyo and Pec 2020; Tjia 1964). The slickenside data can ascertain the stress on the faulting plane and slip on the bedding plane faults on the flolding regimes (Michael 1984). The general agreement is that the collision of continents/plates formed the Himalayan fold-thrust belt (Argand 1924; Klootwijk 1984). The Indian plate and Eurasuan plate collided about 55 Ma (Klootwijk 1984) forming the Himalayan range of 2400 km long. The collision of the two continental plate and continuous convergence (post collisional deformation relults in mega thrusting and folding in the Himalaya. The Himalyan range will be subdicided into Sub-Himalayas, Lower (Lesser) Himalayas, Higjer Himalayas and Tibetan Himalayas (Gansser 1964). The study focused on the severely folded, thrusting, and deformed Lesser Himalaya in Far West Nepal. The ongoing convergence (Gansser 1964; Windley 1996),

The study area is located in the Baitadi District of the Far Western Nepal between latitudes 29°24′0″ to N 29°30′0″ and longitudes 80°32′0″ to 80°32′0″ (Figure 1). The area is situated about 840 km west of Kathmandu, and it is connected to other parts of the country through the Mahakali Highway, running north-south and joining with the East-West Highway.The study area belongs to the complexly folded, thrusted, and deformed zone of the Lesser Himalaya. The fold-thrust belt consists of stratigraphical (Bashyal 1982, 1986; Dhital 2008, 2022) and structural (DeCelles et al. 2001) complex belt of predominantly Proterozoic sedimentary and

* Corresponding author:
Email: phuyalkabiraj@gmail.com (Kabiraj Phuyal)

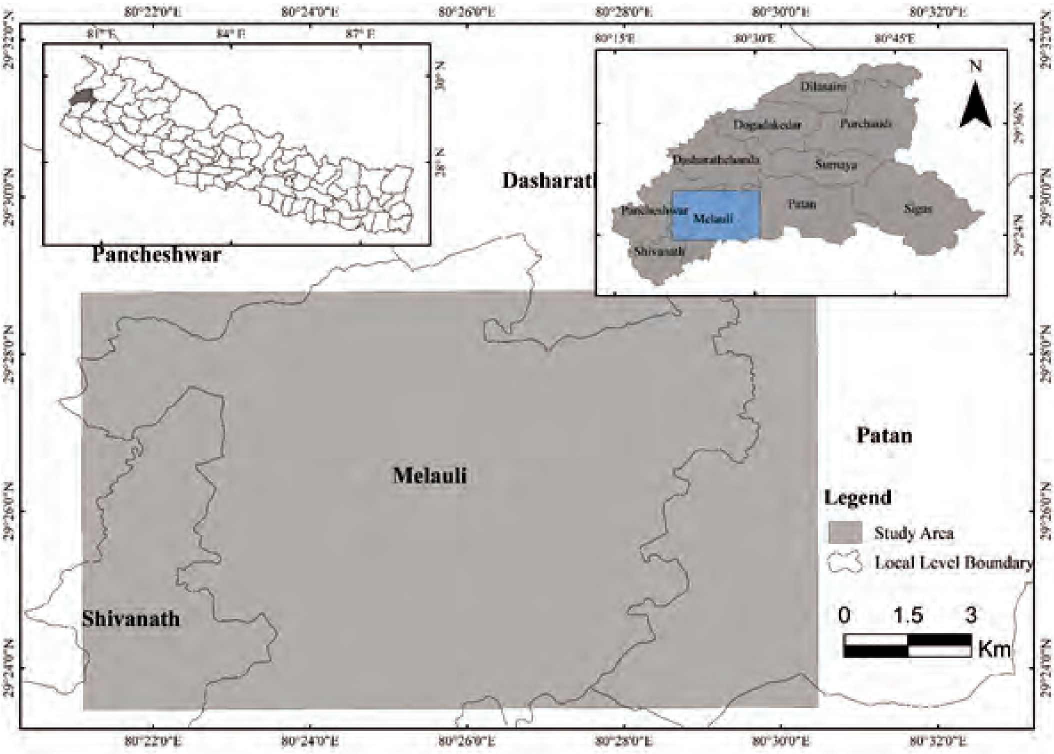

Fig. 1: Political map of Nepal and Baitadi district showing the study area.

metasedimentary rock sequences (Bashyal 1986; Hagen 1969; Heim and Gansser 1939; Khan 1969; Thapa 1977; Upreti 1999).

This paper's key objectives are to present the findings from recent structural and paleostress analyses using the slip data observed in the folded and thrusted zone of Far West Nepal. This part of the Lesser Himalaya has received limited study in the past. The paper aims to contribute to the understanding of the geological characteristics of the region by presenting the paleostress analysis findings.

In the research area, significant slip directions and gently to moderately plunging slickensides and lineations were exposed. Slickenside data are utilized to determine the stress regime that led to the formation and reactivation of these fractures and faults. Paleostress was calculated using fault slip data, including fault plane orientations and slide directions, collected in the field. The paleostress tensors were generated by using a stress inversion technique following a geological field investigation was carried out in the study region.

According to the relative scale of the intermediate axis, which is determined by the stress ratio R, the stress regime is divided into three categories: extensive/pure/compressive strike-slip, radial/pure/strike-slip extensive, and strike-slip/pure/radial compressive. (Delvaux et al. 1995). Fault plane and slip line orientations are used to compute the four parameters of the reduced stress tensor, and they are; the principal stress axes σ1 (maximum compression), σ2 (intermediate compression), σ3 (minimum compression), and the ratio of principal stress differences $R = (\sigma2 - \sigma3)/(\sigma1 - \sigma3)$ (Angelier 1989).

METHODOLOGY

Several materials have been used to meet the objectives of the present research (Figure 2). The topographic map of Melauli (sheet no 2980 10B) is used in the field to make a comprehensive geological map. Research papers, journals, bulletins, and documents were collected from the Central Library (Tribhuvan University), the Department of Mines and Geology (DMG), Survey Department and other sources.

The fieldwork primarily focused on the preparation of the geological map and the identification of slickensides in the exposures. Traverses were conducted along rivers, valleys, ridges, gravel roads, and foot trails. In the field study, rock types were identified based on the color of the rock, grain size variation, composition, texture, fabrics, and mineralogical relations. Lithology was observed and recorded, and various structural features such as foliation plane, bedding plane, the fold axis's trend and dip , hinge trend and plunge, slickenside trend and plunge, and lineations were measured.

The measured slickenside trend and plunge data from the field, along with bed attitudes distinguishing

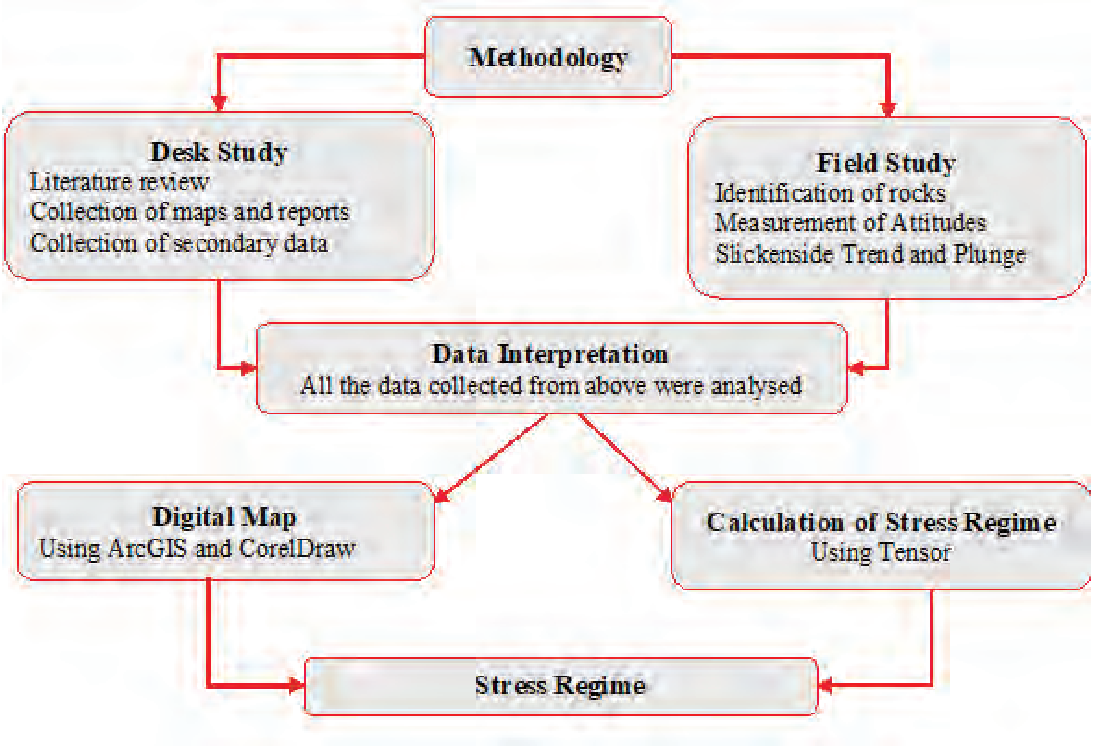

Fig. 2 : Flow chart represents the procedure used during the research.

footwall and hanging wall, are plotted in the Tensor software. The "TENSOR" process uses progressive rotation to maximize the outcomes using the graphic inversion method. It calculates the tensor around each axis by experimenting with different values of R. Fault categories are then ascertained by comparing the acquired value, or R, with the standard values.

GEOLOGICAL SETTING

The study region belongs to the Lesser Himalayan sequence of Baitadi district around Melauli, consisting of the Salena Formation and Chachura Formation (Dhital 2008; Phuyal 2022; Sapkota 2022), (Figure 3). The Pachkora Thrust (PT) separates the lithounits. The Salena Formation, which consists of quartzite and slates, is positioned between the north-dipping Dudilakhan Thrust (DT) and the south-dipping Pachkora Thrust. The Salena Formation in the area is intensely folded. The region has a complicated folding pattern with numerous fractures, local faults, tight to isoclinal folds, and quartz veins that point to a robust tectonic effect. The Lamalake Syncline and Malena Anticline are the major regional folds in the area, where numerous local and field-scale folds are observed. (Figure 3) in the area indicating the strong tectionic activities. This formation comprises of laminated, thinly - to thickly -bedded, fine-grained to crystalline quartzite interbedded with wavy to planar, weak to highly foliated, light grey to dark black slates. Well-preserved mud cracks and cross-lamination indicate the sedimentary origin. Slickensides and stretching lineations are predominantly observed in the beds of the Salena Formation. The complicated folding in the area can be described as superimposed folds due to the presence of recumbent to tight folds, lengthy axial traces, and tight hinges.

The beds regularly strike S 80° E, and the dip is 30°. In some sections, northeast of Salena, the rocks dip at angles ranging from 35° to 58° to the north. The light grey to green slate is intensely deformed with a pencil cleavage structure. A few small magnetite bands are traced in this section. Similarly, in the southern section of Salena, white quartzite with black slate is continuously interbedded. This region is also profoundly folded and deformed, with dips averaging between 15° and 70° in the northwest and southwest directions.

Along the road cut from Lamalek to Melauli, a sharp fault exposes the Tertiary rocks consisting of red-purple shale transitioning to grey shale, light grey and white quartzite, sandstone in green color, and ferruginous quartzite of the Chachura Formation. The Paleocene and Eocene Chachura Formation represents an interesting section of the Lesser Himalaya.

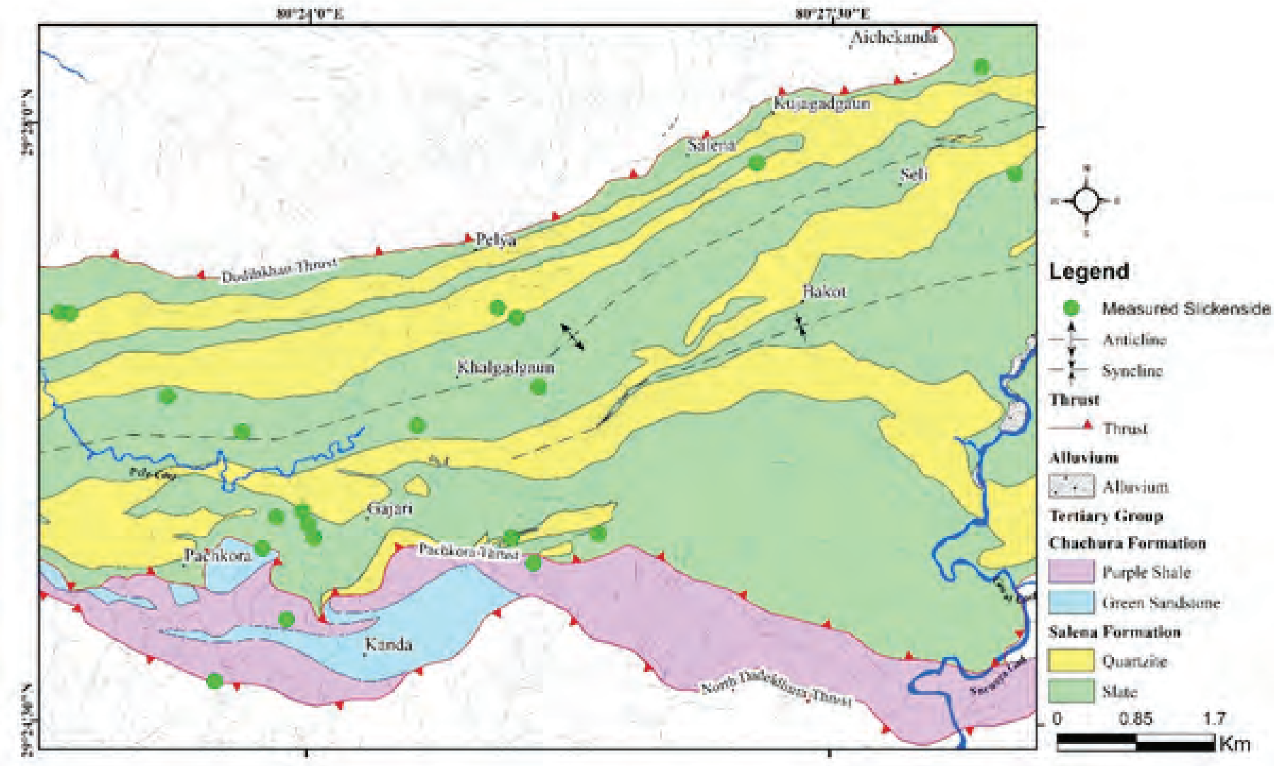

Fig. 3: Geological Map of Study area showing lithology distribution and location of measured Slickenside.

the Tertiary Group is situated between the north-dipping Pachkora Thrust and the south-dipping North Dadeldhura Thrust with overturned sequences. This zone is the Allochthonous one of the Lesser Himalaya (Dhital 2015). The sequence consists of interbed of red and grey fragile mudstone and shale with grey-green greywacke sandstone and subordinates light grey thinly bedded and compacted limestone consisting of lenticular Nummulites (Dhital 2008; Sapkota 2022). The slickenside and stretching lineation are sparsely observed on the bed of green sandstone. The exposure shows an upward finning sequence indicating the deposition in the shallow marine environment. The new Melauli Bajar consists of fragile purple shale interbedded with green sandstone. About 100 m north of new Melauli Bajar, grey shale consists of Bivalvia fossils.

PALAEOSTRESS RECONSTRUCTION

The research area's thrusting and folding zone, which has significant slip directions and gentle to moderately plunging slickenside lineation, is utilized to determine the stress regime that led to the formation and reactivation of these fractures, folds and faults. Several folds are formed in the area, during the folding, slip often occurs on the plane between different lithologic or bedding units (Michael 1984). The slickenside formed on these bedding surfaces have the same information as slickensides on the true faults. Thus, it can be used in the stress inversion (Michael 1984).

Palaeostress was calculated using data on fault slip (fault plane orientations and slide directions) collected in the field (Figure 4). A extensive geological field investigation was conducted in the study area to collect the slip data (slickenside); and the palaeostress tensors were obtained by applying a stress inversion technique. Palaeostress was initially constructed by the Right Dihedron method developed by Angelier and Mechler (1977) as a graphical method for determining the range of possible orientations of o1 and G3 stress axes in fault analysis.

The orientation reference grid used in the Right Dihedron technique is pre-determined to show up as a rectangular grid on the stereonet in the Schmidt projection of the lower hemisphere. (Delvaux and Sperner 2003). The right Dihedron method has been used to conduct the plaeostress reconstruction along the Salena Shivnath area in the study area. The type of tnsor is represented by stress regime calculation (Delvaux et al. 1995; Delvaux et al. 1997).

The stress ratio R has not yet been estimated using the Right Dihedron approach: only the orientations of $\sigma1$, $\sigma2$, and $\sigma3$ have been studied previously. However, upon closer examination of the Right Dihedron counting nets, it becomes apparent that their patterns vary depending on whether the stress tensor is compressional, strike-slip, or extensional. To represent this pattern as a parameter function would provide an estimate of the stress ratio R.(Delvaux and Sperner 2003). Brittle structures such as slickensides can also be used as stress indicators. The inversion method is based on supposing that a) stress is uniform and never changing in space and time and b) the fault plane slip in the maximum direction of the applied shear stress (Bott 1959; Delvaux and Barth 2010; Etchecopar et al. 1981). For this. slickenside lineation is used for calculating movement between the footwall block and the hanging wall block (Ju et al. 2012).

The stress regime is classified into radial/pure/strike-slip extensive, extensive/pure/ compressive strike-slip, or strike-slip/pure/radial compressive, as a role of the relative scale of the intermediate axis, given by the stress ratio R (Delvaux et al. 1995). Fault plane and slip line orientations are used to compute the four parameters of the reduced stress tensor, and they are; the principal stress axes σ1 (maximum compression), σ2 (intermediate compression), σ3 (minimum compression), and the ratio of principal stress differences R = (σ2 - σ3)/(σl - σ3) (Angelier 1989). The vertical stress axes represent the stress regime; if σ1 is vertical, it is extensional, and if σ2 is vertical, it is strike-slip, and it is compressive if σ3 is vertical. Furthermore, the stress regime relates to the ratio of principal stress differences R (Ju et al. 2012).

Slip data (slickenside) were measured during the field observation, and paleostress was computed by applying a stress inversion technique to the slickenside measurements. Paleostress is calculated and displayed using Tensor software (Figure 5).

Fig. 4: Stress-response structures in the study area showing slickenside and thearrow line showing the direction.

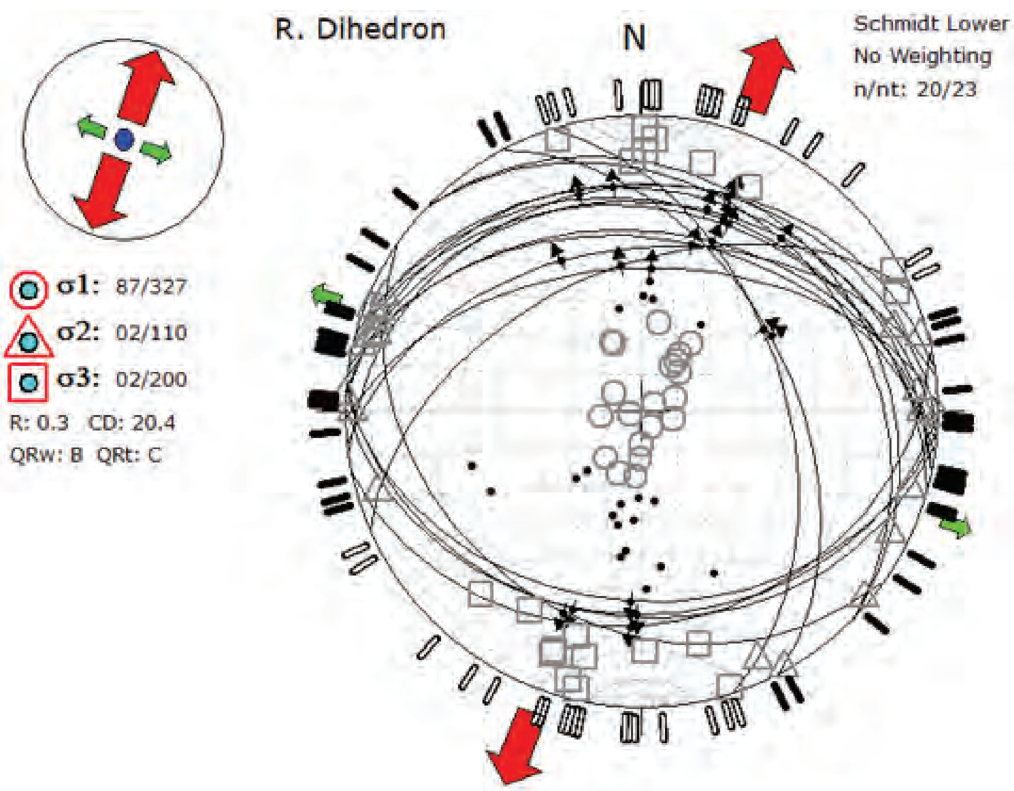

Fig. 5: Palaeostress tensor graphic solutions along the Melauli-Salena route. Slip lines are shown by a black dot with two arrows for strike-slip faulting, an inward direction arrow represents reverse faulting, and an outward direction arrow represents normal faulting. Extensional deviatoric stress is indicated by the outward arrow, while compressional deviatoric stress is indicated by the inward arrow.

DISCUSSION

The different tensor types are defined using stress regimes (Delvaux et al. 1995; Delvaux et al. 1997). Each of the Tensor's vertical regimes is either extensional or strike-slip depending on whether σ1 or σ2 are vertical; if σ3 is the vertical axis, the regime is compressive. The ratio of principal stress differences, R, is related to the stress regime (Figure 6).

faulting during folding in the NE-SW direction. The folds' axial traces also reveal the direction of stress, which is NE-SW.

CONCLUSION

The tectonic stress in Shivanath-Salena is reconstructed using stress-response structures (slickensides). Maximum (σ1) principal compressive

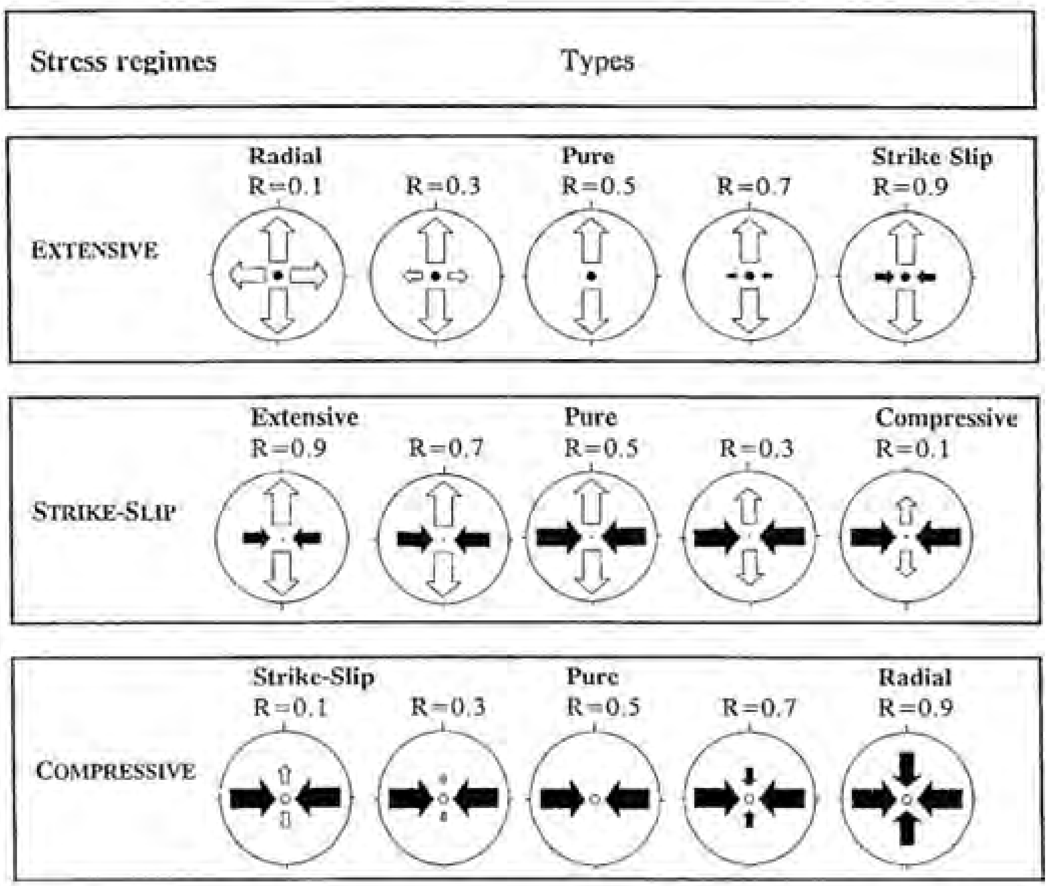

Fig. 6: Different stress regimes and their representation. In the function of the stress ratio R, arrows show the azimuth of the horizontal stress axes, with their length corresponding to the relative stress magnitude. Tensile deviatoric stress axes are represented by white outward arrows, whereas compressive deviatoric stress axes are indicated by black inward arrows. The solid circle for extensive regimes (a1 vertical), the dot for strike-slip regimes (a2 vertical), and the empty circie for compressive regimes (03 vertical) represent the vertical stress axis (Deivaux et al. 1995).

The Himalayan tectonic stress regime was investigated from the stress pattern of earthquakes. Such a study revealed that it is represented by NNE-SSW compressional stress in Nepal and India and NNW-SSE in Pakistan and Hindukush Himalaya (Ali et al. 2021). Paudyal et al. (2008) used the orientation of compressional and tensile stress axes using a fault plane, and they found NE-SW compressional stress in Eastern and Western Nepal.

In a recent study using slip data (slickensides), the stress index was calculated through the inversion method (Right Dihedron method). The study identified an extensional region supporting normal

stress occurs on average 87/327 (dip angle/strike), intermediate (σ2) principal compressive stress occurs on average 02/110 (dip angle/strike), and minimum (σ3) principal compressive stress occurs on average 02/200 (dip angle/strike). The stress index R in the study area averages 0.30, indicating an extensive stress regime in Shivanath-Salena.

Tectonic deformation can be better understood by reconstructing the tectonic stress field in the studied area. The analysis suggests extensive stress in the NE-SW direction, indicating the region's probable involvement in folding processes, demonstrated by bedding slip faults under extensive stress.

ACKNOWLEDGMENT

We would like to thank the Central Department of Geology (CDG), Tribhuvan University, for this research's steadfast support and supervision. We would also like to thank University Grant Commission for supporting the research financially. We would also like to thank Mr. Sijan Acharya, Mr. Sujan Bhattarai, and Mr. Bharat Raj Pant for their gracious support during the research.

REFERENCES

Ali, S.M., Abdelrahman, K., and Al-Otaibi, N., 2021. Tectonic stress regime and stress patterns from the inversion of earthquake focal mechanisms in NW Himalaya and surrounding regions. Jour. King Saud Univ. Sci., v. 33(2), pp. 101-351.

Angelier, J., 1989. From orientation to magnitudes in paleostress determinations using fault slip data. Journal of Structural Geology, v. 11(1-2), pp. 37-50.

Angelier, J., and Mechler, P., 1977. Sur une methode graphique de recherche des contraintes principales egalement utilisables en tectonique et en seismologie: la methode des diedres droits. Bull. Soc. Geol. France, v. 7(6), pp. 1309-1318.

Argand, E., 1924. La tectonique de IHAsie. 13th International Geological Congress: Brussels, v. 7, pp. 171-372.

Bashyal, R., 1982. Geological framework of far western Nepal. Him. Geol., Wadia Institute of Himalayan Geology, v. 12, pp. 40-50.

Bashyal, R., 1986. Geology of Lesser Himalaya, Far Western Nepal. Sci. Ter. Mem., v. 47, pp. 31-42.

Bott, M.H.P., 1959. The mechanics of oblique slip faulting. Geol. Mag., v. 96(2), pp. 109-117.

DeCelles, P.G., Robinson, D.M., Quade, J., Ojha, T., Garzione, C.N., Copeland, P., and Upreti, B.N., 2001. Stratigraphy, structure, and tectonic evolution of the Himalayan fold-thrust belt in western Nepal. Tectonics, v. 20(4), pp. 487-509.

Delvaux, D., and Barth, A., 2010. African stress pattern from formal inversion of focal mechanism data. Tectonophysics, v. 482(1-4), pp. 105-128.

Delvaux, D., Moeys, R., Stapel, G., Melnikov, A., and Ermikov, V., 1995. Palaeostress reconstructions and geodynamics of the Baikal region, Central Asia, Part I. Palaeozoic and Mesozoic pre-rift evolution. Tectonophysics, v. 252(1-4), pp. 61-101.

Delvaux, D., Moeys, R., Stapel, G., Petit, C., Levi, K., Miroshnichenko, A., Ruzhich, V., and San'kov, V., 1997. Paleostress reconstructions and geodynamics of the Baikal region, Central Asia, Part 2. Cenozoic rifting. Tectonophysics, v. 282(1), pp. 1-38.

Delvaux, D., and Sperner, B., 2003. New aspects of tectonic stress inversion with reference to the TENSOR program. Geol. Soc. London, Sp. Pub., v. 212(1), pp. 75-100.

Dhital, M.R., 2008. Lesser Himalayan Tertiary rocks in west Nepal and their extension in Kumaun, India. Jour. Nepal Geol. Soc., v. 37, pp. 11-24.

Dhital, M.R., 2015. Geology of the Nepal Himalaya: regional perspective of the classic collided orogen. Springer,

Dhital, M.R., 2022. Juxtaposition of Greater and Lesser Himalayan nappes in west Nepal: implications for delineating Main Central Thrust. Him. Geol., v. 43(1 B), pp. 231-240.

Etchecopar, A., Vasseur, G., and Daignieres, M., 1981. An inverse problem in microtectonics for the determination of stress tensors from fault striation analysis. Jour. Str. Geol., v. 3(1), pp. 51-65.

Gansser, A., 1964. Geology of the Himalayas. John Wiley and Sons, London. 289p.

Hagen, T., 1969. Report on the Geological survey of Nepal, Vol. 1: preliminary reconnaissance. Denkschriften der Schweizerischen Naturforschenden Gesellschaft Memoires de la Societe Helvetique des Sciences Naturelles, pp. 185.

Heim, A., and Gansser, A., 1939. Central Himalayan geological observations of the Swiss expedition. Zürich : Gebrüder Fretz, v. 1 246p.

Ju, W., Hou, G., Li, L., and Xiao, F., 2012. End Late Paleozoic tectonic stress field in the southern edge of Junggar Basin. Geoscience Frontiers,

v. 3(5), pp. 707-715.

Khan, R.H., 1969. Reconnaissance geological mapping of Far Western Nepal. Preliminary geological note in West-central part of Makahali Anchal. Department of mines and Geology, Kathmandu, unpublished. p. 16.

Klootwijk, C.T., 1984. A review of Indian Phanerozoic paleomagnetism: implications for the India-Asia collision. Tectonophysics, v. 105(1-4), pp. 331-353.

Michael, A.J., 1984. Determination of stress from slip data: faults and folds. Jour. Geophy. Res.: Sol. Earth, v. 89(B13), pp. 11517-11526.

Ortega-Arroyo, D., and Pec, M. 2020. A Closer look into Slickenlines: The link between surface roughness and microstructure. AGU Fall Meeting Abstracts, pp. MR010-0001.

Paudyal, H., Singh, H., Shanker, D., and Singh, V., 2008. Stress pattern in two seismogenic sources in Nepal-Himalaya and its vicinity. Acta Geophy., v. 56(2), pp. 313-323.

Phuyal, K., 2022. Geology and Structure of Shivnath-Salena, Baitadi, Far-West Nepal with special reference to Microstructure, Strain Analysis and Stress Regime. MSc. thesis, Tribhuvan University. Central Department of Geology, Kirtipur.

Sapkota, M., 2022. Lithostratigraphy, Petrography, Paleontology and Mineral Resources of the Shivnath-Melauli-Salena Area, Lesser Himalaya in Baitadi District, Sudurpaschim Province, Nepal. MSc. thesis, Tribhuvan University. Kirtipur, Kathmandu.

Thapa, D.B., 1977. Report on reconnaissance geological mapping of parts of Dandeldhura and Baitadi Districts.D. o. M. a. Geology Department of Mines and Geology, Lainchur, Kathmandu. p. 39.

Tjia, H., 1964. Slickensides and fault movements. Geo. Soc. Am. Bull., v. 75(7), pp. 683-686.

Upreti, B., 1999. An overview of the stratigraphy and tectonics of the Nepal Himalaya. Jour. Asian Earth Sci., v. 17(5-6), pp. 577-606.

Windley, B.F., 1996. The evolving continents. Oceanographic Lit. Rev., v. 8(43), pp. 785.

Bulletin of Department of Geology, Tribhuvan University, Kathmandu, Nepal, vol. 24, 2023, pp. 37-46
DOI:https://doi.org/10.3126/bdg.v24i.68376

A Comparison of Statistical Validity of In-Situ Hydraulic Conductivity Prediction Models of Rock Mass Inferred from Borehole Logs and Lugeon Test Data

Ujjwal Kharel* and Suman Panthee
Central Department of Geology, Tribhuvan University, Kirtipur, Nepal

ABSTRACT

In-situ hydraulic conductivity is a vital property in rock engineering for jointed rock mass. Understanding its correlation with rock mass parameters is crucial for water circulation. Therefore, a study was carried out to develop statistically significant empirical relationships between hydraulic conductivity and various rock mass parameters to estimate in-situ hydraulic conductivity from Lugeon test and various rock mass parameters obtained from borehole logs.

The study initially aimed to establish a correlation between hydraulic conductivity and Rock Quality Designation (RQD). However, the outcomes were unsatisfactory, prompting further research. Later, two more robust models were developed, namely the HC-model and modified HC-model. The HC-model incorporated four rock mass parameters, including Rock Quality Designation Index, Depth Index, Gouge Content Designation Index, and Lithology Permeability Index, achieving a maximum coefficient of determination (R^2) of 0.46. The modified HC-model included six parameters, encompassing fracture frequency and theoretical aperture, resulting in an improved R^2 of 0.69. Both models significantly outperformed RQD-alone predictions ($R^2 < 0.10$), highlighting the need for incorporating multiple rock mass parameters in predicting hydraulic conductivity due to a complex interplay of various factors. However, the effects of joint persistence and roughness are limiting in the present analysis.

Key words: Hydraulic conductivity, Rock mass parameters, Lugeon Test, HC-model, Modified HC-model.

Received : 14 May 2023 **Accepted:** 25 October 2023

INTRODUCTION

Hydraulic conductivity is a physical property which measures the ability of a material to transmit fluid through pore spaces and fractures in the presence of an applied hydraulic gradient (Darcy, 1856). Measurement and quantification of hydraulic conductivity and understanding of water flow inside jointed rock mass has a wide range of applications in mining and civil engineering. Many civil engineering tasks such as tunnel construction, dam construction, mine development, petroleum extraction work and slope stabilization require the estimation of hydraulic conductivity for fractured rock mass. Hydraulic conductivity data are crucial to estimate the grouting volume and grouting type to seal the subsurface joints, fracture and cavities to prevent underground water seepage and for foundation purpose.

It is commonly known that the fluid flow in rock masses mainly occurs in fractured and cavities associated with stratification, joints, tectonic activities, karst dissolution etc. Therefore, knowledge of exact distribution and rock mass parameters, such as dip, dip direction, aperture, spacing, frequency, roughness, infill, alteration, persistence, is essential for identifying as the key measures to describe the fluid flow.

There are several methods of quantifying the hydraulic conductivity of fine- and coarse-grained soil from constant head and falling head test method in field and laboratory. But the hydraulic conductivity of subsurface fractured rock mass can only be quantified more accurately from in-situ field tests known as water pressure test or Lugeon test or packer test or rock mass permeability test. This test was initially proposed by Maurice Lugeon, a Swiss geologist in 1933 which is later modified by Houlsby (1976). Lugeon's test (Lugeon 1933) is a constant head type test which is conducted in an isolated section of boreholes by injecting water at constant pressure into the rock mass through a perforated pipe bounded by the pneumatic packers and this discharge is measured using flow meter.

The calculation and interpretation of water pressure test data can also be done by the equations developed by Hvorslev (1951), United States Department of the Interior Bureau of Reclamation, USBR (1960)

*Corresponding Author
Email: ujjwal.kharel1234@gmail.com (Ujjwal Kharel)

and Moye (1967). Besides from field and laboratory method, several researchers have proposed the empirical equations for the estimation of hydraulic conductivity which were based on the concept that rock mass permeability decreases with depth (Snow 1970; Louis 1969 and Wei et al. 1995).

Determining of permeability values for rock formations is difficult than for soil formations due to factors like rock quality, joint density and fracture values. In-situ testing of permeability is often expensive and time-consuming. Therefore, it is necessary to estimate statistically significant relationship between apparent in-situ permeability with various rock mass parameters from boreholes. This approach will assist in the planning detailed field investigations during design and construction, contributing to time and cost efficiency. Ultimately, it will improve the overall effectiveness of detailed investigations for a specific site.

GEOLOGICAL SETTING OF THE STUDY AREA

Geologically, the study area lies on the Lesser Himalaya of Mid-Western Nepal. The major rock types observed in the exposures and drilled rock cores in the vicinity of the study area are grayish black slate to graphitic slate and light gray to dark gray dolomitic limestone and gray limestone (Fig.1). The rock in and around the vicinity of the investigation area can be divided into two lithological units viz. Dolomite unit and Slate unit (Lamsal et.al.,2021). The dolomite unit in the study area is dark gray to medium dark gray color, medium to thickly bedded Dolomitic limestone rock with the presence of few domed shaped stromatolites structures. The slate unit in the study area comprises dark black, thin to medium bedded slate to graphitic slate rock with slaty cleavage appearances. An alluvial fan was developed by Andheri Khola, which is morphologically flat and marshy.

METHODOLOGY

Data from two drill hole sites up to the depth of 80m were chosen to compare the statistical significance between in-situ hydraulic conductivity and various rock mass parameters in the form of HC-model and modified HC-model. The in-situ permeability of rock mass was performed and interpreted using modified Lugeon water Pressure tests as per the requirements and methods suggested by Houlsby (1976). Other relevant rock mass parameters like recovery, RQD index, at each depth of investigations were obtained from the core logs.

In present research, the in-situ permeability of rock mass was delineated by conducting water pressure test of rock using modified lugeon water pressure test methods as proposed by Houlsby (Eqn.1).

$$\text{Lugeon value} = \text{water intake (Litres/meter/min)} \times \frac{10\ (\text{bars})}{\text{Test presure (bars)}} \quad \text{......................... (Eqn.1)}$$

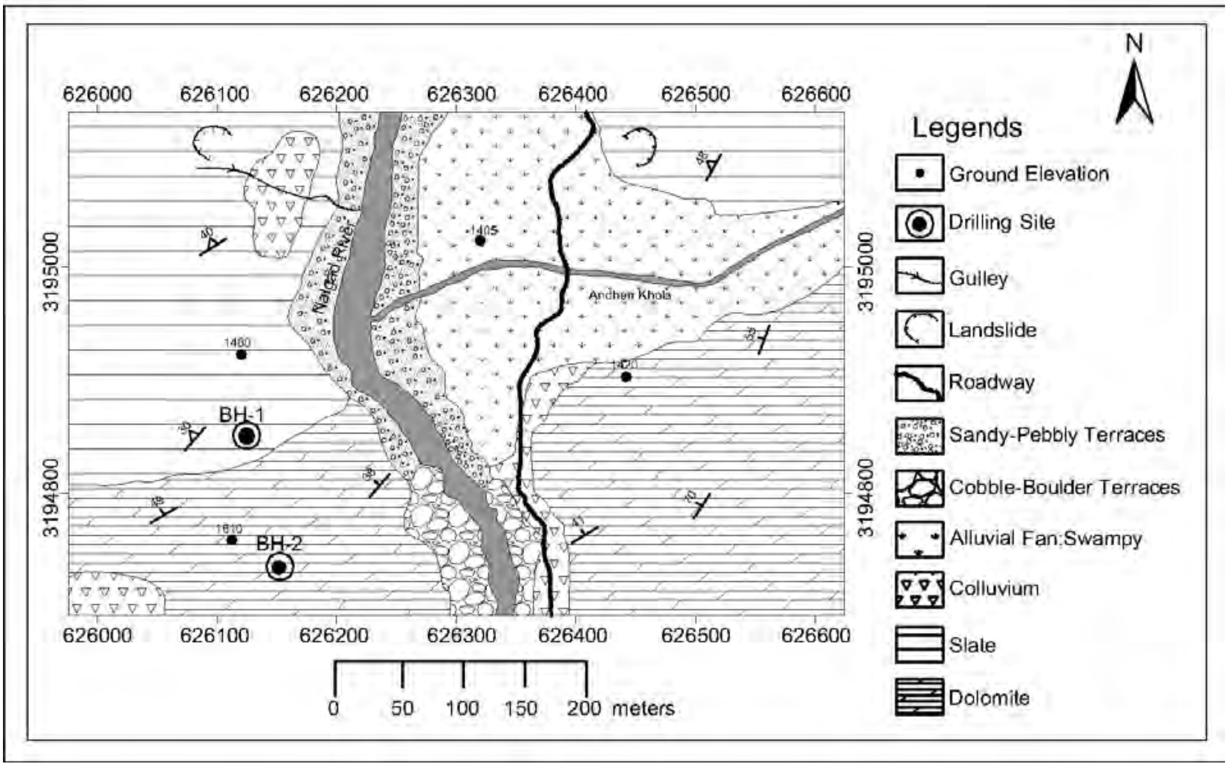

Fig. 1: Engineering geological map of the study area.

According to Fell et.al. (2005) the value of one Lugeon is equivalent to 1.3× 10^{-5} cm/sec. Zoorabadi (2023) had reported that the long ago established lugeon value of 1.3× 10^{-5} cm/sec only consists of one boundary conditions and does not cover all the potential boundary conditions encountered in the field.

a) The empirical HC-Model

The HC model is based on new rock mass classification system known as HC- System first proposed by Hsu et al. (2011) and consists of four component rock mass parameters: Rock Quality Designation (RQD), Depth Index (DI), Gouge Content Designation (GCD) and Lithology permeability index (LPI) which is calculated as the product of four parameters and can be given by the following equation 2.

$$HC = \left(1 - \frac{RQD}{100}\right)(DI)(1 - GCD)(LPI) \ldots \text{(Eqn.2)}$$

Hence using Eqn.2, the HC- value was calculated.

b) Modified HC-Model

The concept of modified HC-model for the prediction of rock mass hydraulic conductivity is a new approach in this research but was inspired from the HC-model of Hsu et al. (2011). Initially proposed HC-model consists of only four component rock mass parameters but this modified HC-model incorporates other two influential rock mass parameters like Fracture Frequency (FF) and theoretical aperture (e) which can be easily obtained from the borehole log data. Hence the modified HC model presented in this study consists of following six components parameters as: Rock Quality Designation (RQD), Depth Index (DI), Lithology permeability Index (LPI), Fracture Frequency (FF) and theoretical aperture (e) where the first four parameters are from HC-model of Hsu et al. (2011).The data set for parameter like Fracture Frequency was measured in the field from the core sample by simply counting the number of natural fractures and breaks identified per meter through the visual observation of the obtained core samples by neglecting mechanically induced fracture as far as possible. On the other hand, theoretical aperture (e) was obtained from the back calculation of aperture from cubic law of parallel plate analogy as shown in equation 3.

Since, we know the equation 3 from cubic law of parallel plate analogy (Snow 1969) as:

$$k = \frac{ge^2}{12V} \ldots\ldots\ldots\ldots\ldots\ldots\ldots\ldots \text{(Eqn.3)}$$

Where, the parenthesis k=isotropic coefficient of hydraulic conductivity, g=gravity, e=joint theoretical aperture, v=coefficient of kinematic viscosity of fluids.

$$\text{or, } e = \sqrt{\frac{12kv}{g}} \qquad \text{[Rearranging Eqn.3]}$$

$$\text{or,} e = \sqrt{\frac{12 \times 1.307 \times 10^{-6} (m^2/s) \times k(m/s)}{9.8\ (m/s^2)}}$$

; kinematic viscosity of water(v)=1.307× 10^{-6} m^2/s

or, $e = 1.265 \times 10^{-3} \sqrt{k}$; units in m……..(Eqn.4).

Hence, on the basis of aforementioned six parameters the new rock mass classification system was developed called as "modified HC-system" and can be calculated as;

Modified HC- value=

$$\left(1 - \frac{RQD}{100}\right)(DI)(1 - GCD)(LPI)(FF)(e) \ldots \text{(Eqn.5)}$$

RESULTS

The borehole logs and packer (Lugeon) test data obtained from field were carefully processed and analyzed to obtain various results which were discussed in brief in this section. Altogether 80 Lugeon test data performed in 40 test section of 2 drill holes site, in the discontinuous dolomite and slate rock unit were reviewed. The obtained value of hydraulic conductivity from water pressure test on field ranges on average from a minimum of 4LU (5.20× 10^{-5}cm/sec) to a maximum of 91LU (1.18×10^{-3}cm/sec) for both first cycle test and second cycle test carried out at same section of boreholes. The majority of flow patterns obtained were turbulent flow. The permeability results were classified using Quinones-Rozo (2010) classification and found that 34% of the flow is highly conductive (i.e. Many open discontinuities), 33% medium conductive (i.e. Some Open discontinuity), 19.5% moderately conductive (i.e. Few Partly Open discontinuities) and 13.5% low conductive (i.e. Tight discontinuities).

Estimating hydraulic conductivity from HC-Model

The HC- model of predicting hydraulic conductivity was initially proposed by Hsu et al. (2011) and is based on new rock mass classification system which incorporates the following four component parameters as: Rock Quality Designation Index (RQD), Depth Index (DI), Gouge Content

Designation Index (GCD) and Lithology Permeability Index (LPI). On the basis of these four aforementioned parameters, HC-values can be calculated using equation 4. After calculating HC values related to the respective depth interval from rock core log data, regression analysis was performed between HC- index values and in-situ hydraulic conductivity obtained from packer test to estimate the dependence of HC on hydraulic conductivity. The regression results indicated that a power law relationship exists with a greater coefficient of determination between HC values and hydraulic conductivity for both the borehole BH-1 and BH-2. The calculated results of HC-values from HC-System is shown in Table 2 for BH-1 and in Table 3 for BH-2. Similarly, the graphical representation figure of obtained HC-model of BH-1 and BH-2 are shown in Fig.2 and Fig. 3 respectively. From the HC model of two boreholes, the following set of equations (6 and 7) were obtained by conducting power law regression analysis between HC-value and hydraulic conductivity.

For borehole BH-1;

$K=0.0006\ (HC)^{0.7251}$, $R^2=0.46$……… (Eqn. 6)

For Borehole BH-2;

$K=0.00001\ (HC)^{-0.626}$, $R^2=0.25$ …….. (Eqn. 7)

The HC-value always lies between 0 and 1. The HC-value close to 1 indicates zone of highly conductive rock mass.

Lithology Permeability Index (LPI) was accounted on new rock mass classification system of Hsu et al. (2011) as shown in Table 1. It should be noted that the value of (1-GCD) in Table 2 and 3 is equal to 1 as because in this research the core sample is assumed to be gouge free (i.e. GCD=0).

Table 1: Rating for lithology permeability index (Modified after B.B.S Singhal and R.P. Gupta 1999; Bear 1972; Hsu et al. 2011)

Lithology	Average hydraulic conductivity Range	Range of LPI rating	Suggested LPI Rating
Sandstone	$10^{-7.5}$	0.8-1.0	1
Silty Sandstone	-	0.9-1.0	0.95
Shale interbedded with some Sandstone	-	0.5-0.7	0.6
Dolomite	10^{-8}	0.6-0.8	0.7
Limestone	10^{-9}	0.6-0.9	0.7
Shale	$10^{10.5}$	0.4-0.6	0.5
Sandy Shale/Slate	-	0.5-0.6	0.6
Siltstone / Claystone	10^{-11}	0.2-0.4	0.3
Granite /Basalt	$10^{11.5}$	0.1-0.2	0.15

Table 2: Calculated results for HC-system for borehole BH-1, data set of first cycle test only

Bore hole	Test Interval	RQD	1-RQD/100	$DI=1-\frac{Lc}{Lt}$	1-GCD	LPI	HC-Value	$K_{in\text{-}situ}$ cm/sec
BH-1	6-9	53	0.47	0.90	1	0.6	0.2538	1.38E-04
	9-12	0.01	0.99	0.86	1	0.6	0.5159	3.56E-04
	12-15	26	0.74	0.82	1	0.6	0.3640	4.27E-04
	15-18	21	0.79	0.78	1	0.6	0.3697	1.45E-04
	21-24	9.6	0.90	0.70	1	0.77	0.4872	1.78E-04
	24-27	13	0.87	0.66	1	0.77	0.4421	1.22E-03
	27-30	49.7	0.50	0.62	1	0.75	0.2338	1.08E-04
	30-33	66	0.34	0.58	1	0.6	0.1183	4.05E-04
	37-40	38	0.62	0.49	1	0.6	0.1810	6.46E-04
	40-43	18.4	0.87	0.45	1	0.77	0.2806	4.00E-04
	43-46	23.9	0.76	0.41	1	0.77	0.2382	2.96E-04
	46-49	34	0.66	0.37	1	0.75	0.1815	1.76E-04
	49-52	4.08	0.96	0.33	1	0.65	0.2036	2.48E-04
	52-55	15.2	0.85	0.29	1	0.65	0.1580	4.56E-05
	58-61	16.6	0.83	0.21	1	0.65	0.1120	1.18E-04
	64-67	17	0.83	0.13	1	0.6	0.06308	3.29E-05
	72-75	28.7	0.71	0.02	1	0.6	0.00855	2.51E-05

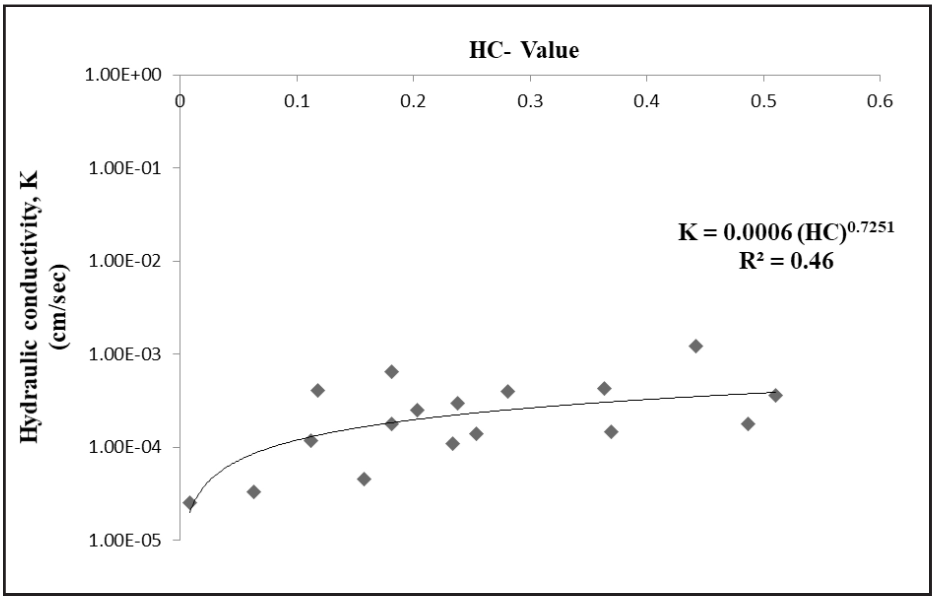

Fig. 2: Relationship between hydraulic conductivity and HC- values estimated from HC-model for BH-1

Table 3: Calculated results for HC-system for borehole BH-2, data set of first cycle test only.

Bore hole	Test Interval	RQD	1-RQD/100	$DI=1-\frac{Lc}{Lt}$	1-GCD	LPI	HC-Value	$K_{in-situ}$, cm/sec
BH-2	21-24	0.01	1.000	0.71	1	0.7	0.4980	1.23E-04
	24-27	10.44	0.896	0.67	1	0.7	0.4220	2.34E-04
	27-30	6.66	0.933	0.63	1	0.7	0.4146	8.94E-05
	30-33	13.83	0.862	0.60	1	0.7	0.3596	5.32E-05
	36-39	0.01	1.000	0.52	1	0.7	0.3634	7.45E-04
	39-42	0.01	1.000	0.48	1	0.7	0.3365	8.08E-04
	42-45	1.6	0.984	0.44	1	0.7	0.3047	9.07E-04
	45-48	5.61	0.944	0.40	1	0.7	0.2668	5.26E-04
	48-51	31.32	0.687	0.37	1	0.7	0.1757	2.83E-04
	51-54	26.4	0.736	0.33	1	0.7	0.1684	5.06E-04
	54-57	19.33	0.807	0.29	1	0.7	0.1629	7.09E-04
	57-60	19.33	0.807	0.25	1	0.7	0.1412	7.90E-04
	60-63	37	0.630	0.21	1	0.7	0.0933	1.31E-04
	63-66	12.2	0.878	0.17	1	0.7	0.1064	7.48E-04
	66-69	9.33	0.907	0.13	1	0.7	0.0854	1.10E-03
	69-72	20.66	0.793	0.10	1	0.7	0.0534	8.09E-04
	72-75	4.76	0.952	0.06	1	0.7	0.0385	1.11E-03

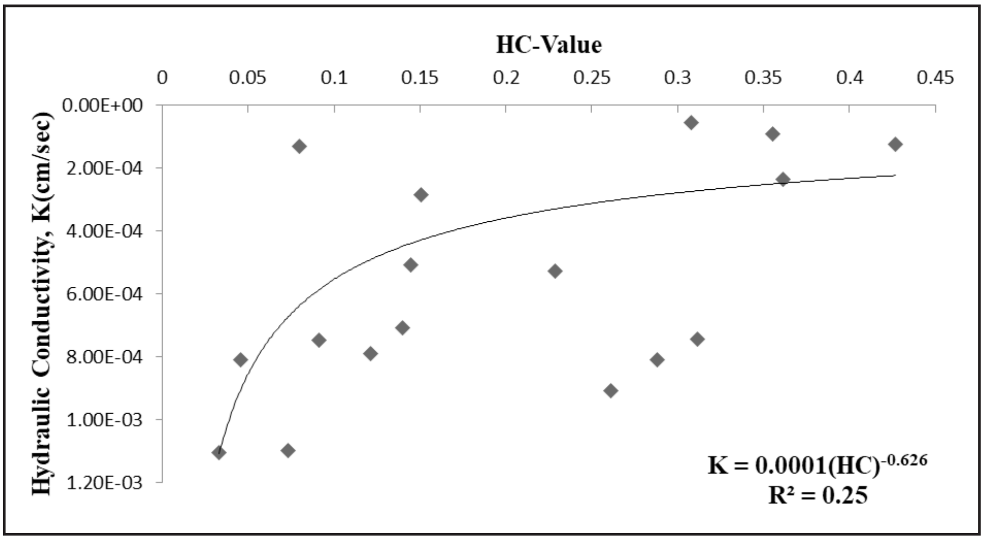

Fig.3: Relationship between hydraulic conductivity and HC- values estimated from HC-model for BH-2

Estimating hydraulic conductivity from modified HC-model

The concept of modified HC-model for the prediction of rock mass hydraulic conductivity was inspired from the HC-model of Hsu et al. (2011). Since, the HC-model developed in the previous section consists of only four component parameters but this new and updated HC model attempts to integrate two more influential rock mass parameters, namely fracture frequency and fracture aperture. Hence the modified HC model presented consists of following components parameters as: Rock Quality Designation (RQD), Depth Index (DI), Lithology permeability Index (LPI), Fracture Frequency (FF) and theoretical aperture (e). The parameters like RQD, DI and LPI are obtained in a similar way as that of the HC-model mentioned in the methodology section whereas the data for additional parameters used in the modified HC-model like fracture frequency was extracted from the borehole logs and the theoretical aperture (e) was obtained from the reverse calculation from the cubic law of parallel plate analogy using equation 3 and 4, as mentioned in the methodology section. Using the above six aforementioned parameters, the modified HC index value was calculated using equation 5.

Modified HC- value=

$$\left(1-\frac{RQD}{100}\right)(DI)(1-GCD)(LPI)(FF)(e) \quad \text{… [From Eqn. 5]}$$

After calculating the modified HC values related to the respective depth interval, regression analysis was performed between HC- index values and in-situ hydraulic conductivity obtained from the packer test to estimate the dependence of modified HC values on hydraulic conductivity. The calculated modified HC-index values and the regression analysis result performed between modified HC-values and in-situ hydraulic conductivity of borehole BH-1 are shown in Table 4 and Fig.4 respectively. The regression analysis is by a power-law relationship with coefficient of determination of 0.69. The empirical equation for modified HC-model obtained from the analysis is presented below.

$K=0.0032(H.C)^{0.6128}$, $R^2 = 0.69$ …………………… (Eqn. 8)

Discussions

El Naqa (2000) and Qureshi (2014) had successfully developed the statistically significant logarithmic and exponential empirical relationship between hydraulic conductivity and RQD with maximum coefficients of determination (R^2) of 0.61 and 0.74 respectively. Similar methodology was employed as a part of this research to see the statistical dependence of rock mass hydraulic conductivity with RQD but in present research the coefficient of determination obtained from regression analysis between hydraulic conductivity and RQD of all the observed set of equation is very low for both

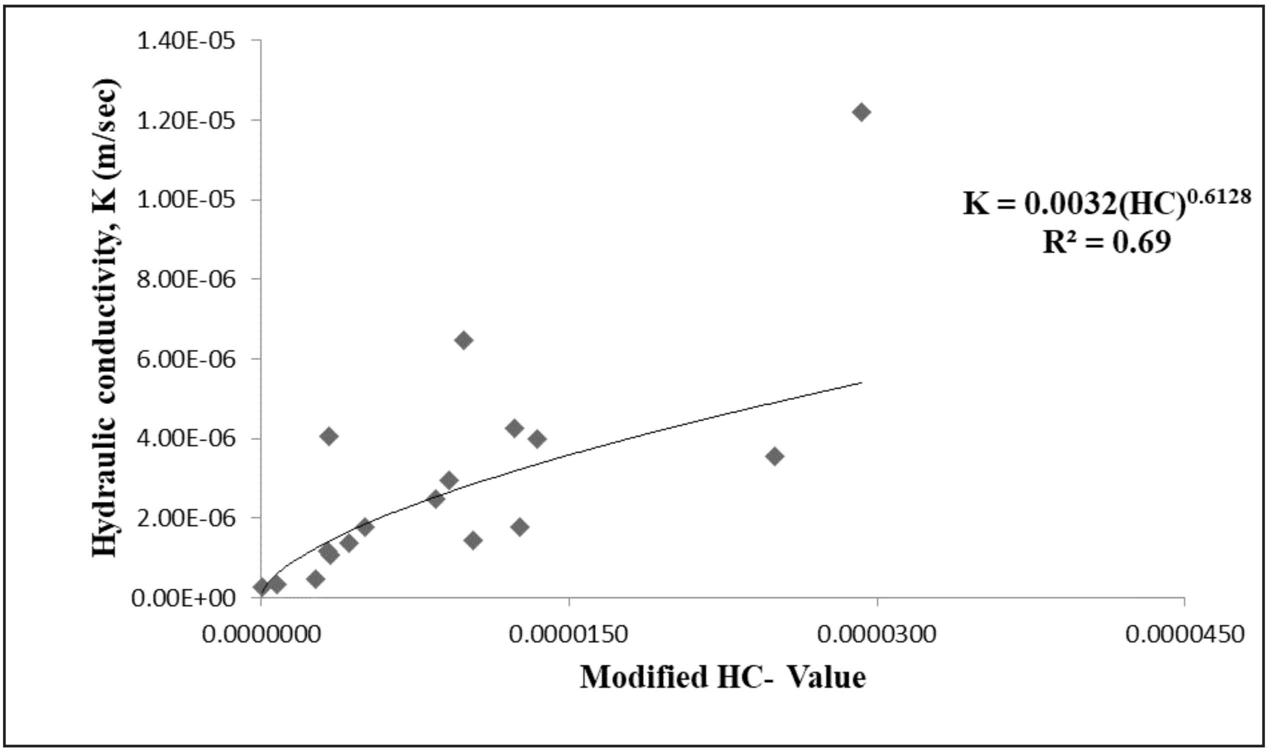

Fig. 4: Empirical relationship between hydraulic conductivity and modified HC-value estimated from modified HC-model for BH-1

Table 4: Calculated result for modified HC-value from borehole BH-1.

Bore hole	Test Depth (m)	RQD	1-RQD/100	DI	1-GCD	LPI	No. of fracture per 3m	Fracture Frequency per meter (FF)	Fracture aperture (e), m	Modified HC-value	$K_{in-situ}$, (m/sec)
BH-1	6-9	53.0	0.47	0.90	1	0.60	34	11.3	1.49E-06	4.27E-06	1.38E-06
	9-12	0.01	0.9999	0.86	1	0.60	61	20.3	2.39E-06	2.51E-05	3.56E-06
	12-15	26.0	0.74	0.82	1	0.60	39	13.0	2.61E-06	1.24E-05	4.27E-06
	15-18	21.0	0.79	0.78	1	0.60	55	18.3	1.52E-06	1.03E-05	1.45E-06
	21-24	9.6	0.904	0.70	1	0.77	46	15.3	1.69E-06	1.26E-05	1.78E-06
	24-27	13.0	0.87	0.66	1	0.77	45	15.0	4.42E-06	2.93E-05	1.22E-05
	27-30	49.7	0.503	0.62	1	0.75	33	11.0	1.31E-06	3.38E-06	1.08E-06
	30-33	66.0	0.34	0.58	1	0.60	33	11.0	2.54E-06	3.31E-06	4.05E-06
	37-40	38.0	0.62	0.49	1	0.60	51	17.0	3.22E-06	9.90E-06	6.46E-06
	40-43	18.4	0.816	0.45	1	0.77	57	19.0	2.53E-06	1.35E-05	4.00E-06
	43-46	23.9	0.761	0.41	1	0.77	53	17.7	2.18E-06	9.17E-06	2.96E-06
	46-49	34.0	0.66	0.37	1	0.75	50	16.7	1.68E-06	5.07E-06	1.76E-06
	49-52	4.08	0.9592	0.33	1	0.65	63	21.0	1.99E-06	8.52E-06	2.48E-06
	52-55	15.2	0.848	0.29	1	0.65	59	19.7	8.55E-07	2.66E-06	4.56E-07
	58-61	16.6	0.834	0.21	1	0.65	64	21.3	1.37E-06	3.28E-06	1.18E-06
	64-67	17.0	0.83	0.13	1	0.60	50	16.7	7.25E-07	7.63E-07	3.29E-07
	72-75	28.7	0.713	0.02	1	0.60	42	14.0	6.34E-07	7.59E-08	2.51E-07

exponential and logarithmic fit, which is clearly evident in figure 5, making the statistical validity of all the observed set of equations between hydraulic conductivity and RQD almost insignificant and questionable.

The possible geological explanation behind the limited correlation observed between hydraulic conductivity and RQD could be attributed to factors such as the presence of a dolomitic terrain, potentially containing caverns and cavities in the study area that complicate permeability estimation, leading to inaccuracies in permeability calculation and unsuccessful correlation with RQD. The study carried out by Lamsal (2020) also suggested the presence of cavities through the analysis of Electrical Resistivity Tomography (ERT) results in

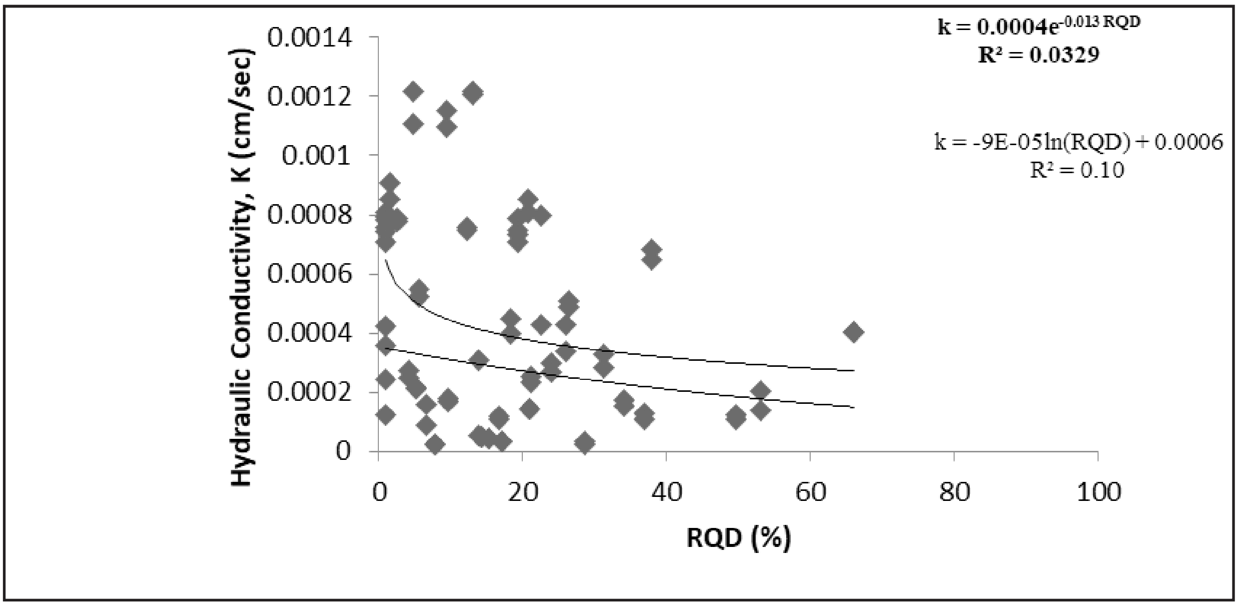

Fig. 5: Exponential and logarithmic regression analysis between representative hydraulic conductivity and RQD obtained using combined data of both boreholes.

the same area whose ERT alignment subsequently passes through BH-2. Additionally, the overall geotechnical properties of the core samples obtained are very poor, with core recovery and RQD both falling below 25%, possibly exerting a significant influence. It is noteworthy that the hydraulic conductivity of a rock mass is intricately linked to a combination of various parameters, including RQD, fracture frequency, aperture, persistence, joint infill etc. and is also highly dependent upon the geological and geotechnical criteria specific to the investigation area further influenced the complexity of the relationship. Consequently, this research suggests that developing a reliable predictive model solely based on the correlation between hydraulic conductivity and RQD alone may not always be feasible without considering the interplay of other influential rock mass parameters.

In the process of establishing a predictive model for hydraulic conductivity based solely on the Rock Quality Designation (RQD), regression analysis from the available data source did not yield the desired accuracy. This limitation prompted a broader exploration into a more comprehensive statistical model, referred to as the HC model, in the current research. Originally proposed by Hsu et al. (2011), the HC model considers hydraulic conductivity as a combined function of various rock mass parameters. This model incorporates four key parameters: Rock Quality Designation Index (RQD), Depth Index (DI), Gouge Content Designation Index (GCD), and Lithology Permeability Index (LPI), all readily obtainable from borehole data.

Hsu et al. (2011) successfully established a power-law empirical relationship between hydraulic conductivity and HC-value based on their innovative rock mass classification scheme, achieving a maximum coefficient of determination of 0.86. Building upon this foundation, similar research was undertaken in the present study to develop an empirical relationship between hydraulic conductivity and the HC-value. The resulting HC model exhibits a power-law relationship with a maximum coefficient of determination of 0.46 and 0.25 for boreholes BH-1 and BH-2, respectively (Fig. 2 and Fig. 3).While the coefficient of determination for the empirical equation derived from the HC model in the current research is not very high as that of Hsu et al. (2011) but, the outcome is very promising for the research conducted on limited time frame and limited data source in the sense that the accuracy of hydraulic conductivity prediction model goes on increasing on adding some more influential rock mass parameters on the model. This underscores the significance of incorporating these factors in refining the predictive capability of the model.

The HC-model, as formulated by Hsu et al. (2011), incorporate four key parameters in predicting permeability. However, it falls short of encompassing all potential influential parameters within the rock mass hydraulic conductivity system. Recognizing this limitation, the concept of a modified HC-model emerged in our research. This adapted hydraulic conductivity model integrates two additional influential parameters, namely Fracture Frequency (FF) and theoretical aperture (e), alongside the four parameters (RQD, GCD, DI, and LPI) used in the original HC-model.

Consequently, the modified HC-model, based on the incorporation of these six parameters, has been successfully developed in present research for BH-1. This modified model exhibits a superior fit with a power-law relationship and a significantly higher coefficient of determination of 0.69 (Fig. 4). Notably, our findings reveal that the accuracy and validity of hydraulic conductivity prediction using the modified HC-model (R^2=0.69 for BH-1) surpass those of the initially developed HC-model (R^2=0.46 for BH-1).

Nevertheless, when applied to BH-2, the modified HC-model doesn't fit well with greater accuracy and show the anomalous outcomes. This discrepancy can be attributed again to a notable factor—namely, very low core recovery resulting due to presence of cavities within the drill holes, as highlighted by Lamsal (2021). This circumstance poses challenges in accurately calculating the hydraulic conductivity value for the tested section and can be represented falsely. Additionally, the borehole data for BH-2 fails to truly represent the actual rock mass conditions, given the deficient core recovery, thereby resulting in a limited correlation. It is also essential to take note of the R^2 value for the HC-model applied to BH-2, which stands at a mere correlation of 0.25 most probably due to the similar challenges for this specific borehole.

Overall, present research highlights a positive trend in the coefficient of determination for different hydraulic conductivity prediction models with the inclusion of more influential rock mass parameters. This shows the importance of considering a broader spectrum of rock mass factors for more accurate predictions in the realm of rock mass hydraulic conductivity.

CONCLUSIONS

The research investigated the connection between hydraulic conductivity and Rock Quality Designation (RQD), concluding that RQD alone was not always sufficient to build a statistically significant model with higher accuracy. However, an empirical relationship between hydraulic conductivity and the HC- value known as the HC-model was successfully developed by incorporating four parameters with a coefficient of determination of 0.46 for BH-1 and 0.25 for BH-2. A more robust model, known as the modified HC-model was developed incorporating six parameters, demonstrated a maximum coefficient of determination of 0.69 for BH-1. These relationships offer practical alternatives to costly in-situ permeability testing, enhancing efficiency and cost-effectiveness in civil structure design. The findings emphasize the significance of multiple parameters hydraulic conductivity model, revealing that hydraulic conductivity in rock mass is a function of RQD, Gouge Content Designation Index, Lithology Permeability Index, Depth Index, Fracture Frequency, and fracture aperture. The research contributes valuable insights for planning field investigations which requires rock mass hydraulic conductivity, particularly in areas with similar geological and geotechnical characteristics.

ACKNOWLEDGEMENTS

The authors would like to express the sincere gratitude to Nalgad Hydropower Development Committee with special thanks for providing the necessary data sets to carry out this research. Furthermore, we would like to extend our special appreciation to the entire team involved in extensive geotechnical site investigations project carried out by Nalgad Hydropower Development Committee.

REFERENCES

Bear, J., 1972. Dynamics of Fluids in Porous Media. American Elsevier Publication Co., New York. 738 p.

Darcy, H., 1856. Les fontaines publiques de la ville de Dijon, exposition et application. Paris, Victor Dalmont.

Deere, D.U., 1964. Technical description of rock cores for engineering purpose. Rock Mechanics and Engineering Geology, v. 1, pp. 17-22.

El-Naqa, A., 2001. The hydraulic conductivity of the fractures intersecting Cambrian sandstone rock masses, central Jordan. Env. Geol., v. 40, pp. 973-982.

Fell, R., MacGregor, P., Stapledon, D., and Bell, G., 2005. Geotechnical engineering of dams. Tailor and Francis, London, UK. 1338 p.

Houlsby, A.C., 1976. Routine interpretation of the Lugeon water-test. Quart. Jour., Engg. Geol. Hydrogeol., v. 9, pp. 303-313.

Hvorslev, M. L., 1951. Time lag and soil permeability in groundwater observations. Waterways Experiment Station Corps of Engineers, U.S. Army, Vicksburg, Mississippi. v. 36, pp.50.

Hsu, S.M., Lo, H.C., Chi, S.Y., and Ku, C.Y., 2011. Rock mass hydraulic conductivity estimated by two empirical models. Developments in hydraulic conductivity research, pp. 1-27.

Lamsal, I., Ghimire, S., and Acharya, K.K., 2020. Geological and Geophysical Study in Udheri Khola Area, Nalgad Hydroelectric Project, Jajarkot District, Lesser Himalaya, Western Nepal. Bull. Dept. Geol., v. 22, 11-16. 10.3126/bdg.v22i0.33409.

Lugeon, M., 1933. Barrages et géologie. library de l'Université. Paris, Dunod. 430 p.

Louis, C., 1969. A study of groundwater flow in jointed rock and its influence on the stability of rock masses. Rock Mechanics Research Report, Imperial College, London, UK.

Moye, D. G., 1967. Diamond drilling for foundation exploration. Inst Engrs Civil Eng. Site Investigation Symposium.

Quiñones, C., 2010. Lugeon test interpretation, revisited. Collaborative management of integrated watersheds, US Society of Dams, 30th annual conference, pp. 405-414.

Qureshi, M.U., Khan, K. M., Bessaih, N., Al-Mawali, K., and Al-Sadrani, K., 2014. An empirical relationship between in-situ permeability and RQD of discontinuous sedimentary rocks. Elect. Jour. Geotech. Engg. v. 19, pp. 4781-4790.

Singhal, B.B.S., and Gupta, R.P., 1999. Applied hydrogeology of fractured rocks. Kluwer Academic Publishers, The Netherlands. 400 p.

Snow, D.T., 1969. Anisotropie permeability of fractured media. Water Resources Research, v. 5, pp. 1273-1289.

Wei, G., Kirby, J.T., Grilli, S.T., and Subramanya, R., 1995. A fully nonlinear Boussinesq model for surface waves. Part 1. Highly nonlinear unsteady waves. Journal of fluid mechanics, v. 294, pp. 71-92.

United States Bureau of Reclamation (USBR)., 1987. Design of small dams. US Department of the Interior, Bureau of Reclamation.

Zoorabadi, M. 2023. Lugeon Test: New insights Into the Calculated Hydraulic Conductivity. Quarterly Jour. Engg. Geol. Hydrogeol. qjegh 2023- 006.

Bulletin of Department of Geology, Tribhuvan University, Kathmandu, Nepal, vol. 24, 2023, pp. 47-55
DOI:https://doi.org/10.3126/bdg.v24i.68377

Recent Trends in the Study of Springs in Nepal: A Review

Gunanidhi Pokhrel and Moti Lal Rijal*
Central Department of Geology, Tribhuvan University, Kirtipur, Kathmandu, Nepal

ABSTRACT

Springs, a component of groundwater systems, are a vital source of fresh water for fulfilling people's demand for drinking water, household uses, and irrigation, especially in the Middle Hill region of Nepal. Springs provide water for base flows and lifelines for many rivers originating from the Middle Hill regions. The present study reviews a recent trend of spring studies and investigations in Nepal through a systematic search of published and unpublished works related to springs, which are freely available. The results show 47 publications, out of 30 are published, and 17 are unpublished. The origin of published work is mainly related to project-related works, whereas unpublished works come from the academic sector for fulfilling academic criteria for thesis research. According to the physiographical division of Nepal, the study area falls in the Middle Hills of Nepal, with the maximum area located in Bagmati Province. Most of the studies that qualitative rather than quantitative information of springs. Studies are not linked with spring source and their seasonal dynamics. However, clearly available data, attributes and information about springs from 47 reviewed documents are noted. Systematic data generation and a standard framework for data collection are also missing. Nevertheless, out of 47 studies, including 11 published and 4 unpublished, the total number of springs per sq. km. in the Middle Hill region of Nepal is estimated as 2.57, which can be integrated after more research on future springs–related work.

Keywords: Groundwater, Nepal Himalaya, Spring water quality, Water resources

Received : 12 May 2023 **Accepted:** 11 November 2023

INTRODUCTION

Spring represents a groundwater component of hydrological systems, which appears as freely flowing groundwater at the earth's surface. Springs are vital natural resources crucial in sustaining ecosystems and meeting communities' water needs worldwide. A spring is an out flow groundwater, i.e. an aquifer or into a body of water, such as a stream, lake, or sea. It happens when water from underground sources reaches the Earth’s surface or the water level of a nearby water body (Britannica, 2020). In Nepal, where most of the land is covered with hills and mountains, springs are vital drinking water sources for households, agriculture, and hydropower generation (Nepal et al., 2021; Ghimire et al., 2019; Gurung et al., 2019). The hydrology of springs involves investigating the sources of groundwater that feed the springs, the factors influencing their flow patterns, and the mechanisms that control their discharge.

Although, an overall recognition of springs' distribution and seasonal dynamics with natural processes and anthropogenic activities is less understood. A significant study of springs in Nepal, which aims for an inventory of springs with a primary focus on gathering qualitative and quantitative parameters, is at the initial stage now. Such studies are dispersed in terms of types of parameters because studies are either project-based or academic-based. Therefore, this study attempts to determine the current stage of spring studies and works concerning springs in Nepal. The study includes reviewing published and unpublished freely available academic thesis reports and published works on web sources.

METHODOLOGY

A comprehensive search was conducted in the study to find published (PS) and unpublished (UPS) studies relevant to the study of spring water in Nepal. The selection criteria are defined for searching documents (Figure 1). A total freely available 30 PS and 17 UPS in national and international journals were included in this review.

* Corresponding author:
Email: moti.rijal@gmail.com (Moti Lal Rijal)

Among them, 41 include typical studies related to springs and generating primary data in different areas of Nepal. The springs studies used to prepare this article are listed in Annex 1 and 2.

At first, Research4Life, Google Scholar, and Google were used to search for literature. Using two groups of keywords—one identifying GROUNDWATER or MOUNTAIN AQUIFER and the other characterizing the location of NEPAL—in the title, abstract, or keywords of the publications, the advanced search method was applied for Research4Life. The same set of keywords was also utilized to find additional papers that were contributed to the Mendeley literature database using Google Scholar and the Google search engine. A separate search was conducted for WATER QUALITY and GROUNDWATER SPRING, yielding a total of 2190 literature records initially, of which 1000 papers remained when surface water was eliminated.

First, the papers were reviewed using the title, abstract, and keyword filters to ensure they met the review's goals. Excluded from consideration were studies on Middle hill springs in Nepal that did not address surface water, groundwater in plain regions, or groundwater wells. As a result, just 30 articles of literature were left allowed for the final screening, and those were downloaded. The literature containing information about spring water in Nepal was identified through skim reading and added for review. A total of thirty full text online publications were found as a result, ready for a thorough review.

The studies were first grouped according to the variable of interests, which included the title, authors, affiliations, publication year, subject focus, and locations. After that, the final sorted documents were reviewed, and data was extracted from the literature regarding geographical distribution to create the checklist of springs. For the spring water study, bibliometric and study area-specific analyses were performed to achieve the predetermined research goals.

RESULTS

Status of spring-related studies

Out of 30 published articles and 17 unpublished but approved for academic degrees related to springs, the publication of PS shows the progression of research advancements over three years, namely 2019, 2020, and 2021. Moreover, the number of UPS peaked in 2021, showing a significant increase in research activity and data collection (Figure 2).

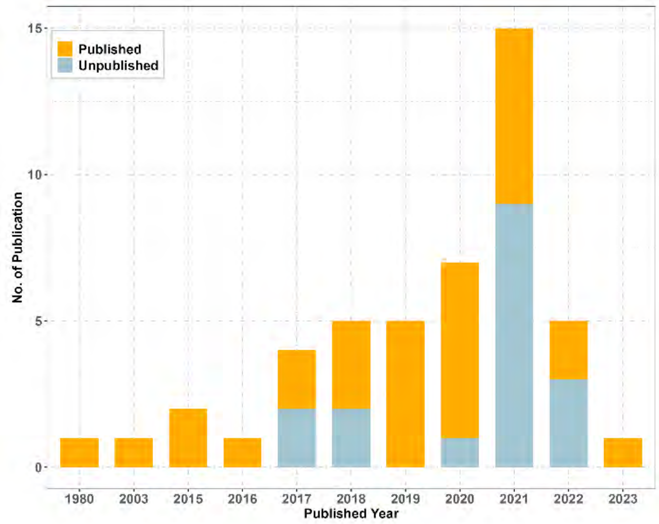

Fig. 2: Stack diagram of published and unpublished articles of springs study in Nepal.

The PS articles were sourced from various national and international agencies. Five articles were published by the International Centre for Integrated Mountain Development as working papers (Sharma et al., 2016), a manual, and a management plan (ICIMOD, 2021). As an imperative policy document, a PS was included from the National Water Conservation Foundation (Dahal et al., 2021). Six articles were included from national journals such as Banko Jankari, Bulletin of the Department of Geology, Journal of Nepal Geological Society, Journal of Institute of Science and Technology, and

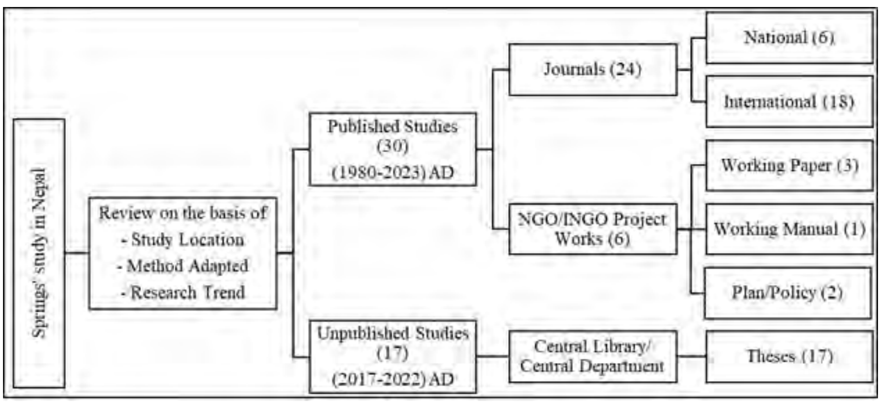

Fig. 1: Flowchart of springs study in Nepal.

Bulletin of Nepal Hydrogeological Association.

Out of thirty published articles, a total of 18 PS were published in international journals such as Tectonophysics, Mountain Research and Development, Groundwater of South Asia, Environment, Development and Sustainability, Journal of Geoscience and Environment Protection, Science of The Total Environment, Journal of Earth System Science, Hydrogeology Journal, Environmental Earth Sciences, Journal of Geographical Research, Water Practice and Technology, Environmental Earth Sciences, Journal of Hydrology: Regional Studies, Environmental Challenges, Research Square, and Mountain Research and Development.

Study area and data collection approach

A total of 47 (PS and UPS) spring related documents and articles were sampled to assess spring studies in different provinces of Nepal. Among the provinces, Koshi stands out with 3 PS and 4 UPS, showing a significant research focus on springs in the region. Bagmati Province displays many studies, with 12 PS and 7 US, showcasing a robust exploration of springs in the region. Similarly, Gandaki Province has 4 PS and 2 US, suggesting moderate research activity. Lumbini Province reveals a moderate research interest with 6 PS and 2 US. Karnali Province has fewer studies, with 2 PS and 2 US, indicating a lower level of research attention. Lastly, Sudurpaschim Province demonstrates a strong research inclination, boasting 12 PS. The spring studies highlighted variations in research activity on springs across the provinces of Nepal, directing potential disparities in knowledge and understanding of this vital natural resource.

Nepal shows a wide range of altitudes, from 64 m at Kechana in the southeastern plains to the towering height of 8,848.86 m at the world's highest peak Mount Everest. Remarkably, these extreme altitudes are found within a relatively short aerial distance of approximately 150 km, resulting in rapid changes in climate from subtropical conditions to arctic environments (Dhital, 2015), as shown in a physiographic map of Nepal (Figure 3). Geologically, the studies of springs were conducted in the dominant rocks of Nepal Himalaya, such as Shale, Slate, Phyllite, Schist, Gneiss, Mudstone, Siltstone, Sandstone, Quartzite, from Siwalik, Lesser Himalaya, and Higher Himalaya.

The gathered information was synthesized and interpreted after reviewing available documents and articles identify common trends, knowledge gaps, significant findings, and other pertinent details related to springs in Nepal. The findings and insights were compiled and organized from the review into a cohesive article on groundwater springs in Nepal. The studies collected primary data using standardized forms, including a spring inventory, geological inventory, focus group discussions (FGD), and key informant interviews (KII), ensuring consistency and reliability in the data collection process. The Geographic Information System (GIS) and Remote Sensing (RS) tools help identify potential recharge zones and aid in

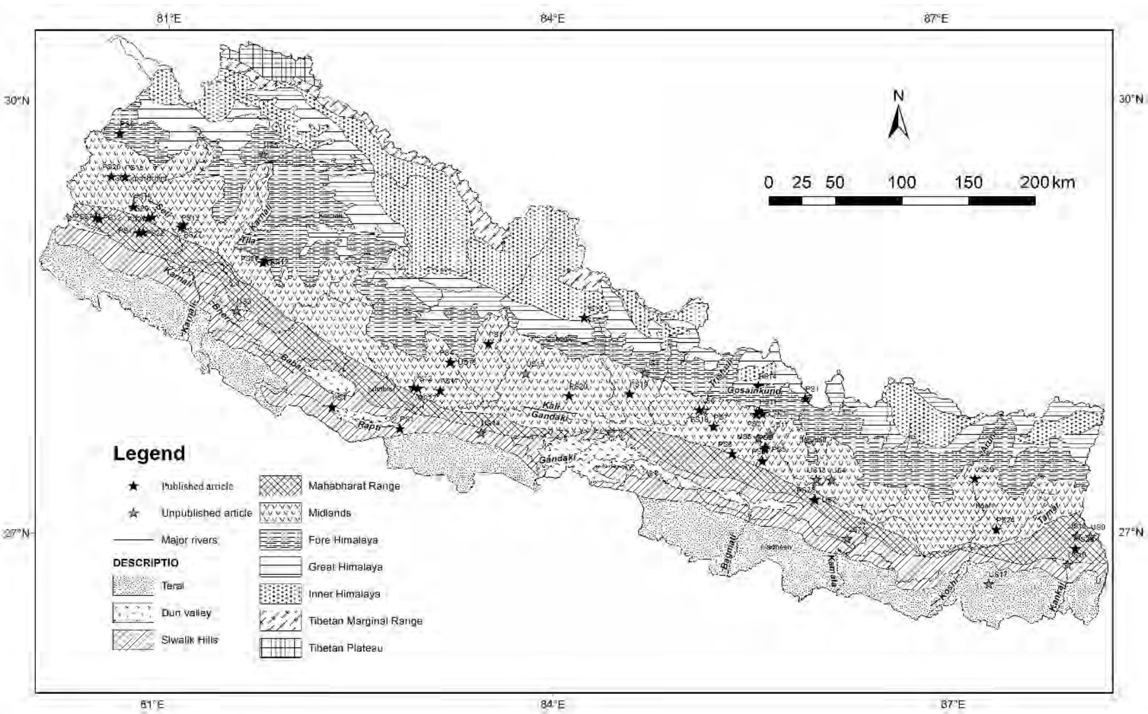

Fig. 3: Springs distribution study in Nepal's Physiography (Dhital, 2015).

better planning for increasing recharge potential. The managed potential recharge areas and spring water sources direct the future water availability to fulfil the increasing water need of the communities (Shrestha, 2020).

The potential solutions to water scarcity in the rural watersheds of Nepal conclude that catchment protection can effectively prevent contaminants from being deposited in the springs and groundwater recharge areas. In closely populated areas, delineation of recharge zones may be impracticable, but careful management of these zones is possible with the involvement of communities. The paper emphasizes the need for a collaborative approach to maximize access to critical research and promote sustainable scholarly publishing (Merz et al., 2003).

The integrated approach of geospatial and field exploration techniques effectively assesses potential groundwater zones in a hard-rock aquifer Himalayan watershed (Sapkota et al., 2021). The groundwater spring potential validation is successful, implying that the method can be replicated in a similar biophysical environment (Ghimire et al., 2019). The hydrologic modelling was carried out in a spring catchment of western Nepal to understand the changing hydrological processes. The study suggests that understanding the likely response of hydrologic variables to potential future climate scenarios is critical for water resource management (K.C. et al., 2021).

An opinion paper Yadav (2018) discusses challenges, governance, and management of groundwater resources in Nepal. It highlights the importance of sustainable management of groundwater resources and the need for policy reorientation to address potential vulnerabilities of groundwater to climate change, changing economy, and diverse social contexts.

Dahal et al. (2021) argue that a combined set of policies and practices prioritizing the sustainability of Himalayan spring sources could have a transformative impact. Regarding management-related studies of springs, Rijal (2016) emphasized a springshed approach to ensure water security in hilly communities. The author mentioned that springshed ('muladhar') should address springs rather than watershed ('jaladhar') to focus on spring revival and conservation. As such, the study was conducted in springshed approach by Lamichhane et al., (2020).

Similarly, the importance of hydrogeological science in managing watersheds, springsheds, and groundwater is demonstrated in the manual of protocol for reviving springs by Shrestha et al. (2018). It describes that the location and extent of recharge areas, where water enters the ground and replenishes aquifers, are determined by local hydrogeology rather than administrative or socio-economic boundaries. The perspective requires a paradigm shift in how we think about watersheds and springsheds.

Spring water discharge

The studies incorporated various techniques to measure spring discharge, namely the bucket stopwatch, area velocity, and water level drop methods were used to obtain discharge. Several studies classified springs into different types to comprehensively understand spring behavior across different time periods and locations. The widely adopted classifications of Tolman (1937) include Depression, Fracture, Contact, Fault, and Karst springs. Many studies incorporated Meinzer (1923) for the springs categorization based on their discharge, emphasizing the importance of considering the variability of spring discharge. The studied springs are categorized as constant, semi-constant, and variable springs as adapted by Pokhrel and Rijal (2020).

Groundwater is available in most parts of the country, but the amount and depth vary from place to place (Shrestha et al., 2018). The study by Ghimire et al. (2019) identified 11 influencing factors related to spring occurrence and groundwater movement and surveyed 412 springs in the study area. The water stress in the Rel Gad watershed is evident, accentuating the proper recharge area management. Only 16 percent of the total watershed area is under a remarkably high recharge potential zone, while 31 percent falls under minimal recharge potential. The average spring discharge is higher on the Northern Slope but lower on the southern slope (Shrestha, 2020). The 2015 Nepal earthquake had a huge and immediate impact on the water volume of the springs in the study, with an drying effect about 18% of the springs (Chapagain et al., 2019). Moreover, the discharge of springs increases highly after monsoon indicating that springs are highly dependent on precipitation (K.C. and Rijal, 2017).

Spring water quality

The in-situ water quality parameters employed in studies include EC (Electrical Conductivity), pH, Temperature, TDS (Total Dissolved Solids), and Salinity. Davis and DeWiest (1966) provided a classification system that divides water into fresh, brackish, salty and brine water to assess the TDS levels. Similarly, the classification of water based on EC, as proposed by Detay (1997), consists of six classes: very weakly, weakly, slightly, moderately, highly, and excessively mineralized water.

Piper (1944) presents a visual method for separating and analyzing dissolved substances in water. It helps study the origins of these constituents, changes in water characteristics as it moves through an area, and other geochemical issues. The primary factors governing the chemical composition of water mechanisms are atmospheric precipitation, geological influence, and the evaporation-crystallization process (Gibbs, 1970). The Stiff (1951) pattern is a visual representation of chemical analyses to illustrate the primary ion composition of a water sample. Bhattarai (1980) discusses the investigations on four thermal springs in Nepal of tectonic origin close to and south of either the Main Central Thrust or the Main Boundary Fault. Thermal waters outflowing in Greater Himalaya Sequence show a lower HCO_3 interpreted as reflecting changes in CO_2 outgassing possibly related to the 25 April 2015 Gorkha earthquake (Ghezzi et al., 2019).

The water quality of spring resources of the Badigad Catchment was found under the permissible limit of the National Standard for Drinking and Irrigation (NSDI) and WHO standards for drinking and irrigation water. Spring originated from non-carbonate rocks have slightly lower value of chemical parameters than those from the carbonate rocks (Bhusal and Gyawali, 2015). Dumaru et al. (2021); Tiwari et al. (2020); Thapa et al. (2020); Shrestha et al. (2023); Silwal et al. (2022) and Pantha et al. (2022) did suitability analysis to evaluate the quality and potential usability of spring water for drinking and irrigation purposes by using WQI and compare with national standards.

DISCUSSION

The Midland region of Nepal covers a total area of 43,141 sq. km. (Dhital, 2015) as Figure 3, the average density of the springs in the studied area is 2.57 springs per sq. km. Based on this information, it is estimated that there are approximately 111,045 springs in the Midland of Nepal.

Spring water quality and water quantity studies

Out of 30 PS, 11 discussed spring discharge quantity and 10 discussed spring water quality, and all 17 UPS included water quality and quantity. However, most scientific studies focus on quantifying spring water and other assessed spring water quality. Scientific measurements and statistical analyses provided measurable insights into spring characterizations.

Semi-quantitative studies

Out of 47 articles, 8 PS and 17 UPS discussed potential groundwater zones incorporating the different thematic layers as discussed below. Within 17 UPS, one had discussed the water poverty index using the parameters resource, use, access, capacity, and environment. Groundwater potential studies have been conducted continuously in Nepal, considering various factors contributing to increasing groundwater spring potentiality. It is found that the role of such factors assigned solely depends on the site-specific condition and authors' observation.

The validated influencing factors utilized in 14 UPS and 3 PS are hydrogeomorphology, geomorphology, water ratio index, topographic wetness index, rainfall, drainage density, degree of slope, degree of slope aspect, relative relief, elevation, geology, lineament, soil thickness, land use/land cover,

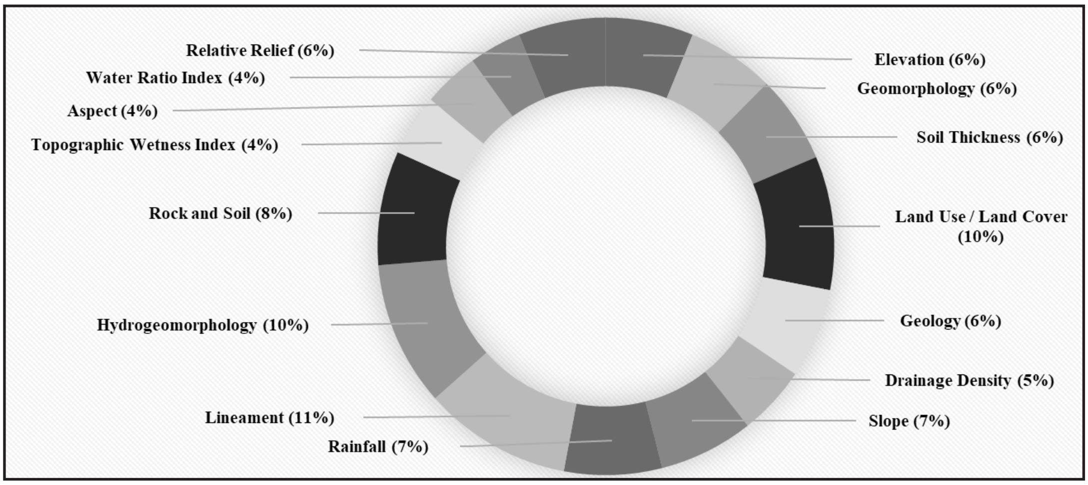

Fig. 4: Influencing factors of groundwater potential from the research of Nepal

and rock-soil characteristics (Figure 4). Each aspect carries a specific weightage, reflecting its significance in determining the suitability of an area for groundwater development and management.

Scientific data and social information of springs

The studies of springs utilized both scientific and social information. The most adapted parameters of scientific studies are hydrogeological mapping, groundwater potential zonation using GIS and RS applied in 25 articles and isotopes in 1 article (Matheswaran et al., 2019). Estimating the water quality index by applying laboratory and in-situ analyses of water samples are parameters to describe spring water quality. The scientific aspect focuses on understanding the physical processes, hydrogeological characteristics, and environmental factors influencing springs.

The societal parameters are found to be very crucial as springs hold cultural, historical, and socio-economic significance for communities relying on them for their water needs. It includes recognizing the cultural values attached to springs, the customary water use and management practices, and the social dynamics of water access and distribution. The tools for social surveys are Questionnaire, FGD, and KII. The spring inventory done by various researchers Adhikari et al. (2021) and Gurung et al. (2019) of large number of springs i.e., 4,222 from five different watersheds in Nepal incorporating social sciences is significant spring research in Nepal. (Poudel and Duex, 2017) recommends for building community capacity for water sustainability and climate change adaptation.

Drinking and other uses of spring water

Springs play an important role in providing drinking water to communities, particularly in rural areas, where they are often the primary source of water supply. The quality and quantity of water from springs are critical factors in determining their suitability for drinking. Springs have multiple uses beyond drinking water. They are vital water sources for agricultural irrigation, livestock watering, and other domestic and commercial activities. Understanding the different water demands and usage patterns associated with springs is crucial for effective water resource management.

Project-dependent and academic studies of spring

Academic studies focus on advancing scientific knowledge and understanding of springs, employing rigorous methodologies and scientific approaches to investigate various aspects such as hydrogeology, water quality, and hydrological processes. These studies contribute to the theoretical understanding of springs, expanding the scientific knowledge base.

Project-based studies are initiated by governmental organizations, non-governmental organizations, or development projects to assess springs' availability, sustainability, and management for various purposes such as drinking water supply, irrigation, or ecosystem preservation. Practical considerations and specific objectives drive the studies of springs. Dhakal et al. (2021) mentioned springshed management practices, including improved forest management, rainwater harvesting, and awareness campaigns, are recommended to enhance water security and building socio-ecological resilience in the region.

CONCLUSIONS

A recent trend in spring studies in Nepal is revealed from reviewing and in-depth analysis of publications on springs and spring water resources. This trend primarily focuses on fundamental parameters of springs such as spring discharge, in-situ physio-chemical parameters and some chemical water quality parameters. Besides that, the societal status of spring water users is included in some studies. In addition, conservation and management-related studies have also identified applying a concept of the springshed approach. However, origin, seasonal dynamics, anthropogenic impact on spring origin, and gender issues related to spring water uses are rarely focused on in these studies. The science of spring hydrogeology linking their origin with aquifers and their contribution to environmental flow and base flow for sustaining ecosystems in hill and mountain regions of Nepal Himalaya is far less focused.

ACKNOWLEDGEMENT

The authors extend their gratitude to the Central Library and Central Departments of Tribhuvan University, Kirtipur, for granting access to the available literature about studies in springs.

REFERENCES

Adhikari, S., Gurung, A., Chauhan, R., Rijal, D., Dongol, B.S., Aryal, D., and Talchabhadel, R. 2021. Status of springs in mountain watershed of western Nepal. Water Policy, v. 23(1), pp.142–156. https://doi.org/10.2166/wp.2020.187

Bhattarai, D.R. 1980. Some geothermal springs of Nepal. Tectonophysics, v. 62(1–2), pp.7–11. https://doi.org/10.1016/0040-1951(80)90071-2

Bhusal, J., and Gyawali, P. 2015. Water quality of springs in Badigad Catchment, Western Nepal. Bull. Dept. Geol., v.18, pp.67–74. https://doi.org/10.3126/bdg.v18i0.16458

Britannica, T. Editors of Encyclopaedia 2020. spring. Encyclopedia Britannica. https://www.britannica.com/science/spring-water

Chapagain, P.S., Ghimire, M., and Shrestha, S. 2019. Status of natural springs in the Melamchi region of the Nepal Himalayas in the context of climate change. Env. Dev. Sustain., v.21(1), pp.263–280. https://doi.org/10.1007/s10668-017-0036-4

Dahal, N., Bhattarai, C., Thapa, B., Tiwari, S., Shrestha, K., Agrawal, N.K., Bhuchar, S., Shrestha, A. B., and Dhakal, M. 2021. Reviving Springs of the Himalayas: An Imperative for Policy Support (Issue December). NWCF and ICIMOD.

Davis, S.N., and DeWiest, R.J.M. 1966. Hydrogeology. Wiley.

Detay, M. 1997. Water Wells Implementation, Maintenance and Restoration.

Dhakal, M.P., Khadka, K., Pokhrel, G., Desai, J., Kingsley, C., Barola, Y., and Bhuchar, S. 2021. Springs in the Godavari Landscape, Nepal. ICIMOD, pp.1–51.

Dhital, M. R. 2015. Geology of the Nepal Himalaya. Springer International Publishing Switzerland.

Dumaru, B., Kayastha, S.P., and Pandey, V.P. 2021. Spring water assessment for quality and suitability for various uses: The case of Thuligaad watershed, western Nepal. Environmental Earth Sciences, v.80(17), pp.586. https://doi.org/10.1007/s12665-021-09826-w

Ghezzi, L., Iaccarino, S., Carosi, R., Montomoli, C., Simonetti, M., Paudyal, K.R., Cidu, R., and Petrini, R. 2019. Water quality and solute sources in the Marsyangdi River system of Higher Himalayan range (West-Central Nepal). Science of The Total Environment, v. 677, pp.580–589. https://doi.org/10.1016/j.scitotenv.2019.04.363

Ghimire, M., Chapagain, P. S., and Shrestha, S. 2019. Mapping of groundwater spring potential zone using geospatial techniques in the Central Nepal Himalayas: A case example of Melamchi–Larke area. Jour. Earth Sys. Sci., v.128(2), pp.1-26. https://doi.org/10.1007/s12040-018-1048-7

Gibbs, R.J. 1970. Mechanisms Controlling World Water Chemistry. Science, v.170(3962), pp.1088–1090.

Gurung, A., Adhikari, S., Chauhan, R., Thakuri, S., Nakarmi, S., Rijal, D., and Dongol, B.S. 2019. Assessment of Spring Water Quality in the Rural Watersheds of Western Nepal. Jour. Geosci., Env., v.07(11), pp.39–53. https://doi.org/10.4236/gep.2019.711004

ICIMOD. 2021. Nibuwa—Tankhuwa Watershed Management Plan (Nepali Version).

K.C., J.K., Dhaubanjar, S., Pandey, V.P., and Subedi, R. 2021. Water balance component analysis of a spring catchment of western Nepal. Banko Janakari, v.31(1), pp.23–32. https://doi.org/10.3126/banko.v31i1.37341

K.C., P. C., and Rijal, M. L. 2017. Study of Springs of Khar Area , Darchula , Far-Western Nepal. Bull. Nepal Hydrogeol. Asso., v.2, pp.39–48.

Khadka, K., and Rijal, M. L. 2020. Hydrogeochemical assessment of spring water resources around Melamchi, Central Nepal. Water Pract. Tech., v.15(3), pp.748–758. https://doi.org/10.2166/wpt.2020.066

Lamichhane, N., Dandekhya, S., Shrestha, K., and Rajendra, S. 2020. Springshed research: A study from Charghare Village Development Committee in the mid-hills of Nepal. HI-AWARE, 48 p.

Matheswaran, K., Khadka, A., Dhaubanjar, S., Bharati, L., Kumar, S., and Shrestha, S. 2019. Delineation of spring recharge zones using environmental isotopes to support climate-resilient interventions in two mountainous catchments in Far-Western Nepal. Hydrogeol. Jour., 27(6), 2181–2197. https://doi.org/10.1007/s10040-019-01973-6

Meinzer, O.E. 1923. The Occurrence of Ground Water in the United States—With a Discussion of Principles. U.S. Government Printing Office.321 p..

Merz, J., Nakarmi, G., and Weingartner, R. 2003. Potential solutions to water scarcity in the rural watersheds of Nepal's Middle Mountains. Mount. Res. Dev., v.23(1), pp.14–18. https://doi.org/10.1659/0276-4741(2003)023[0014:PS

TWSI]2.0.CO;2

Nepal, S., Neupane, N., Belbase, D., Pandey, V.P., and Mukherji, A. 2021. Achieving water security in Nepal through unravelling the water-energy-agriculture nexus. Int. Jour. Water Res. Dev., 37(1), 67-93.

Pantha, S., Timilsina, S., Pantha, S., Manjan, S.K., and Maharjan, M. 2022. Water quality index of springs in mid-hill of Nepal. Env. Challenges https://doi.org/10.1016/j.envc.2022.100658

Piper, A.M. 1944. A Graphic Procedure in the Geochemical Interpretation of Water Analyses. American Geophysical Union, pp.914–928.

Pokhrel, G., and Rijal, M.L. 2020. Seasonal Variation of Springwater In-Situ Parameters in the Bhusundi Catchment, Gorkha, Nepal. Jour. Inst. Sci. Tech., v.25(1), pp.45–51. https://doi.org/10.3126/jist.v25i1.29450

Poudel, D.D., and Duex, T.W. 2017. Vanishing Springs in Nepalese Mountains: Assessment of Water Sources, Farmers' Perceptions, and Climate Change Adaptation. Mount. Res. Dev., v.37(1), 35 p. https://doi.org/10.1659/MRD-JOURNAL-D-16-00039.1

Rijal, M.L. 2016. The importance of springshed approach for the conservation of springs in Nepal Himalaya. Bull. Nepal Geol. Soc., v.33, pp.61–64.

Sapkota, S., Pandey, V.P., Bhattarai, U., Panday, S., Shrestha, S.R., and Maharjan, S.B. 2021. Groundwater potential assessment using an integrated AHP-driven geospatial and field exploration approach applied to a hard-rock aquifer Himalayan watershed. Jour. Hydro.: Regional Studies, v.37. https://doi.org/10.1016/j.ejrh.2021.100914

Sharma, B., Nepal, S., Gyawali, D., Pokhrel, G.S., Wahid, S., Mukherji, A., Acharya, S., and Shrestha, A.B. 2016. Springs, Storage Towers, and Water Conservation in the Midhills of Nepal. 56 p.

Shrestha, A., Shrestha, S.M., and Pradhan, A.M.S. 2023. Assessment of spring water quality of Khandbari Municipality in Sankhuwasabha District, Eastern Nepal. Research Square, pp.1–23. https://doi.org/10.21203/rs.3.rs-2518326/v1

Shrestha, R.B., Desai, J., Mukherji, A., Dhakal, M., Kulkarni, H., Mahamuni, K., Bhuchar, S., and Bajracharya, S. 2018. Protocol for Reviving Springs in the Hindu Kush Himalayas: A Practitioner's Manual 2018/4. ICIMOD Manual 2018/4. https://doi.org/978 92 9115 606 1

Shrestha, S. 2020. Groundwater Recharge Potential Mapping in Far Western Middle Mountain of Nepal: A GIS-based Approach. Jour. Geol. Res., v.3(3), pp.1–12. https://doi.org/10.30564/jgr.v3i3.2160

Shrestha, S.R., Tripathi, G.N., and Laudari, D. 2018. Groundwater Resources of Nepal: An Overview. In Groundwater of South Asia. Springer Singapore, pp. 169–193. https://doi.org/10.1007/978-981-10-3889-1_11

Silwal, C.B., Karkee, B., Dahal, K., Nepal, M., Acharya, S., Khanal, M., and Pathak, D. 2022. Hydro-geochemical characterization and suitability analysis of spring water of the Mai Khola Watershed, Ilam, eastern Nepal. Jour. Nepal. Geol. Soc., August, pp.123–132. https://doi.org/10.3126/jngs.v63i01.50847

Stiff, H.A. 1951. The Interpretation of Chemical Water Analysis by Means of Patterns. Jour. Pet. Tech., v.3(10), 15–33 https://doi.org/10.2118/951376-G

Thapa, B., Pant, R.R., Thakuri, S., and Pond, G. 2020. Assessment of spring water quality in Jhimruk River Watershed, Lesser Himalaya, Nepal. Env. Earth Sci., v.79(22). https://doi.org/10.1007/s12665-020-09252-4

Tiwari, S., Chamlagain, D., Atwood, A., and Sayami, M. 2020. Quality assessment and status of spring water in Helambu area, Sindhupalchok district, central Nepal. Jour. Nepal Geol. Soc., v.60, pp.59–74. https://doi.org/10.3126/jngs.v60i0.31274

Tolman, C.F. 1937. Ground Water. In McGraw-Hill Book Company.

Yadav, S.K. 2018. Groundwater Challenges, Governance, and Management in Nepal. In Groundwater of South Asia. Springer Singapore. pp.707–734 https://doi.org/10.1007/978-981-10-3889-1_42

ANNEXURES

Annex 1: Number of studied springs of PS and corresponding authors.

Area code	No. of springs studied	Author(s)	Area code	No. of springs studied	Author(s)
PS1	4	(Bhattarai, 1980)	PS17	102	(Thapa et al., 2020)
PS3	40	(Dhakal et al., 2021)	PS18	69	(Lamichhane et al., 2020)
PS4	30	(Bhusal and Gyawali, 2015)	PS19	44	(Pokhrel and Rijal, 2020)
PS5	286	(Sharma et al., 2016)	PS20	90	(S. Shrestha, 2020)
PS6	57	(P. C. K.C. and Rijal, 2017)	PS21	18	(Khadka and Rijal, 2020)
PS7	41	(Poudel and Duex, 2017)	PS22	160	(Dumaru et al., 2021)
PS11	412	(Chapagain et al., 2019)	PS24	97	(ICIMOD, 2021)
PS12	155	(Gurung et al., 2019)	PS25	61	(Sapkota et al., 2021)
PS13	9	(Ghezzi et al., 2019)	PS27	4222	(Adhikari et al., 2021)
PS14	412	(Ghimire et al., 2019)	PS28	147	(Silwal et al., 2022)
PS15	7	(Matheswaran et al., 2019)	PS29	3	(Pantha et al., 2022)
PS16	57	(Tiwari et al., 2020)	PS30	85	(A. Shrestha et al., 2023)

Annex 2: Number of studied springs of UPS and corresponding authors.

Area code	No. of springs studied	Author(s)	Area code	No. of springs studied	Author(s)
UPS1	28	(Gautam, 2017)	UPS10	10	(Shah, 2021)
UPS2	107	(Adhikari, 2017)	UPS11	15	(Pandey, 2021)
UPS3	8	(B.C., 2018)	UPS12	147	(Karkee, 2021)
UPS4	33	(Khadka, 2018)	UPS13	12	(Bhattarai, 2021)
UPS5	8	(Sunar, 2020)	UPS14	11	(Maharjan, 2021)
UPS6	80	(Aryal, 2021)	UPS15	23	(Aryal, 2022)
UPS7	18	(Magar, 2021)	UPS16	122	(Sapkota, 2022)
UPS8	15	(Dhungana, 2021)	UPS17	20	(Dahal, 2022)
UPS9	129	(Acharya, 2021)			

Annex 3: Water Quality, Water Quantity, and Semi Quantitative-Qualitative categories of PS.

Published Studies (PS)		
Water Quality	**Water Quantity**	**Semi Quantitative-Qualitative**
(Bhattarai, 1980)	(Sharma et al., 2016)	(Merz et al., 2003)
(Bhusal and Gyawali, 2015)	(K.C. and Rijal, 2017)	(Yadav, 2018)
(Poudel and Duex, 2017)	(Chapagain et al., 2019)	(Shrestha et al., 2018)
(Ghezzi et al., 2019)	(Pokhrel and Rijal, 2020)	(Shrestha et al., 2018)
(Gurung et al., 2019)	(Lamichhane et al., 2020)	(Ghimire et al., 2019)
(Tiwari et al., 2020)	(Khadka and Rijal, 2020)	(Matheswaran et al., 2019)
(Thapa et al., 2020)	(Dhakal et al., 2021)	(Shrestha, 2020)
(Dumaru et al., 2021)	(ICIMOD, 2021)	(Sapkota et al., 2021)
(Pantha et al., 2022)	(K.C. et al., 2021)	(Dahal et al., 2021)
(Shrestha et al., 2023)	(Adhikari et al., 2021)	(Rijal, 2016)
	(Silwal et al., 2022)	

Bulletin of the Department of Geology
Tribhuvan University, Kathmandu, Nepal
ISSN: 1996-3491

Volume 24 **December 2023**

Printed at: Tribhuvan University Press, Kirtipur, Kathmandu, Nepal
Telephone: 00977 1 4331320, 4331321